UILU-ENG-83-2014

CIVIL ENGINEERING STUDIES
STRUCTURAL RESEARCH SERIES NO. 510

ISSN: 0069-4274

# INVESTIGATION OF METHODS FOR STRUCTURAL SYSTEM RELIABILITY

By
R. M. BENNETT
and
A. H-S. ANG



Technical Report of Research
Supported partially by the
NATIONAL SCIENCE FOUNDATION
(Under Grants CEE 80-02584 and CEE 82-13729)

UNIVERSITY OF ILLINOIS
at URBANA-CHAMPAIGN
URBANA, ILLINOIS
SEPTEMBER 1983

50272-101

| REPORT DOCUMENTATION PAGE | 1. REPORT NO. UILU-ENG-83-2014 | 2. | 3. Recipient's Accession No. |
|---|---|---|---|

**4. Title and Subtitle**

INVESTIGATION OF METHODS FOR STRUCTURAL SYSTEM RELIABILITY

**5. Report Date** SEPTEMBER 1983

**6.**

**7. Author(s)**

R. M. Bennett and A. H-S. Ang

**8. Performing Organization Rept. No.** SRS No. 510

**9. Performing Organization Name and Address**

Department of Civil Engineering
University of Illinois
208 N. Romine Street
Urbana, IL 61801

**10. Project/Task/Work Unit No.**

**11. Contract(C) or Grant(G) No.**

(C)

(G) NSF PFR 80-02584
NSF CEE 82-13729

**12. Sponsoring Organization Name and Address**

National Science Foundation
Washington, D.C.

**13. Type of Report & Period Covered**

**14.**

**15. Supplementary Notes**

**16. Abstract (Limit: 200 words)**

The failure mode approach, based on ways in which a structure can fail, and the stable configuration approach, based on ways in which a structure can carry an applied load, were examined and developed for the determination of the reliability of general redundant structural systems including systems with brittle components. For a class of structures, in which the load effects on the surviving elements never decrease with the failures of other elements, simplified formulations are introduced. Such simplifications result from the fact that the reliability of a system becomes independent of the sequence in which the elements may fail. Results of the simplified formulation are generally on the conservative side.

The failure graph, which is a directed graph of all possible sequences of component failures that will lead to the prescribed limit state, is introduced to aid in the formulation. Each path from the initial node to the terminal node of a graph represents a failure mode. A branch represents a component failure and each node of the graph (except the terminal node) represents a stable configuration of a structure. A cut is defined as a set of branches containing one branch from every path.

The failure mode approach leads to the probability of the union of the individual failure modes (paths); each failure mode is the intersection of all the branches in the corresponding path. The stable configuration approach leads to the probability of the intersection of the failures of the cuts; the failure of a cut is the union of the branches comprising the cut.

**17. Document Analysis a. Descriptors**

Failure Modes
Failure Probability
Reliability
Safety
Stable Configurations
Structures
System Reliability

**b. Identifiers/Open-Ended Terms**

**c. COSATI Field/Group**

| 18. Availability Statement | 19. Security Class (This Report) UNCLASSIFIED | 21. No. of Pages 134 |
|---|---|---|
| | 20. Security Class (This Page) UNCLASSIFIED | 22. Price |

# ACKNOWLEDGMENTS

This report is based on the doctoral thesis of Dr. R. M. Bennett submitted in partial fulfillment of the requirements for the Ph.D. in Civil Engineering at the University of Illinois.

The study is part of a program on the safety and reliability of structures to seismic and other hazards, supported partially by the Division of Civil and Environmental Engineering of the National Science Foundation under grants PFR 80-02584 and CEE 82-13729. Supports for this study are gratefully acknowledged.

TABLE OF CONTENTS


| CHAPTER | | Page |
|---|---|---|
| 1 | INTRODUCTION | 1 |
| | 1.1 General Remarks | 1 |
| | 1.2 Object and Scope of Study | 2 |
| | 1.3 Previous Related Work | 2 |
| | 1.4 Organization | 3 |
| | 1.5 Notation | 4 |
| 2 | RELIABILITY OF COMPONENTS | 6 |
| | 2.1 Gaussian Framework | 6 |
| | 2.2 First-Order Methods | 7 |
| | 2.2.1 Basic Concepts | 7 |
| | 2.2.2 Accuracy of First-Order Methods | 8 |
| | 2.3 Improved Methods | 9 |
| 3 | PROBABILISTIC METHODS FOR SYSTEM RELIABILITY | 14 |
| | 3.1 Union of Failure Events | 14 |
| | 3.1.1 Elementary Bounds | 14 |
| | 3.1.2 Second-Order Bounds | 15 |
| | 3.1.3 Approximate Methods | 17 |
| | 3.2 Intersection of Failure Events | 18 |
| | 3.2.1 Elementary Bounds | 18 |
| | 3.2.2 Second-Order Bounds | 19 |
| | 3.3 Multivariate Normal Integral | 20 |
| | 3.3.1 Solutions for Special Cases | 20 |
| | 3.3.2 Bivariate Normal Integral | 23 |
| | 3.3.3 Trivariate Normal Integral | 24 |
| | 3.3.4 Bounds Based on Slepians's Inequality | 25 |
| | 3.3.5 First-Order Solution | 26 |
| 4 | FORMULATIONS OF STRUCTURAL SYSTEM RELIABILITY | 29 |
| | 4.1 Introductory Comments | 29 |
| | 4.2 Failure Graphs | 30 |
| | 4.3 Conceptual Models | 30 |
| | 4.3.1 Failure Mode Approach | 30 |
| | 4.3.2 Stable Configuration Approach | 32 |
| | 4.3.3 Examples | 34 |
| | 4.4 Monotonically Loaded Structures | 37 |
| | 4.4.1 Definition | 37 |
| | 4.4.2 Formulation of Failure Modes | 38 |
| | 4.4.3 Formulation of Cuts | 39 |

Page


4.4.4 Relationships Between Formulations ..... 41
4.4.5 Minimal Forms ..... 42
4.4.6 Physical Interpretations ..... 42
4.4.7 Examples ..... 43
4.5 General Structures ..... 44
4.5.1 Remarks ..... 44
4.5.2 Conservative Approximations ..... 45
4.5.3 Examples ..... 46

5 COMPUTATIONAL METHODS ..... 57

5.1 Introductory Comments ..... 57
5.2 Failure Mode Approach ..... 57
5.2.1 Systematic Determination of Significant Failure Modes ..... 57
5.2.2 Determination of the Reliability of Each Mode ..... 60
5.2.3 Combining of Modes ..... 61
5.2.4 Algorithm for Analysis of General Structural Systems ..... 63
5.3 Stable Configuration Approach ..... 67
5.4 Monte Carlo Methods ..... 69

6 ILLUSTRATIVE APPLICATIONS ..... 83

6.1 Introductory Comments ..... 83
6.2 A Four-Member Parallel Structure ..... 83
6.2.1 Failure Mode Analysis ..... 84
6.2.2 Stable Configuration Analysis ..... 87
6.2.3 Monte Carlo Simulations ..... 88
6.3 A Fixed-Fixed Beam ..... 89
6.3.1 Case I--Ductile Sections ..... 90
6.3.2 Case II--Brittle Sections ..... 90
6.3.3 Case III--Combined Ductile and Brittle Sections ..... 91
6.3.4 Case IV--Semi-Ductile Sections ..... 93
6.3.5 Case V--General Nonlinear Behavior ..... 95
6.4 A Simple Grid System ..... 97
6.5 A Simple Rigid Frame ..... 100
6.5.1 Failure Mode Analysis ..... 101
6.5.2 Stable Configuration Analysis ..... 102
6.5.3 Monte Carlo Analysis ..... 103
6.6 An Unsymmetrical Two-Story Two-Bay Frame ..... 104
6.7 A Two-Tier Truss ..... 106
6.8 A Truss Structure ..... 109
6.8.1 Failure Mode Analysis ..... 110
6.8.2 Stable Configuration Analysis ..... 113

Page

7 SUMMARY AND CONCLUSIONS ..... 122

7.1 Summary ..... 122
7.2 Conclusions ..... 123
7.3 Critical Overview and Recommendations for Further Study ..... 124

APPENDIX

A QUADRATIC PROGRAMMING ALGORITHM FOR FINDING THE FAILURE POINT OF FAILURE MODES ..... 125

REFERENCES ..... 128

# LIST OF TABLES


| Table | | Page |
|---|---|---|
| 2.1 | Accuracy of First-Order Methods: Nonnormal Variables | 12 |
| 5.1 | Accuracy of Different Linearizations of the Failure Surface | 74 |
| 5.2 | Failure Regions of Modes Shown in Fig. 5.2 | 75 |
| 5.3 | Comparison of Results Using Approximate Planes with Direction Cosines as Sensitivity Coefficients and of the Failure Point of the Mode | 76 |
| 6.1 | Statistics of Random Variables of Grid System (Fig. 6.8) | 99 |
| 6.2 | Statistics of Random Variables of Two-Story Two-Bay Frame (Fig. 6.11) | 105 |
| 6.3 | Statistics of Random Variables of Two-Tier Truss (Fig. 6.12) | 107 |
| 6.4 | Statistics of Random Variables of Truss Structure (Fig. 6.13) | 111 |

# LIST OF FIGURES


| Figure | | Page |
|---|---|---|
| 2.1 | Failure and Safe Regions in Design Space | 13 |
| 2.2 | Linearized Failure Surface | 13 |
| 2.3 | Shifting of First-Order Plane | 13 |
| 3.1 | "Failure Surfaces" for Conditional Probabilities | 28 |
| 4.1 | Typical Failure Graph | 49 |
| 4.2 | Three-Member Parallel System with Active Redundancy | 50 |
| 4.3 | Failure Graph for 3-Member Structure of Fig. 4.2 | 50 |
| 4.4 | Stable Configurations of 3-Member Structure of Fig. 4.2 | 51 |
| 4.5 | Possible Cuts of Failure Graph of Fig. 4.3 | 52 |
| 4.6 | Load-Deformation Characteristics of Members of Structure of Fig. 4.2 | 52 |
| 4.7 | Reduced Failure Graph and Cuts for Structure of Fig. 4.2 | 53 |
| 4.8 | Simple Frame Structure of Example 4.2 | 54 |
| 4.9 | Failure Graph for Frame of Fig. 4.8 | 54 |
| 4.10 | Three Possible Loading Paths for Frame of Fig. 4.8 | 55 |
| 4.11 | Structure of Example 4.3 | 55 |
| 4.12 | Load-Deformation Characteristics of Members of Structure of Fig. 4.11 | 55 |
| 4.13 | Non-Monotonically Loaded Structure of Example 4.4 | 56 |
| 5.1 | Linearization of Failure Surfaces | 77 |
| 5.2 | Linearization of Failure Modes | 78 |
| 5.3 | Identical Approximate Planes | 80 |
| 5.4 | Failure Graph for Illustrating Algorithm | 81 |

Page

5.5 Error in Probability of Failure from Monte Carlo Calculations ..... 82

5.6 Error in Reliability Index from Monte Carlo Calculations ..... 82

6.1 Four-Member Parallel Structure ..... 114

6.2 Stable Configurations Considered ..... 114

6.3 A Fixed-Fixed Beam ..... 115

6.4 Moment-Curvature Diagram for Beam, Case III ..... 115

6.5 Failure Graph for Beam, Case III ..... 115

6.6 Modelling of Beam, Case V ..... 116

6.7 Portion of Failure Graph for Beam, Case V ..... 116

6.8 A Simple Grid System ..... 117

6.9 Failure Graph for Grid System ..... 118

6.10 One-Story One-Bay Frame ..... 119

6.11 Two-Story Two-Bay Frame ..... 119

6.12 Two-Tier Truss System ..... 120

6.13 A Truss Structure ..... 121

6.14 $\beta$ vs. $\overline{P}$ ..... 121

6.15 Retrofitted Truss Structure ..... 121

# CHAPTER 1

# INTRODUCTION

## 1.1 General Remarks

The structural engineer is responsible for the design of structures in which the safety and performance must be ascertained, generally without the benefit of complete information. Essentially, prediction of the future loading, resistances, and behavior under conditions of uncertainty is involved. To account for these uncertainties, factors of safety are traditionally introduced into the design process. For many years, safety has been assured in a more or less qualitative manner. In his classic paper, Freudenthal (1947) introduced the use of probability theory as a tool for the rational analysis of safety. Since that time, there have been many advances in the analysis of safety, both in terms of theoretical developments and applications to design codes.

The design of civil engineering structures generally proceeds element by element; for instance, in a frame structure the beams, columns, connections, etc. are designed individually and separately. Decomposing the design process further, each element is designed so that it has a desired level of safety against various modes of failure; for example, a beam is examined for its flexural and shear capacity as well as other potential modes of failure. The safety against these various failure modes is certainly of interest; equally important, however, is the safety of the entire structure. This latter point was emphasized by Frankland (1947). It is this concern that has prompted studies into methods for the determination of the reliability of structural systems. Civil engineering structures, invariably being one-of-a-kind type of systems, require that the reliability of a system be determined from the information on the reliabilities of the components.

Failure is often thought of as collapse; however, other lesser degrees of damage, or limit states (e.g., excessive deflection or drift) may also be defined as failure.

## 1.2 Object and Scope of Study

The primary objective of the present study is the investigation and development of methods for determining the reliability of structural systems. Specifically, various formulations are examined and (whenever possible) simplifications are made. Computational methods are also examined with particular emphasis on the extension of first-order methods for component reliability to the analysis of structural system reliability.

Redundant structural systems in which some of the elements may exhibit brittle behavior are emphasized, i.e. structures in which the failure probability depends on the sequence of component failures. The failure of a component in a brittle manner obviously causes the structure to be physically altered and the load to be redistributed among the surviving members.

Structures in this study are assumed to be subjected to a single static load application.

## 1.3 Previous Related Work

Previous studies on structural system reliability are largely limited to the determination of the collapse probability of ductile systems, such as frames and trusses. Grimmelt and Schueller (1982) provided an extensive review of available methods and also comparisons of the capabilities of the various techniques.

Research has included the reliability of bundles of threads, which is a form of parallel-component structures. Daniels (1945) may have been the first to look at this type of system. Representative of recent

works are the studies by Shinozuka and Itagaki (1966), Phoenix (1979), and Hohenbichler and Rackwitz (1983a), that examine different load-sharing rules including chains of parallel structures.

General structural systems, in particular systems with brittle components, have been examined by Shinozuka, et al. (1965), Ang and Amin (1967), Yao and Yeh (1967,1969), and Ishizawa (1968). Most of these studies, while important, have extremely limited applications. Recently, there were additional studies directed at both the computational aspects (Ma and Ang, 1981) and formulation (Rackwitz and Peintinger, 1982) of the reliability of more general structures.

## 1.4 Organization

This chapter discussed some of the motivations for the study and related previous research.

Chapter 2 contains a brief review of methods for determining the probability of failure of components. Particular emphasis is given to first-order methods. The usefulness of the methods in relation to determining the failure probability of structural systems is discussed.

In Chapter 3, methods for determining the probabilities of unions and intersections are discussed, focusing on bounding techniques and solutions to the multivariate normal integral.

Chapter 4 develops various formulations for determining the reliability of structural systems. The failure mode approach is examined and a new formulation, the stable configuration approach, is introduced. A special type of structure, herein called a monotonically loaded structure, is defined and a number of simplifications in the formulations are delineated.

Chapter 5 combines the material of Chapters 2 through 4 to develop practical computational techniques for the analysis of the reliability of structural systems.

Illustrative examples are given and discussed in Chapter 6. They are used to verify the developments of this study and to suggest

possible practical applications.

Finally, Chapter 7 contains a summary and the conclusions of the study. Possible areas of further research are also suggested.

## 1.5 Notation

The notation and symbols used are defined where they first appear in the text. However, for ease of reference, the most important symbols are summarized as follows:

$B_{ij}$ = event that branch ij fails

$C_{a-a}$ = event that cut a-a fails

$E(.)$ = expected value

$f(.)$ = probability density function

$F(.)$ = cumulative distribution function

$F_{ij}$ = set of random variables such that if the structure fails, it will fail through branch ij.

$g(.)$ = performance function

$I(.)$ = indicator function

$M_i$ = event mode i fails

$p_F$ = probability of failure

$P(E)$ = probability of event E occuring

$U$ = independent standard normal variable

$X$ = basic random variable

$\alpha$ = direction cosine

$\beta$ = reliability index; also distance from plane to origin in independent standard normal space

$\mu$ = mean value

$\rho$ = correlation coefficient

$\sigma$ = standard deviation

$\phi_n(.)$ = standard normal density function of dimension n; if subscript is omitted, it is assumed to be 1

$\Phi_n(.)$ = standard normal integral of dimension n; if subscript is omitted, it is assumed to be 1

$\underline{X}$ = vector of $x_1,\ldots,x_n$

$\underline{\underline{X}}$ = matrix of values $x_{ij}$

$\bar{E}$ = denotes complement of event E

$\cup$ = denotes union of events

$\cap$ = denotes intersection of events

$\varepsilon$ = denotes is a member of

# CHAPTER 2

# RELIABILITY OF COMPONENTS

For obvious reasons, the accurate determination of the component reliabilities is important in the analysis of system reliability. In a recent study on methods for determining the reliability of frame structures against plastic collapse (Grimmelt and Schueller, 1982), one of the conclusions was that the discrepancies in the different methods of analysis were mainly due to errors in the calculation of the probability of failure of the individual modes. Therefore, in the study of structural system reliability, the accuracy of the calculated component reliability is essential.

## 2.1 Gaussian Framework

Define a performance function of a component, $g(X_1,\ldots,X_n)$, such that when $g(\underline{X})<0$ failure occurs and when $g(\underline{X})>0$ the component survives. The limit state surface or failure surface is

$$g(X_1,\ldots,X_n) = 0 \tag{2.1}$$

This surface divides the state space into the safe and failure regions as shown in Fig. 2.1. The random variables, $X_i$, could include material strengths, member dimensions, applied loads, and model parameters.

Assume that the random variables are independent standard normal variables, i.e., all the random variables are normal with zero means and unit standard deviations. Assume also that the performance function is linear. A reliability index can be defined as (Ang and Cornell, 1974):

$$\beta = \frac{\mu_g}{\sigma_g} \tag{2.2}$$

where:

$\mu_g$ = mean of $g(\underline{X})$;
$\sigma_g$ = standard deviation of $g(\underline{X})$.

The reliability index will be the distance from the origin to the failure surface. The probability of failure is determined exactly as:

$$p_f = \Phi(-\beta) \tag{2.3}$$

where $\Phi(.)$ is the standard normal integral. Ditlevsen (1979a) proposed that a "generalized" reliability index be defined such that Eq. 2.3 is valid for a general failure surface, including nonlinear surfaces.

Although the problem is formulated in Gaussian space, the random variables may not be Gaussian. Oftentimes the available information is limited to the first two moments of the random variables. In this case, it is consistent and reasonable to assume the random variables to be Gaussian. If the full joint distribution of the random variables is known, the random variables can be transformed into independent standard normal variables (Rosenblatt, 1952). If more than the first two moments are known but the full distribution is not known, a distribution can be prescribed that fits all available information (Ang, 1973).

## 2.2 First-Order Methods

### 2.2.1 Basic Concepts

Often the failure surface is nonlinear. The exact evaluation of the probability of failure and corresponding reliability index will be difficult; generally, this requires multidimensional integration. As an approximation, first-order methods have been suggested in which the

performance function is expanded in a Taylor series and only the linear terms in the series are retained. In other words, a nonlinear failure surface is approximated by a linear failure surface.

The point about which the performance function is expanded should be such that the difference between the estimated probability of failure, based on the approximate linear failure surface, and the true probability of failure is minimized. It has been shown that the expansion point is the point on the failure surface closest to the origin in independent standard normal space (Shinozuka, 1983). This point is often referred to as the most-probable failure point, i.e., it is the point with the maximum probability density in the failure region.

Therefore, the performance function can be approximated by:

$$g(\underline{U}) \simeq \underline{\alpha}^t (\underline{U} - \underline{u}_o) = \underline{\alpha}^t \underline{U} + \beta \qquad (2.4)$$

where:

$\underline{U}$ = independent standard normal variates;

$\underline{u}_o$ = the expansion point;

$\underline{\alpha}$ = direction cosines: $\frac{\partial g}{\partial \underline{U}}$ evaluated at $\underline{u}_o$;

$\beta$ = the distance from the origin to $\underline{u}_o$.

The physical interpretations of $\underline{\alpha}$ and $\beta$ are shown in Fig. 2.2 for two dimensions. $\beta$ is an estimate of the reliability index, on the basis of which the probability of failure can be estimated using Eq. 2.3.

### 2.2.2 Accuracy of First-Order Methods

Nonnormal Variables--Nonlinearity of the performance function in independent standard normal space can arise in two ways. One is when the basic variables are nonnormal. The transformation to the normal space is generally nonlinear. The accuracy of the first-order approximation is examined for five cases with a variety of distributions, including the lognormal, extreme types I, II, and III,

and the gamma distribution. The results are summarized in Table 2.1. The maximum error in the probability of failure is 20% whereas the error in the reliability index is less than 4%. Table 2.1 also includes seven other cases that were examined by other researchers.

As demonstrated in Table 2.1, first-order methods are quite accurate except when the distribution deviates significantly from the normal, such as the exponential distribution. In structural reliability problems, the random variables will generally be well behaved, i.e., unimodal and no discontinuities in the probability density function. Therefore, first-order methods should be suitable for handling nonnormal variables.

Nonlinear Performance Function--Nonlinearity of the performance function in independent standard normal space can, of course, be expected when the performance function in the original space is nonlinear. The accuracy of first-order methods in this case obviously depends on the degree of nonlinearity. In the worst case, such as a concentric circular failure surface, poor results may be expected with the first-order method. In fact, in such cases, the estimated probability could be an order-of-magnitude in error. However, most failure surfaces are reasonably flat and first-order methods should be adequate in most practical problems.

A number of examples involving nonlinear failure surfaces have been examined by other researchers, both with normal and nonnormal variables (Rackwitz and Fiessler, 1978; Ang and Tang, 1983). In general, first-order methods appear to give fairly accurate estimates. Although there could be large error (e.g., as much as 60%) in the probability of failure, there is much less error (a few percent) in the reliability index.

## 2.3 Improved Methods

Although first-order methods are generally sufficiently accurate, it may be necessary or desirable to improve the accuracy, especially

when dealing with structural systems. Various computational methods have been proposed for obtaining improved estimates of the probability content of the failure region.

An obvious extension to first-order methods would be second-order approximations, whereby a quadratic surface is fitted to the failure surface (Fiessler, et al., 1979). This method requires the second derivatives of the performance function and may introduce difficulties in determining the probability content of quadratics; the method remains a single point checking method, i.e., the failure surface is being examined at only one point.

Ditlevsen (1979b) has suggested that the failure surface be approximated by linear failure surfaces at a number of points, e.g., the locally most dangerous points. System techniques (see Chapter 3) may then be used to obtain an estimate of the probability of failure. Another multiple point checking method is the control variable approach proposed by Grigoriu (1982) in which a polynomial is fitted to the failure surface at a number of points. The points on the failure surface that should be used are generally not obvious.

A number of methods have been developed in which the distribution of the performance function is approximated by another more tractable distribution. Generally, the first few moments of $g(\underline{X})$ are obtained, often through Monte Carlo simulations, and then a distribution is fitted with these moments. Parkinson (1980) suggests using the Johnson translation systems (Johnson, 1949). Grigoriu and Lind (1980) find the "best" linear combination of a number of distributions such that the first two moments agree and higher moments are estimated as accurately as possible. By fitting a polynomial to the performance function (Grigoriu, 1982), the moments of the performace function may easily be calculated, thus simplifying this method. Problems with these methods are that the lower tail of the performance function may not be accurately fitted as it requires large samples to obtain statistical accuracy in the higher moments.

Monte Carlo techniques, including variance reduction techniques, may also be used (Shinozuka, 1983). More details are given in Sect. 5.4.

Chen and Lind (1982) suggest that a scaled form of the normal distribution be substituted for the original distribution at the failure point. The method is limited essentially to independent random variables.

For system probability calculations, the failure surface may need to be approximated by a plane. If the above methods are used, the plane obtained using first-order methods can be shifted so that the distance from the origin to the plane is equal to the reliability index. In other words, the plane is shifted so the probability of failure evaluated on the basis of the planar failure surface is the same as the best estimate of the probability content of the true failure region. This is shown conceptually in Fig. 2.3. The shifted linear failure surface will be referred to as the equivalent (in terms of probability) linear failure surface.

Table 2.1 Accuracy of First-Order Methods: Nonnormal Variables

| Ref. | Performance Function | Distribution | First-Order | | Exact | | % Error | |
|---|---|---|---|---|---|---|---|---|
| | | | $P_F$ | $\beta$ | $P_F$ | $\beta$ | $P_F$ | $\beta$ |
| - | $X_1-X_2$ | $X_1$: Lognormal $X_2$: Normal | .00320 | 2.727 | .00296 | 2.752 | 8. | -0.9 |
| - | $X_1-X_2$ | $X_1$: Lognormal $X_2$: Ex. Type I | .00813 | 2.403 | .00839 | 2.392 | -3. | 0.5 |
| - | $X_1-X_2$ | $X_1$: Ex. Type III $X_2$: Ex. Type I | .01039 | 2.312 | .01290 | 2.229 | -19. | 3.7 |
| - | $X_1-X_2$ | $X_1$: Lognormal $X_2$: Gamma | .00539 | 2.550 | .00519 | 2.563 | 4. | -0.5 |
| - | $X_1-X_2$ | $X_1$: Lognormal $X_2$: Ex. Type II | .01133 | 2.279 | .01088 | 2.294 | 4. | -0.7 |
| a | $X_1-X_2$ | $X_1$: Normal $X_2$: Ex. Type I | .000089 | 3.75 | .000100 | 3.72 | -11. | 0.8 |
| a | $X_1-X_2$ | $X_1$: Normal $X_2$: Ex. Type I | .000095 | 3.73 | .000101 | 3.72 | -6. | 0.3 |
| b | $2-X_1-X_2$ | $X_1$: Normal $F(x_2) = x$; $x\varepsilon(0,1)$ | .0748 | 1.441 | .0807 | 1.401 | -7. | 2.8 |
| b | $2-X_1-X_2$ | $X_1$: Normal $F(x_2) = x^{1/3.52}$; $x\varepsilon(0,1)$ | .0440 | 1.706 | .0393 | 1.758 | 12. | -3.0 |
| b | $2-X_1-X_2$ | $X_1$: Normal $F(x_2) = x^{1/6}$; $x\varepsilon(0,1)$ | .0362 | 1.797 | .0271 | 1.925 | 34. | -6.6 |
| c | $5-X_1-X_2$ | $F(x_1,x_2) = 1-e^{-x_1}-e^{-x_2}+e^{-x_1-x_2}$ | .0246 | 1.97 | .0404 | 1.75 | -39. | 12.6 |
| c | $5-X_1-X_2$ | $F(x_1,x_2) = 1-e^{-x_1}-e^{-x_2}+e^{-x_1-x_2-x_1x_2}$ | .0113 | 2.28 | .0173 | 2.11 | -35. | 8.1 |

[a]From Dumonteil (1980)

[b]From Ditlevsen and Madsen (1980)

[c]From Hohenbichler and Rackwitz (1981)

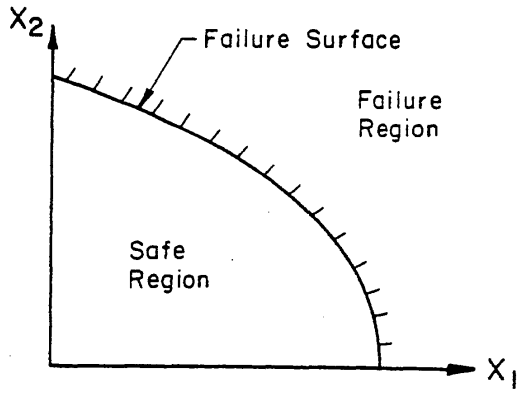


Fig. 2.1 Failure and Safe Regions in Design Space

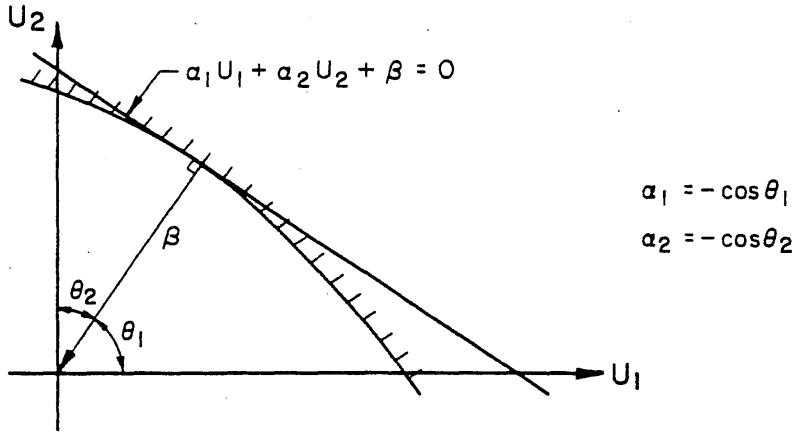


Fig. 2.2 Linearized Failure Surface

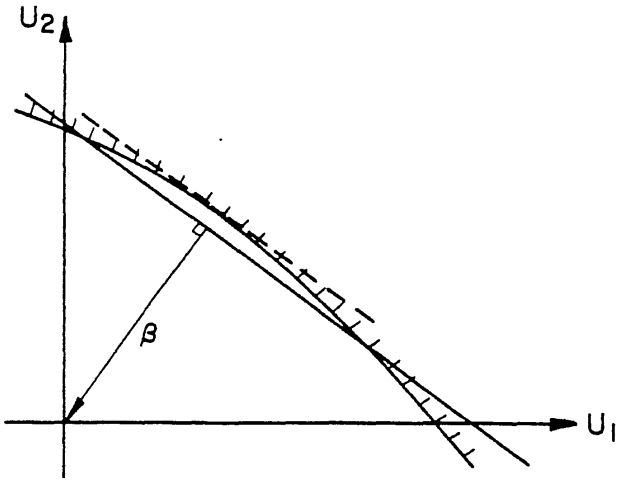


Fig. 2.3 Shifting of First-Order Plane

# CHAPTER 3

# PROBABILISTIC METHODS FOR SYSTEM RELIABILITY

The failure of a system may be formulated as the combination of unions and intersections of events. Each of the events represents the failure of a certain component or the occurence of a failure mode in a system. A union of events will result when the failure of any component leads to the failure of the system, whereas an intersection of events will result if the failure of the system requires the failure of all the components.

## 3.1 Union of Failure Events

### 3.1.1 Elementary Bounds

The determination of the exact probability of a union is generally difficult; it involves the multiple integration of joint density functions. Bounding methods may often be necessary. The simplest bounds are the uni-modal or first-order bounds as follows (Ang and Amin, 1967; Cornell, 1967):

$$\max\{P(E_i)\} \leq P(F) \leq \min\{\sum_{i=1}^{n} P(E_i), 1\} \tag{3.1}$$

where:

$E_i$ = failure event i;
$F = (E_1 \cup \ldots \cup E_n)$.

The lower bound represents the failure probability if all the events are

perfectly correlated, whereas the upper bound is the failure probability if all the the events are mutually exclusive. If all the events, $E_i$, are mutually positively dependent, i.e., $P(E_i|E_j) \geq P(E_i)$, the upper bound becomes

$$P(F) \leq 1 - \prod_{i=1}^{n} (1 - P(E_i)) \tag{3.2}$$

which is the failure probability for statistically independent events.

3.1.2 Second-Order Bounds

The first-order bounds could be very wide. Narrower bi-modal or second-order bounds are available (Kounias, 1968; Hunter, 1976) involving the pairwise intersection of all failure events. Although the derivation of these second-order bounds can be found elsewhere, a derivation similar to that of Ma and Ang (1981) and Ang and Tang (1983) is developed below.

The failure event, F, can be decomposed into mutually exclusive events as follows:

$$F = E_1 \cup \bar{E}_1 E_2 \cup \bar{E}_1 \bar{E}_2 E_3 \cup \ldots \cup \bar{E}_1 \bar{E}_2 \ldots \bar{E}_{n-1} E_n \tag{3.3}$$

The probability of failure, therefore, can be represented as

$$P(F) = P(E_1) + P(\bar{E}_1 E_2) + \ldots + P(\bar{E}_1 \bar{E}_2 \ldots \bar{E}_{n-1} E_n) \tag{3.4}$$

The probability of any event $E_i$, i=2,...,n, may be obtained as:

$$P(E_i) = P(\bar{E}_1 \ldots \bar{E}_{i-1} E_i) + P(\overline{\bar{E}_1 \ldots \bar{E}_{i-1}} E_i) \tag{3.5}$$

Therefore,

$$P(\bar{E}_1 \ldots \bar{E}_{i-1} E_i) = P(E_i) - P(\overline{\bar{E}_1 \ldots \bar{E}_{i-1} E_i})$$

$$= P(E_i) - P((E_1 \cup \ldots \cup E_{i-1}) E_i) \tag{3.6}$$

$$= P(E_i) - P(E_1 E_i \cup \ldots \cup E_{i-1} E_i)$$

Using the first-order bounds for $P(E_1 E_i \cup \ldots \cup E_{i-1} E_i)$, the second-order bounds are:

$$P(F) \begin{cases} \geq P(E_1) + \sum_{i=2}^{n} \min\{P(E_i) - \sum_{j=1}^{i-1} P(E_i E_j), 0\} & (3.7) \\ \leq \min\{\sum_{i=1}^{n} P(E_i) + \sum_{i=2}^{n} \max_{j<i}\{P(E_i E_j)\}, 1\} & (3.8) \end{cases}$$

Different improved bounds may be developed by applying higher-order bounds to $P(E_1 E_i \cup \ldots \cup E_{i-1} E_i)$. For example, if all the events are positively dependent, the pairwise intersections are positively dependent (Esary, et al., 1967) and Eq. 3.2 can be used to obtain a slightly closer lower second-order bound. Little improvement is usually observed beyond the second-order bounds (Hohenbichler and Rackwitz, 1983b). Using higher order bounds will eventually lead to Boole's formula (Johnson and Kotz, 1969).

For structural systems, where the probability of failure is usually very small, the second-order bounds will often be narrow enough for practical purposes. The closeness of the second-order bounds will depend on the ordering of the failure events. An algorithm is available (Hunter, 1976) for obtaining the sharpest upper bound as follows:

1. Determine $P^*(F) = \sum_i P(E_i)$.

2. Find the maximum of $\{P(E_1,E_i)\}$, $i>1$. Without loss of generality, assume that this occurs at $i=2$. Subtract $P(E_1 E_2)$ from $P^*(F)$ to obtain a sharper upper bound.
3. Find the maximum of $\{P(E_1 E_i),P(E_2 E_i)\}$, $i>2$. Again without loss of generality, assume that the maximum is $P(E_1 E_3)$. Subtract $P(E_1 E_3)$ from $P^*(F)$ to obtain a still sharper upper bound.
4. Continue the process, i.e., at step k subtract the maximum of $\{P(E_j E_i)\}$, $j\leq k$, $i>k$, where it is assumed that the maximum occurs at $i=k+1$.

Obviously each step improves the upper bound; the algorithm may be terminated at any point to give a valid upper bound.

The intersection of failure events is discussed in general in Sect. 3.2. For the case of normal distributions, simple bounds for the intersection of two events were proposed by Ditlevsen (1979b); using these bounds leads to a weaker version of the second-order bounds of Eqs. 3.7 and 3.8. If the individual events follow an extreme Type I distribution, Garson (1980) has given charts that can be used to determine the probabilities for the pairwise intersections; however, no information is given as to which of the various bivariate extreme Type I distributions (Johnson and Kotz, 1972) is appropriate.

### 3.1.3 Approximate Methods

A number of approximate methods (Vanmarke, 1973; Ang and Ma, 1979; Gorman and Moses, 1979) have been developed for obtaining point estimates of the probability of a union. The accuracy of these approximate methods, however, is difficult to assess. The geometric average of the second-order bounds may also be used as a suitable point estimate.

One approximate method that has a desirable feature is the PNET method (Ang and Ma, 1979). In the PNET method, events that have a high correlation, greater than $\rho_o$, are assumed to be perfectly correlated.

Thus, a number of groups of events can be developed; each group is represented by the event within that group with the highest probability of failure. It is then assumed that the representative events are statistically independent; Eq. 3.2 can then be used to determine the probability of failure. A value of 0.7 should be used for $\rho_o$, the demarcation correlation coefficient, for systems with a probability of failure on the order of $10^{-3}$, and $\rho_o = 0.8$ for systems with a probability of failure on the order of $10^{-4}$ or smaller (Ma and Ang, 1981).

The PNET method can be used to obtain a suitable point estimate if certain events are neglected provided they are highly correlated with other events. This is advantageous, especially if the events represent failure modes and it is possible to obtain some, but not necessarily all, of the significant modes.

## 3.2 Intersection of Failure Events

### 3.2.1 Elementary Bounds

As with the union of events, it will be difficult also to determine the exact probability of an intersection of events. Bounding methods are also available; however, the bounds for the intersection of multiple events will not, in general, be as close as the bounds for the union of events.

The first-order or elementary bounds for an intersection are:

$$\max\{1 - \sum_{i=1}^{n} (1 - P(E_i)), 0\} \leq P(F) \leq \min\{P(E_i)\} \tag{3.9}$$

where:

$$F = E_1 E_2 \ldots E_n .$$

The lower bound is invariably zero. The upper bound is exact if the

events are perfectly correlated. For positively dependent events, the lower bound becomes:

$$P(F) \geq \prod_{i=1}^{n} P(E_i) \tag{3.10}$$

The equality holds if the events are statistically independent.

3.2.2 Second-Order Bounds

Second and higher order bounds can be developed for the intersection of events. The second-order bounds are given below without derivation since the derivation is similar to that for the second-order bounds for the union of events.

$$P(F) \begin{cases} \geq \max\{\sum_{i=1}^{n} P(E_i) - \sum_{i=2}^{n} \min_{j<i}\{P(E_i \cup E_j)\},0\} & (3.11) \\ \leq P(E_1) + \sum_{i=2}^{n} \{\min\ i-2 + P(E_i) - \sum_{j=1}^{i-1} P(E_i \cup E_j),0\} & (3.12) \end{cases}$$

The best lower bound can be obtained through an algorithm similar to that for obtaining the best upper bound for the union of events. If the events are positively dependent, the upper bound becomes:

$$P(F) \leq P(E_1) + \sum_{i=1}^{n} \min\{P(E_i) - \prod_{j=1}^{i-1} P(E_i \cup E_j),0\} \tag{3.13}$$

The upper bound often reduces to:

$$P(F) \leq \min\{P(E_i) + P(E_j) - P(E_i \cup E_j)\} \tag{3.14}$$

This upper bound has been proposed as a suitable estimate for the probability of an intersection (Murotsu, et al., 1981a). Another upper bound for the intersection of events that takes into account three events is:

$$P(F) \leq P(E_i) + P(E_j) + P(E_k) - P(E_i \cup E_j) - P(E_i \cup E_k) - P(E_j \cup E_k) + P(E_i \cup E_j \cup E_k) \tag{3.15}$$

However, there is no assurance that this is better than Eq. 3.14.

## 3.3 Multivariate Normal Integral

### 3.3.1 Solutions for Special Cases

If all the underlying random variables follow the normal distribution, the solution for the system failure probability will involve the multivariate normal integral. Even though there are no general closed form solutions, this integral has been studied extensively and some useful results are available.

Consider n failure events as follows:

$$\begin{aligned} E_1&: \ \underline{\alpha}_1^t \underline{U} + \beta_1 < 0 \\ &\vdots \qquad\qquad \vdots \\ E_n&: \ \underline{\alpha}_n^t \underline{U} + \beta_n < 0 \end{aligned} \tag{3.16}$$

where:

$\underline{U}$ = standard normal variates;

$\underline{\alpha}_i$ = direction cosines;

$\beta_i$ = reliability index.

Define the new random variables,

$$Y_i = \underline{\alpha}_i^t \underline{U} \tag{3.17}$$

The $Y_i$'s will be normal with $\mu_{Y_i}=0.0$ and $\sigma_{Y_i}=1.0$; the correlation coefficient between $Y_i$ and $Y_j$ will be:

$$\rho_{ij} = \underline{\alpha}_i^t \underline{\alpha}_j^t \tag{3.18}$$

The probability of the intersection of the n failure events can be shown to be:

$$P(Y_1 < -\beta_1 \cap \ldots \cap Y_n < -\beta_n) = \Phi_n(-\beta_1,\ldots,-\beta_n ; \underline{\underline{C}}) \tag{3.19}$$

where $\Phi_n(.)$ is the n-dimensional multivariate normal integral with correlation coefficient matrix $\underline{\underline{C}}$.

The probability of the union of failure events can also be written in terms of the multivariate normal integral as follows:

$$\begin{aligned} &P(Y_1 < -\beta_1 \cup \ldots \cup Y_n < -\beta_n) \\ &\qquad = 1 - P(Y_1 > -\beta_1 \cap \ldots \cap Y_n > -\beta_n) \end{aligned} \tag{3.20}$$

By virtue of the symmetry of the normal distribution, Eq. 3.20 becomes

$$\begin{aligned} &1 - P(Y_1 > -\beta_1 \cap \ldots \cap Y_n > -\beta_n) \\ &\qquad = 1 - P(Y_1 < \beta_1 \cap \ldots \cap Y_n < \beta_n) \\ &\qquad = 1 - \Phi_n(\beta_1,\ldots,\beta_n ; \underline{\underline{C}}) \end{aligned} \tag{3.21}$$

The solution, therefore, to the multivariate normal integral would allow first-order reliability methods to be extended to systems.

Consider the special case where the $Y_i$'s can be written as:

$$Y_i = \lambda_i V + \sqrt{1 - \lambda_i^2}\, V_i \tag{3.22}$$

where the $V_i$'s and V are all statistically indpendent standard normal random variables. The correlation between $Y_i$ and $Y_j$ is thus:

$$\rho_{ij} = \lambda_i \lambda_j \tag{3.23}$$

The probability of the intersection of the failure events, therefore, is:

$$\Phi_n(-\beta_1,\ldots,-\beta_n ; \underline{\underline{C}}) = P[\bigcap_{i=1}^{n} (Y_i < -\beta_i)]$$

$$= P[\bigcap_{i=1}^{n} (V_i < \frac{-\beta_i - \lambda_i V}{\sqrt{1 - \lambda_i^2}})] \tag{3.24}$$

Using the theorem of total probability, we obtain

$$P[\bigcap_{i=1}^{n} (V_i < \frac{-\beta_i-\lambda_i V}{\sqrt{1-\lambda_i^2}})] = \int_{-\infty}^{\infty} P[\bigcap_{i=1}^{n} (V_i < \frac{-\beta_i-\lambda_i V}{\sqrt{1-\lambda_i^2}})] \,|V=v]P[V=v] \tag{3.25}$$

and by virtue of statistical independence of the $V_i$'s, the multivariate normal integral becomes

$$\Phi_n(-\beta_i,\ldots,-\beta_n;\underline{\underline{C}}) = \int_{-\infty}^{\infty} [\prod_{i=1}^{n} \Phi(\frac{-\beta_i-\lambda_i v}{\sqrt{1-\lambda_i^2}})]\ \phi(v)dv \tag{3.26}$$

where $\phi(v)$ is the probability density function of the standard normal distribution. Therefore, the multivariate normal integral is reduced to

a single integral if the correlation coefficients can be decomposed into the form $\rho_{ij} = \lambda_i \lambda_j$. When $\lambda_i$ approaches 1.0, numerical difficulties may arise; in this case, the integrand will approach a step function.

This special form of the multivariate normal integral has been derived by many researchers; one of the original derivations was by Dunnett and Sobel (1955). The result is valid also for negatively correlated normal variates; however, in such cases complex integration may be required.

### 3.3.2 Bivariate Normal Integral

Various numerical and series solutions have been proposed for the bivariate normal integral. A complete summary is given in Johnson and Kotz (1972). One of the better solutions seems to be that of Owen (1956); the solution is obtained through an infinite series that can be made to converge rapidly.

Bounds for the bivariate normal integral have also been developed (Ditlevsen, 1979b) as follows:

$$\max\{q_1, q_2\} \leq \Phi_2(-\beta_1, -\beta_2; \rho) \leq q_1 + q_2 \quad ; \quad \rho \geq 0 \tag{3.27}$$

$$0 \leq \Phi_2(-\beta_1, -\beta_2; \rho) \leq \min\{q_1, q_2\} \quad ; \quad \rho < 0 \tag{3.28}$$

where:

$$q_1 = \Phi(-\beta_1)\ \Phi\left(-\frac{\beta_2 - \rho\beta_1}{\sqrt{1-\rho^2}}\right)$$

$$q_2 = \Phi(-\beta_2)\ \Phi\left(-\frac{\beta_1 - \rho\beta_2}{\sqrt{1-\rho^2}}\right)$$

The bivariate normal integral is required in the second-order bounds of Eqs. 3.7 and 3.8. The bounds, of course, will be weakened if

the upper bound for the joint events is used in Eq. 3.7 and the corresponding lower bound in Eq. 3.8. The resulting weakened second-order bounds are close enough for reliability problems involving very small failure probabilities. However, for events with high correlations and/or large failure probabilities, it may be necessary to evaluate the exact bivariate integral in order to maintain tight bounds (Bennett and Ang, 1983).

### 3.3.3 Trivariate Normal Integral

Equation 3.26 can be used to solve the trivariate normal integral if the product of all the correlation coefficients is non-negative, and the product of any two correlation coefficients is less than the remaining one (Curnow and Dunnett, 1962). The solution is obtained by choosing the $\lambda_i$'s as follows:

$$\lambda_1 = \sqrt{\frac{\rho_{12}\,\rho_{13}}{\rho_{23}}} \quad ; \quad \lambda_2 = \sqrt{\frac{\rho_{21}\,\rho_{23}}{\rho_{13}}} \quad ; \quad \lambda_3 = \sqrt{\frac{\rho_{31}\,\rho_{32}}{\rho_{12}}}$$

For other cases, the following integral (Curnow and Dunnett, 1962) can be used in conjunction with a method for obtaining the bivariate normal integral.

$$\Phi_3(-\beta_1,-\beta_2,-\beta_3;\underline{\underline{C}}) = \int_{-\infty}^{-\beta_1} \Phi_2\left(\frac{-\beta_2-\rho_{12}u}{\sqrt{1-\rho_{12}^2}},\frac{-\beta_3-\rho_{13}u}{\sqrt{1-\rho_{13}^2}};\frac{\rho_{23}-\rho_{12}\rho_{13}}{\sqrt{1-\rho_{12}^2}\sqrt{1-\rho_{13}^2}}\right)\phi(u)\,du \tag{3.29}$$

where $\Phi_2(-\beta_i,-\beta_j;\rho)$ is the bivariate normal integral with correlation coefficient $\rho$.

### 3.3.4 Bounds Based on Slepians's Inequality

Slepians's inequality (Slepian, 1962) states that if $\underline{U}$ is a vector of standard normal variables with correlation coefficients $\rho_{ij}$, and $\underline{V}$ is another vector of standard normal variables with correlation coefficients $\tau_{ij}$, such that $\rho_{ij} \geq \tau_{ij}$ for all (i,j), then

$$P[\bigcap_{i=1}^{n} (U_i \leq -\beta_i)] \geq P[\bigcap_{i=1}^{n} (V_i \leq -\beta_i)] \tag{3.30}$$

This inequality can be used with Eq. 3.26 to bound the multivariate normal integral. The $\lambda_i$'s in Eq. 3.26 are chosen such that $\lambda_i \lambda_j \leq \rho_{ij}$ to obtain a lower bound to the multivariate normal integral. Choosing the $\lambda_i$'s such that $\lambda_i \lambda_j \geq \rho_{ij}$ will result in an upper bound to the multivariate normal integral.

There is no particular method for determining the $\lambda_i$'s so that the sharpest bounds are obtained. One way is simply to use

$$\lambda_i = \sqrt{\min_j \{\rho_{ij}\}} \quad ; \quad i \neq j \tag{3.31}$$

for the lower bound, whereas for the upper bounds use

$$\lambda_i = \sqrt{\max_j \{\rho_{ij}\}} \quad ; \quad i \neq j \tag{3.32}$$

These values can be improved by setting:

$$\lambda_i = \min_j \{\frac{\rho_{ij}}{\lambda_j}, 1\} \quad ; \quad i \neq j, \lambda_j \neq 0 \tag{3.33}$$

for the lower bound, whereas for the upper bound,

$$\lambda_i = \max_j \{\frac{\rho_{ij}}{\lambda_j}\} \quad ; \quad i \neq j, \lambda_j \neq 0 \qquad (3.34)$$

If some of the correlation coefficients are negative, it is possible to obtain an upper bound without complex integration, for example, by setting $\lambda_i = 0.0$ in Eq. 3.32 if the maximum correlation coefficient is negative. This bounding technique will be referred to as the MVNI (multivariate normal integral) bounds throughout this study.

### 3.3.5 First-Order Solution

An approximate solution to the multivariate normal integral has been suggested (Hohenbichler, 1981; Hohenbichler and Rackwitz, 1983b) based on first-order approximations for the conditional probabilities.

The multivariate normal integral may be separated into two parts as follows:

$$\Phi_n(-\underline{\beta}; \underline{\underline{C}}) = P[\bigcap_{i=2}^{n} (Y_i < -\beta_i) | (Y_1 < -\beta_1)] P[Y_1 < -\beta_1] \qquad (3.35)$$

It can be shown that

$$P[\bigcap_{i=2}^{n} (Y_i < -\beta_i) | (Y_1 < -\beta_1)]$$

$$= P[\bigcap_{i=2}^{n} (\rho_{il} \Phi^{-1}(\Phi(-\beta_1)\Phi(U_1)) + \sqrt{1 - \rho_{il}^2}\, U_2 + \beta_i < 0] \qquad (3.36)$$

$$= P[\bigcap_{i=2}^{n} (g_i(U_1, U_2) < 0)]$$

where $(U_1, U_2)$ are a pair of independent standard normal variables. First-order methods are then used to linearize $g_i(U_1, U_2)$; i.e.,

$$g_i(U_1, U_2) \approx \alpha_{i1} U_1 + \alpha_{i2} U_2 + \beta_i^{(2)} \tag{3.37}$$

New normal variables are then developed as follows:

$$Y_i^{(2)} = \alpha_{i1} U_1 + \alpha_{i2} U_2 \tag{3.38}$$

$$\rho_{ij}^{(2)} = \alpha_{i1} \alpha_{j1} + \alpha_{i2} \alpha_{j2} \tag{3.39}$$

Using these in Eq. 3.36 yields,

$$\begin{aligned} P[\bigcap_{i=2}^{n} (Y_i < -\beta_i) | (Y_1 < -\beta_1)] &= P[\bigcap_{i=2}^{n} (Y_i^{(2)} < -\beta_i^{(2)})] \\ &= \Phi_{n-1}(-\beta^{(2)} ; \underline{\underline{C}}^{(2)}) \end{aligned} \tag{3.40}$$

The process, therefore, reduces the standard normal integral by one dimension.

$$\Phi_n(-\underline{\beta}; \underline{\underline{C}}) = \Phi_{n-1}(-\underline{\beta}^{(2)} ; \underline{\underline{C}}^{(2)}) \Phi(-\beta_1) \tag{3.41}$$

The algorithm can be repeated to further reduce the dimension of the multivariate normal integral.

For $\rho_{i1} \geq 0$, the "failure region,", i.e., $g_i(U_1, U_2) < 0$, will be concave (see Fig. 3.1) meaning the linearization underestimates the true conditional probability. Therefore, if $\rho_{i1} \geq 0$ for all i throughout the algorithm, the solution obtained will be an unconservative (or lower bound) estimate of the multivariate normal integral.

Improvements in the above algorithm have been proposed (Hohenbichler, 1981). However, results outside the second-order bounds are possible, and the method may have limitations when applied to practical problems.

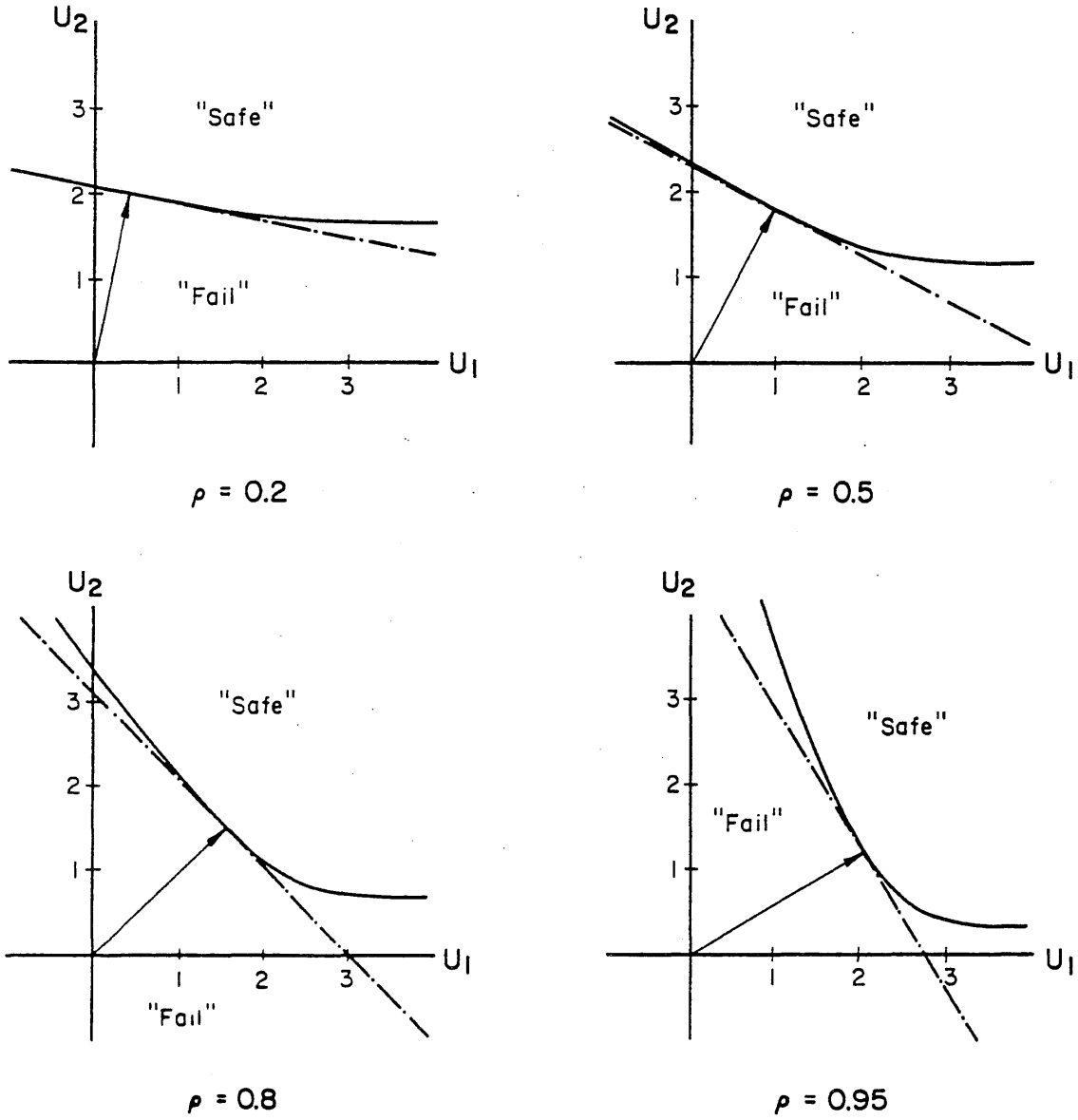


$\rho\,\Phi^{-1}(\Phi(2.0)\,\Phi(U_1)) + \sqrt{1-\rho^2}\,U_2 - 2.0 = 0$ (Eq. 3.36)

$\alpha_1 U_1 + \alpha_2 U_2 + \beta^{(2)} = 0$ (Eq. 3.37)

Fig. 3.1 "Failure Surfaces" for Conditional Probabilities

# CHAPTER 4

# FORMULATIONS OF STRUCTURAL SYSTEM RELIABILITY

## 4.1 Introductory Comments

Most structural systems are redundant systems. Redundancy in structural systems will generally be of the active type, i.e., all the components participate actively in carrying the load (load-sharing system). Standby redundancy, where certain components are activated only after others have failed, rarely exists in structural systems.

The failure of any member of a non-redundant structure is tantamount to collapse of the structure. The probability of system failure is, therefore, the probability of the union of the individual member failure events. A system with standby redundancy will fail only if the redundant components fail. The probability of failure is the probability of the intersection of the individual failure events. The formulation of the probability of failure for systems with active redundancy may be much more involved. The failure of a member causes the load to be redistributed; the redistribution depends on the congiguration of the system components and the nature of the component failure.

Two methods for obtaining the probability of failure (collapse) of structural systems with active redundancy will be formulated; namely, the failure mode approach and the stable configuration approach. Simplifications and approximations for a class of structures will also be developed.

## 4.2 Failure Graphs

The formulation of the reliability of a structural system is aided through the use of graph theory (Henley and Williams, 1973). A directed graph, or directed network, can be constructed of all possible sequences of component failures that will lead to some limit state. This will be called a failure graph; a typical failure graph is shown in Fig. 4.1. Each node of the failure graph (except the terminal node) represents a stable configuration of the structure; that is, any combination of the components of the original structure that is geometrically and statically stable under the applied load. The initial node represents the structure with no failed components and the terminal node represents the prescribed limit state. Each branch in the failure graph represents a component failure. A path is a set of branches connecting the initial and terminal nodes, and thus represents a sequence of component failures. A set of branches containing one and only one branch from every path is called a cut. A cut, therefore, will be crossed only once for any path between the initial node and the terminal node.

Fault trees may also be used to identify potential problems and failures in structural systems (Pinjarkar, 1979). Methods are available for obtaining the failure paths from the fault tree (Barlow and Proschan, 1975; Locks, 1978), and thus the failure graph may also be constructed through the corresponding fault tree.

## 4.3 Conceptual Models

### 4.3.1 Failure Mode Approach

The probability of failure of a structure may be obtained by considering all possible failure modes (Ang and Amin, 1967). In this regard, each path of the failure graph represents a failure mode. Obviously, if the structure fails in any mode it is no longer capable of carrying the load and thus the structure has failed. Therefore, the

failure event of the structural system is the union of the events representing failures in the respective modes, i.e., if any path from the initial node to the terminal node of the failure graph is realized, the system has failed. Thus, the probability of failure of the system may be obtained as:

$$P_F = P[M_1 \cup M_2 \cup \ldots \cup M_n] \tag{4.1}$$

where $M_i$ is the failure of the $i^{th}$ mode. A path will occur only if all the branches comprising the path fail, i.e., the structure cannot carry the load in any of the stable configurations that are represented by the nodes along the pertinent path. In other words, failure through a given mode is the intersection of the failures of all the branches along the pertinent path. Therefore, the probability of failure of mode i is

$$P[M_i] = P[B_{i1} B_{i2} \ldots B_{im}] \tag{4.2}$$

where $B_{ij}$ is the failure of the $j^{th}$ branch in the $i^{th}$ path. For a branch to fail, both the limit state for the component represented by the branch must be exceeded <u>and</u> the structure must be such that it will fail through that branch, i.e.,

$$P[B_{ij}] = P[(g_{ij}(\underline{X}) < 0) \cap (\underline{X} \in F_{ij})] \tag{4.3}$$

where:

$\underline{X}$ = vector of basic variables;

$g_{ij}(\underline{X})$ = performance function for the component represented by branch j in path i;

$F_{ij}$ = set of random variables such that if structure fails, it will fail through branch ij.

The event that a structure will actually fail along a certain branch may be referred to as the constraints on the random variables. It should be noted that the event $(\underline{X} \in F_{ij})$ is the constraint that failure will occur

along branch j as opposed to any other branch emanating from the begining node of branch j. The probability that the structure will fail along path i is thus:

$$P[\underline{X} \in F_i] = P[\bigcap_{j=1}^{m} (\underline{X} \in F_{ij})] \tag{4.4}$$

If the structure fails, it will fail only through one mode; hence, the events in Eq. 4.1 are mutually exclusive and the probability of failure may be obtained as:

$$P_F = P[M_1] + P[M_2] + \ldots + P[M_n] \tag{4.5}$$

The constraints are often difficult to obtain. They may depend on how the loads are applied to the structure (i.e., the loading paths). Also, the constraints will often contain both unions and intersections creating further difficulties in the probabilistic calculations.

In short, the failure mode approach results in the probability of failure being obtained as the union of events (the failure modes) that are composed of the intersection of events (i.e., all the branches in the pertinent path fail).

### 4.3.2 Stable Configuration Approach

The probability of survival of a system may be obtained by considering all possible cuts of the failure graph. If the components represented by the branches in a cut survive, the structure survives; in other words, there is no possible path from the initial node to the terminal node. Thus, the event that the structure survives may be obtained as the union of all the events representing the surviving cuts, i.e.,

$$P_S = P[\bar{C}_1 \cup \bar{C}_2 \cup \ldots \cup \bar{C}_n] \tag{4.6}$$

where $\bar{C}_i$ represents the survival of cut i. The survival of a cut is the intersection of the survivals of all the branches in the cut; in other words, if a branch fails, there may exist a possible path from the initial node to the final node of the failure graph. Thus,

$$P[\bar{C}_i] = P[\bar{B}_{i1}\bar{B}_{i2}\ldots\bar{B}_{im}] \tag{4.7}$$

where $\bar{B}_{ij}$ is the event that the $j^{th}$ branch of the $i^{th}$ cut survives. A branch will survive if either the component represented by the branch can carry the applied load or another component will fail first. Therefore, the probability that a branch survives is:

$$P[\bar{B}_{ij}] = P[(g_{ij}(\underline{X})>0) \cup (\underline{X} \notin F_{ij})] \tag{4.8}$$

Applying de Morgans's rule to Eq. 4.6, we obtain the probability of failure of a system as

$$P_F = P[C_1C_2\ldots C_n] \tag{4.9}$$

Similarly, by de Morgan's rule, Eq. 4.7 yields

$$P[C_i] = P[B_{i1} \cup B_{i2} \cup \ldots \cup B_{im}] \tag{4.10}$$

Finally, applying de Morgan's rule once more, a branch failure can be obtained as the intersection of events that the limit state of the component has been exceeded and the component fails before other components, i.e., Eq. 4.3.

It is not always necessary to include the constraints on a component failure. The constraints on a component need to be included only if the structure can survive in the manner represented by the cut even if the limit state for the component has been exceeded. In other words, a constraint that the component failure represented by one branch of the failure graph occurs before the failure of another branch does not need to be included if both branches are included in the cut. This

may be seen by examining Eqs. 4.7 and 4.8. If $g_{ij}(\underline{X})<0$ but $(\underline{X} \notin F_{ij})$, then branch j survives. However, if $(\underline{X} \in F_{ik})$, where k is another branch in cut i, then since $g_{ij}(\underline{X})<0$, $g_{ik}(\underline{X})<0$ also and branch k fails. Therefore, the constraint that branch k fails before branch j does not have to be included since if $g_{ij}(\underline{X})<0$ and $(\underline{X} \in F_{ik})$, branch k will fail and thus the cut will fail.

The cuts are related to the stable configurations of the structure. If no cut survives, then the structure cannot carry the load through any stable configuration. The stable configuration approach, therefore, is based on the cuts of the failure graph to determine the system probability of failure.

The stable configuration approach has been implicitly the basis for some previous studies. Ishizawa (1968) determined the probability that a structure would go from one configuration to another. The Markov chain was used to determine the system probability of failure. Augusti and Baratta (1972) developed an upper bound to the probability of failure of ductile frames by examining statically admissible moment diagrams. Each statically admissible moment diagram would correspond to a cut in the failure graph.

In short, with the stable configuration approach, the probability of failure is obtained as the intersection of events (failures of the cuts) each of which is composed of the union of component failure events (i.e., at least one of the branches in the cut fails).

### 4.3.3 Examples

Example 4.1--Consider the three member parallel system shown in Fig. 4.2. The load-deformation characteristics of the members are shown in Fig. 4.6. It is assumed that members 1 and 3 will fail in a brittle manner, whereas member 2 will fail in a ductile manner. Assume also that the members share the load equally.

The failure graph for this structure is shown in Fig. 4.3 and the corresponding stable configurations in Fig. 4.4. There are six possible paths in the graph of Fig. 4.3, each composed of three branches. The

failure sequence of member 1 failing, member 2 failing, and member 3 failing is represented by the first path in Fig. 4.3. The graph contains eight nodes. Node 1 represents the initial configuration (configuration 1 in Fig. 4.4) of the structure. Some of the possible cuts of the failure graph are shown in Fig. 4.5.

Examine the first branch of path 1. From Eq. 4.3, the probability of failure of this branch is

$$P[B_{1A}] = P[(R_1 - \frac{P}{3}<0) \cap (R_1<R_2)(R_1<R_3)]$$

where $R_1 - P/3<0$ is the event that the limit state of member 1 is exceeded and $(R_1<R_2)(R_1<R_3)$ are the constraints on the random variables, i.e., the event that member 1 will fail before members 2 and 3. The failure probability of the other branches may be obtained in a similar manner; the resulting probability of failure of path 1 is then

$$P[M_1] = P[(R_1 - \frac{P}{3}<0)(R_2 - \frac{P}{2}<0)(R_3+R_2-P<0)(R_1<R_2)(R_1<R_3)(R_2<R_3)]$$

Corresponding expressions can be developed for the other paths and Eq. 4.5 used to obtain the system probability of failure.

Using the stable configuration approach would require consideration of all possible cuts of the failure graph. For the failure graph shown in Fig. 4.3, there are 18 possible cuts. Consider cut b-b in Fig. 4.5. The probability that cut b-b fails is obtaind using Eq. 4.10 as

$$P[C_{b-b}] = P[(R_2 - \frac{P}{2}<0)(R_2<R_3) \cup (R_3 - \frac{P}{2}<0)(R_3<R_2)$$
$$\cup (R_2 - \frac{P}{3}<0)(R_2<R_1)(R_2<R_3) \cup (R_3 - \frac{P}{3}<0)(R_3<R_1)(R_3<R_2)]$$

However, some of the constraints may be eliminated as discussed earlier. For example, consider the first branch in the cut. The constraint, $R_2<R_3$, implies that this branch fails before the other branch emanating from the same node. This branch is also included in the cut so the constraint is not necessary and may be eliminated. Similar arguments hold for some of the other constraints and the probability of failure of

the cut may be simplified to

$$P[C_{b-b}] = P[(R_2 - \frac{P}{2}<0) \cup (R_3 - \frac{P}{2}<0) \cup (R_2 - \frac{P}{3}<0)(R_2<R_1) \cup (R_3 - \frac{P}{3}<0)(R_3<R_1)]$$

Similar expressions may be developed for all the other cuts and Eq. 4.9 used to obtain the failure probability of the system.

Example 4.2--A simple frame subjected to horizontal and vertical loads $S_1$ and $S_2$ is shown in Fig. 4.8. The resulting moments at the critical sections are also shown. Depending on the magnitudes of the loads, the bending moments at sections 2 and 3 could be in the positive direction, as shown, or in the opposite (negative) direction. Assume that when the moment capacity at a section is exceeded the resistance drops to zero, i.e., failure is brittle. The corresponding failure graph is shown in Fig. 4.9 along with all possible cuts. Six possible failures could occur first. Two involve the moment capacity at section 1 $(M_1^-)$ being exceeded and the moment capacity at section 2 $(M_2^-)$ being exceeded. The respective performance functions for these events are:

$$g_1 = (M_1^-) - \frac{15}{16}S_1 - \frac{75}{8}S_2$$

$$g_2^- = (M_2^-) - \frac{15}{16}S_1 + \frac{45}{8}S_2$$

For the values of the random variables, $s_1$=70.0, $s_2$=4.0, $m_1$=98.0, and $m_2^-$=40.0, both $g_1$ and $g_2^-$ will be less than zero. Which of the two sections will fail first depends not only on the values of the random variables but also on how the structure is loaded. Three conceivable loading paths are shown in Fig. 4.10. For path A, the horizontal load increases from zero to $s_2$=4.0, and then the vertical load increases from zero to $s_1$=70.0. In path B the vertical load is applied first and then the horizontal load; whereas in path C the load is increased along the

line $S_2 = 0.0587S_1$ until either $s_1$ or $s_2$ is reached and then the other load is increased to its given value.

If the structure is loaded along path A, section 1 will fail before section $\bar{2}$, whereas if loading occurs along path B, section $\bar{2}$ will fail before section 1. Path C acts as a demarcation path. Loading paths above path C will cause section 1 to fail first and loading paths below path C will cause section $\bar{2}$ to fail first.

Assuming that the structure is loaded along path B, all failure modes for which section 1 fails first will contain the constraints:

$$(M_1 < M_2 -) \cup (M_2 - > \frac{15}{16} S_1)$$

whereas all failure modes for which section $\bar{2}$ fails first will contain the constaints:

$$(M_2 - < M_1)(M_2 - < \frac{15}{16} S_1)$$

This example shows the complicated nature of the constraints for even a simple structure. Therefore, considerable simplification would ensue if these constraints can be neglected without introducing significant error.

## 4.4 Monotonically Loaded Structures

### 4.4.1 Definition

A structure is monotonically loaded if the load on a surviving member never decreases following the failure of other members. In terms of the performance function, if the limit state for two components is exceeded, then the limit state for either component after the other has failed will also be exceeded. The structure considered in Example 4.1 is obviously monotonically loaded since the load on any surviving member does not decrease with failures of other members. Examining the

performance functions for the initial failure of members 1 and 2, it is seen that if $R_1-P/3<0$ and $R_2-P/3<0$ then $R_1+R_2/2-P/2<0$ and $R_1-P/2<0$.

4.4.2 Formulation of Failure Modes

For a monotonically loaded structure, the formulation of the failure modes may be simplified. In particular, the constraints do not need to be specified, and thus the probability of failure of such a system, Eq. 4.1, is reduced to:

$$P_F = P[(g_1(\underline{X}) < 0) \cup \ldots \cup (g_n(\underline{X}) < 0)] \tag{4.11}$$

where $g_i(\underline{X})$ is the performance function for mode i. The failure modes, however, are no longer mutually exclusive. Moreover, the mutual correlations between the modes may be important in the determination of the system failure probability.

The constraints are not necessary for mode i if the limit state for some other mode is not exceeded, i.e., $g_j(\underline{X})\not<0$, $i \neq j$, when $g_i(\underline{X})>0$, given that the structure will fail through mode i. In other words, if the structure fails through mode i, $g_i(\underline{X})<0$ should occur first as the load is applied. Otherwise, Eq. 4.11 would indicate that the structure has failed when actually no failure has occured. This may be illustrated using a portion of the failure graph shown in Fig. 4.3. The proof for a more complicated monotonically loaded structure would follow similar but lengthier arguments.

Consider branches 1B, 1C, 2B, and 2C of the failure graph in Fig. 4.3. Assume that $\underline{X}$ corresponds to the structure failing through the sequential failures of member 2 and then member 3 after member 1 fails. Assume also that $g_{1A}<0$ and that either $g_{1B}>0$ or $g_{1C}>0$ (mode 1 survives) while $g_{2B}<0$ and $g_{2C}<0$ (mode 2 fails), i.e. it is necessary to include the constraints. Since $\underline{X}$ is such that the structure will fail through mode 1, it means, among other things, that if $g_{2B}<0$ then $g_{1B}<0$. Due to monotonic loading, if both $g_{1B}<0$ and $g_{2B}<0$ then $g_{1C}<0$. Both $g_{1B}<0$ and $g_{1C}<0$ is a contradiction of the postulated situation (mode 1

survives) and, therefore, it is not necessary to include the constraints.

Elastic-plastic frames and trusses have been the subject of many reliability studies (e.g., Jorgenson and Goldberg, 1969; Stevenson and Moses, 1970; Gorman and Moses, 1979; Ang and Ma, 1981; Murotsu, et al., 1981a) Strictly speaking, this type of structure may not be monotonically loaded since a section may yield in one sense (e.g., positive moment) as the load is applied but end up yielding in the other sense (e.g., negative moment) in the final collapse mechanism. However, the structure may be treated as monotonically loaded if it is assumed that there is no hysteresis in the behavior. Therefore, consideration of the plastic collapse mechanisms without any constraints on how the structure will actually fail will give the correct probability of failure, as all past studies have implicitly assumed.

### 4.4.3 Formulation of Cuts

No constraints are necessary in the stable configuration formulation for monotonically loaded structures. To show this, consider cut b-b in Fig. 4.5. The probability that at least one branch in this cut fails is obtained as (see Sect. 4.3.3):

$$P[C_{b-b}] = P[(g_{3A}<0)(\underline{X}\varepsilon F_{3A})\cup(g_{5A}<0)(\underline{X}\varepsilon F_{5A})\cup(g_{1B}<0)\cup(g_{2B}<0)] \quad (4.12)$$

where:

$F_{3A}$ = set of random variables for which member 2 fails before member 1;

$F_{5A}$ = set of random variables for which member 3 fails before member 1.

To show that the constraint $(\underline{X}\varepsilon F_{3A})$ is not necessary, it is sufficient to demonstrate that if $(\underline{X}\notin F_{3A})$ but $g_{3A}<0$, then one of the other events must occur. If $\underline{X}$ is such that member 1 fails first then $g_{1A}<0$ if $g_{3A}<0$. If $g_{1A}<0$ and $g_{3A}<0$, then $g_{1B}<0$ due to the monotonic loading. Thus,

another event in the cut must occur and the constraint is not necessary. Likewise, it can be shown the the constraint ($\underline{X} \in F_{5A}$) is not necessary. Similar proofs may be constructed for all the other cuts.

Actually, only seven of the cuts, those indicated in Fig. 4.5, are necessary to obtain the correct probability of failure. For a cut to be necessary, it must be possible for all the branches in the cut to survive while at least one branch in all the other cuts fails. Otherwise, the failure region of the cut would be entirely contained in the intersection of the failure regions of the other cuts. Consider the cut containing branches 1A, 3B, 4B, 5B, and 6B. If all the branches in this cut survive but at least one branch in cut c-c fails, then $g_{3A}<0$. Similarly, if at least one branch in cut d-d fails, then $g_{5A}<0$. Due to the monotonic loading, if $g_{3A}<0$ and $g_{5A}<0$, then $g_{4B}<0$ and $g_{6B}<0$. Therefore, not all the branches in the specified cut can survive while at least one branch in all the other cuts fails, and thus the cut is not necessary. Similar arguments may be applied for all the other cuts not shown in Fig. 4.5.

The above arguments may be generalized to the failure graph of any monotonically loaded structure. The essence is that if a member cannot carry the applied load in a certain stable configuration, then it cannot carry the same load in any other stable configuration derived from the first configuration with additional failed members. Therefore, the necessary cuts may be obtained by identifying all possible combinations of members that will carry the load, i.e., the members in each stable configuration. The necessary cuts are then obtained by cutting through the branches that represent the failure of these members in any configuration of which they are a part. Consider configuration 2 in Fig. 4.4, which is composed of members 2 and 3. The only other configuration of which members 2 and 3 are both a part is configuration 1. Cutting through the branches representing failure of member 2 and 3 in configurations 1 and 2 (see Figs. 4.3 and 4.5) yields cut b-b, and thus cut b-b is a necessary cut.

### 4.4.4 Relationships Between Formulations

The failure mode approach and the stable configuration approach are dual formulations of each other. The failure mode approach is based on ways in which the structure can fail. It approaches the probability of failure from below, i.e., as more potential failure modes are included, the probability of failure will increase and approach the true probability of failure. Conversely, the stable configuration approach is based on configurations of the structure that can carry the load. It approaches the probability of failure from above, i.e., as more cuts are included, the probability of failure will decrease and approach the true probability of failure. If all failure modes and all stable configurations are included, the two methods should yield the same result. One formulation may be obtained from the other through the use of the distributive properties of sets. The failure mode approach leads to a union of intersections, whereas the stable configuration approach involves the intersection of unions.

Neither method has provision to guard against missing potential failure modes. If the potential failure of certain components is not included in the analysis, both methods will err on the uncovservative side, i.e., not including certain components in the formulation is tantamount to assuming that the probability of failure of the component is zero, and thus is unconservative.

The stable configuration approach and the failure mode approach are embedded in each other. The stable configuration approach is used in the analysis of each failure mode; a particular failure mode will occur only if all the configurations along the path representing the mode fail. Conversely, the failure mode approach is used in analyzing each stable configuration; a cut fails if any of the failure modes contained in the cut fails. This embedding is observed also in other studies (e.g., Der Kiureghian and Moghtaderi-Zadeh, 1982; Rackwitz and Peintinger, 1982). For complex problems, it may prove useful to subdivide the failure graph and analyze different parts by different methods.

### 4.4.5 Minimal Forms

A minimal form is a formulation in which there are no superfluous failure modes or cuts, i.e., there is no event in the formulation that is not necessary. A failure mode is necessary only if the limit state for that mode is exceeded without exceeding the limit state of any other mode, i.e., the mode can fail while all the other modes survive. A cut is necessary only if all the performance functions for the branches in the cut can be greater than zero while at least one performance function for a branch in all the other cuts is less than zero, i.e., the cut can survive while all the other cuts fail. Reduction of a formulation to minimal form will normally result in less computational effort. Unfortunately, no unique minimal form may exist and the reduction to a minimal form may be complicated (Locks, 1978).

In general, reducing to the minimum failure modes can be accomplished through the principle of absorption, i.e., $P[(AB)\cup A)]=P[A]$. For example, when analyzing ductile frames, it is not necessary to include failure modes with hinges that are not part of the collapse mechansism (Murotsu, et al., 1981b) as they will be absorbed by a failure mode that includes only the hinges in the collapse mechanism.

Reducing the stable configurations to minimal form is generally more difficult and requires more than the absorption rule. Two examples will be examined in Sect. 4.4.7. The examples show that the consideration of the plastic collapse mechanisms for ductile structures leads to the minimal form.

### 4.4.6 Physical Interpretations

The physical meaning of a failure mode is straightforward, it is a representation of a given limit state of a structure. The physical interpretation of a cut, however, is less obvious. It represents a configuration derived from the original structure that may carry the load. Consider cut e-e in Fig. 4.5 and the stable configurations shown in Fig. 4.4. Cut e-e corresponds to configuration 7. The cut will fail

if either the structure cannot carry the load in this configuration or the structure never reaches this particular configuration. The structure will not reach configuration 7 if any of the following occurs: member 1 fails in configuration 1, member 1 fails in configuration 3, or member 1 fails in configuration 4. Of course, the cut will also fail if the structure cannot carry the load in configuration 7, i.e., member 1 fails.

4.4.7 Examples

Example 4.3--Consider the monotonically loaded two member system shown in Fig. 4.11. The load-deformation curve for the members is shown in Fig. 4.12, where k and $\alpha$ are deterministic constants. The resistance of a member after it has failed, i.e., reached the maximum load carrying capacity is:

$$R = \max \{- \alpha k (\delta - \delta_y) + R_i, 0\}$$

The probability of failure of one of the two modes, namely member 1 failing followed by member 2 failing, is:

$$P[M_1] = P[(R_1 - \frac{P}{2} < 0)(\max \{- \alpha(R_2 - R_1) + R_1, 0\} + R_2 - P < 0]$$

Consider $\alpha=0$, which corresponds to perfectly elastic-plastic behavior. For mode 1 to occur, $R_1<R_2$. Therefore if $R_1+R_2-P<0$ then $R_1-P/2<0$ and mode 1 reduces to $P[R_1+R_2-P<0]$. Mode 2 would also yield the same result. Thus the system probability of failure is the well known result, $P[R_1+R_2-P<0]$. For $0<\alpha<1$, the probability of failure of the first mode reduces to

$$P[M_1] = P[(- \alpha(R_2 - R_1) + R_1 + R_2 - P < 0)(R_2 - P < 0)]$$

whereas if $\alpha>1$, mode 1 becomes $P[(R_1-P/2<0)(R_2-P<0)]$. It may be observed that in this case, i.e., $\alpha>1$, the probability of failure is no

longer a function of $\alpha$ and in fact leads to the same formulation as for ideal brittle behavior.

Example 4.1 (continued)--Because of the ductile behavior of member 2, the failure graph of Fig. 4.3 may be reduced to that of Fig. 4.7, i.e., each mode is reduced to its minimal form. Based on the stable configuration approach, the probability of failure becomes:

$$P_F = P[\{(R_1 - \frac{P}{3}<0) \cup (R_1 + \frac{R_2}{2} - \frac{P}{2}<0) \cup (R_3 + \frac{R_2}{2} - \frac{P}{2}<0) \cup (R_3 - \frac{P}{3}<0)\}$$

$$\{(R_1+R_2-P<0) \cup (R_1 - \frac{P}{2}<0)\}\{(R_3+R_2-P<0) \cup (R_3 - \frac{P}{2}<0)\}\{R_2-P<0\}]$$

The cuts that correspond to this formulation are also shown in Fig. 4.7. Observe that some of the cuts (three of them) in the earlier stable configuration approach (Sect. 4.4.3) have been eliminated. For example, consider cut a-a: it is easy to show that it is not part of the minimal form. If all the branches in cut a-a survive, then all the branches in cut c-c will also survive, i.e., if $R_1-P/3>0$, $R_2-P/3>0$, and $R_3-P/3>0$ then $R_1+R_2/2-P/2>0$ and $R_3+R_2/2-P/2>0$. No performance function in cut c-c can be less than zero if the performance functions for all the branches in cut a-a are greater than zero.

## 4.5 General Structures

### 4.5.1 Remarks

The simplifications discussed above for monotonically loaded structures may not apply for non-monotonically loaded structures. In particular, the constraints may need to be specified in the formulations to obtain the exact probability of failure.

The probability of failure for general structural systems may depend on the loading path. Proportional loading is often assumed (e.g., Augusti and Baratta, 1972; Klingmuller, 1981; Moses, 1982);

however, this may not be entirely realistic. It may be possible to intuitively determine a reasonable loading path. For instance, in Example 4.2, if $S_1$ is a combined dead load and live load, and $S_2$ is a wind loading, then it seems reasonable to assume the loading path would follow closely that of loading path B in Fig. 4.10, i.e., load $S_1$ is first imposed on the structure and then load $S_2$.

4.5.2 Conservative Approximations

The formulation for monotonically loaded structures, i.e., not taking into account the constraints, may be used to obtain a conservative estimate of the probability of failure of general structural systems. Examining the two formulations for the failure mode approach, Eqs. 4.1 and 4.11, it can be observed that the probability of failure as obtained with Eq. 4.11 is greater than or equal to the probability of failure obtained with Eq. 4.1. Physically, this is because if the limit state for a component is exceeded, the component may still not fail if another component fails first causing the load on the component under consideration to decrease.

Care, therefore, must be taken when there are counteracting loads, such as when a load effect is acting as a "resistance". Whether or not a section will fail obviously depends on how the loads are applied. The possibility of the full counteracting load not being present needs to be included in the formulation when obtaining an estimate of the probability of failure without the constraints. Otherwise, the resulting estimate may not be conservative. Generally, however, counteracting loads will not be a practical problem since the loads may act together instead of counter to each other (e.g., wind induced moments acting counter to gravity moments in a frame). The probability of failure with the loads acting counter to each other will often be insignificant.

The stable configuration approach, without including the constraints, may also be used to obtain a conservative estimate of the probability of failure of general systems. However, the method

developed for determining the necessary cuts of monotonically loaded structures may not apply. Nevertheless, if certain cuts are neglected, the results will always be conservative.

Applying the formulation for monotonically loaded structures to general systems should give a reasonable estimate of the probability of failure. The formulation will be in error only when two or more limit states for events represented by branches emanating from the same node are exceeded. The probability of this may be small compared to the system probability of failure.

### 4.5.3 Examples

Example 4.4--Consider the structure shown in Fig. 4.13. Assume that all four members fail in a brittle manner and the two chains share the load equally. This structure is non-monotonically loaded since a failure of one of the members will induce a reduction (to zero) in the load on the other member in the same chain.

This structure may be treated as a monotonically loaded structure by defining member A as the chain consisting of members 1 and 3, and similarly defining member B as the chain consisting of members 2 and 4. The substitute structure is then similar to that shown in Fig. 4.11 with the strength of member A being $\min\{R_1, R_3\}$ and the strength of member B being $\min\{R_2, R_4\}$, where $R_i$ is the ultimate strength of member i. Using the failure mode approach, the probability of failure is:

$$P_F = P[(\min\{R_1, R_3\} - \frac{P}{2} < 0)(\min\{R_2, R_4\} - P < 0)$$

$$\cup (\min\{R_2, R_4\} - \frac{P}{2} < 0)(\min\{R_1, R_3\} - P < 0)]$$

$$= P[(R_1 - \frac{P}{2}<0)(R_2-P<0) \cup (R_1 - \frac{P}{2}<0)(R_4-P<0)$$

$$\cup (R_3 - \frac{P}{2}<0)(R_2-P<0) \cup (R_3 - \frac{P}{2}<0)(R_4-P<0)$$

$$\cup (R_2 - \frac{P}{2}<0)(R_1-P<0) \cup (R_2 - \frac{P}{2}<0)(R_3-P<0)$$

$$\cup (R_4 - \frac{P}{2}<0)(R_1-P<0) \cup (R_4 - \frac{P}{2}<0)(R_3-P<0)]$$

Now consider the case in which members 1 and 2 will fail in a ductile manner, whereas failures of members 3 and 4 remain brittle. In this case, the structure cannot be modelled as a monotonically loaded structure since the residual strength of member A depends on whether member 1 or 3 is stronger. However, not all constraints need to be included since only the failures of members 3 and 4 will reduce the loads on the other members. The probability of failure is thus obtained as:

$$P_F = P[(R_1+R_2-P<0) \cup (R_1+R_4-P<0) \cup (R_2+R_3-P<0)$$

$$\cup (R_3 - \frac{P}{2}<0)(R_3<R_1)(R_2-P<0) \cup (R_3 - \frac{P}{2}<0)(R_3<R_1)(R_4-P<0)$$

$$\cup (R_4 - \frac{P}{2}<0)(R_4<R_2)(R_1-P<0) \cup (R_4 - \frac{P}{2}<0)(R_4<R_2)(R_3-P<0)]$$

Eliminating the constraints will be conservative. Consider the case in which the random variables have values $r_1=0.4p$, $r_2=0.65p$, $r_3=0.45p$, and $r_4=0.70p$. The structure will survive since member 1 would yield before member 3 breaks and the combined strengths of members 2 and 3 and members 4 and 3 are both greater than the applied load P. However, neglecting the event $R_3<R_1$ in the formulation would show the structure as having failed since $R_3-P/2<0$ and at least one (in fact both) of members 2 and 4 have strengths less than the applied load.

Example 4.2 (continued)--Consider again the non-monotonically loaded structure shown in Fig. 4.8. Some aspects of monotonic loading are inherent. The applied moment at section 1 does not decrease with

the failure of section 4 and vice versa. Also the applied moments on sections $2^+$ and $3^+$ do not decrease with the failure of section 1 and the applied moments on sections $2^-$ and $3^-$ do not decrease with the failure of section 4. Because of this, cut h-h is not necessary.

For this structure it would be unnecessary to include the constraints defining the first failure among sections $2^+$, $3^+$, $2^-$, and $3^-$. If any of these fails, the structure will be in the same physical configuration.

A conservative estimate of the probability of failure may be obtained from either the failure mode approach or the stable configuration approach by eliminating the constraints. The cuts that need to be included in the stable configuration approach are cuts a-a, b-b, c-c, d-d, e-e, and f-f of Fig. 4.9. For a monotonically loaded structure, only the cuts a-a, b-b, c-c, and d-d would have to be included. Thus, two additional cuts need to be included in the formulation to obtain the same probability of failure as with the failure mode approach.

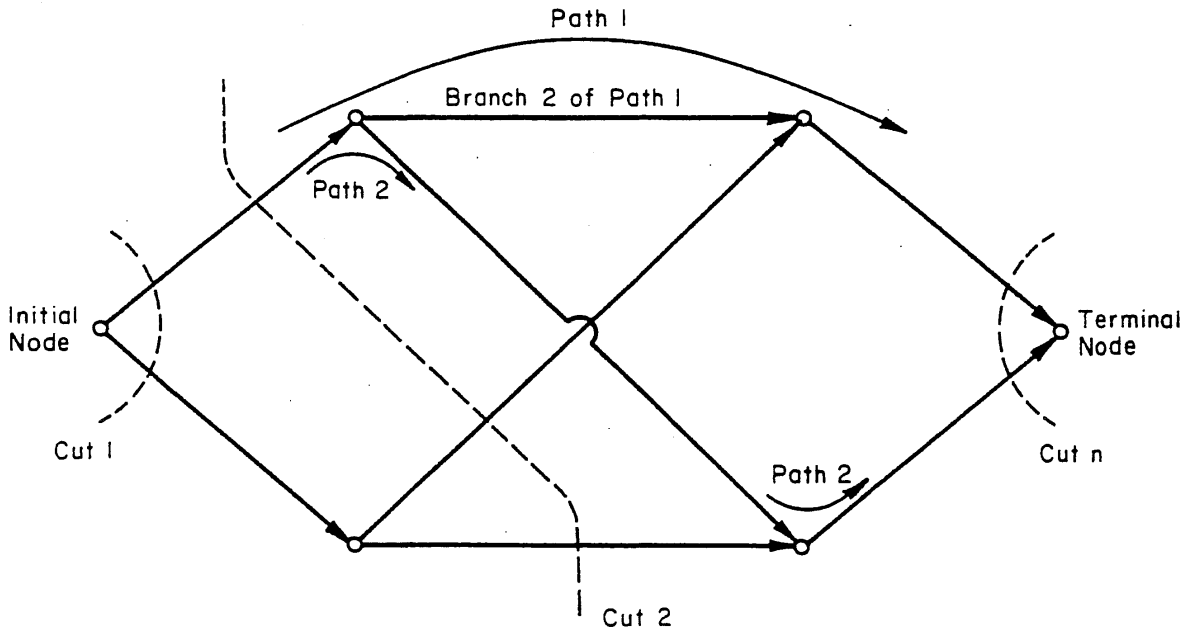


Fig. 4.1 Typical Failure Graph

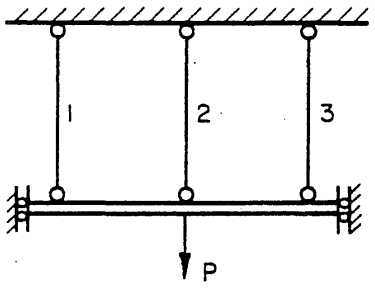


Fig. 4.2 Three-Member Parallel System with Active Redundancy

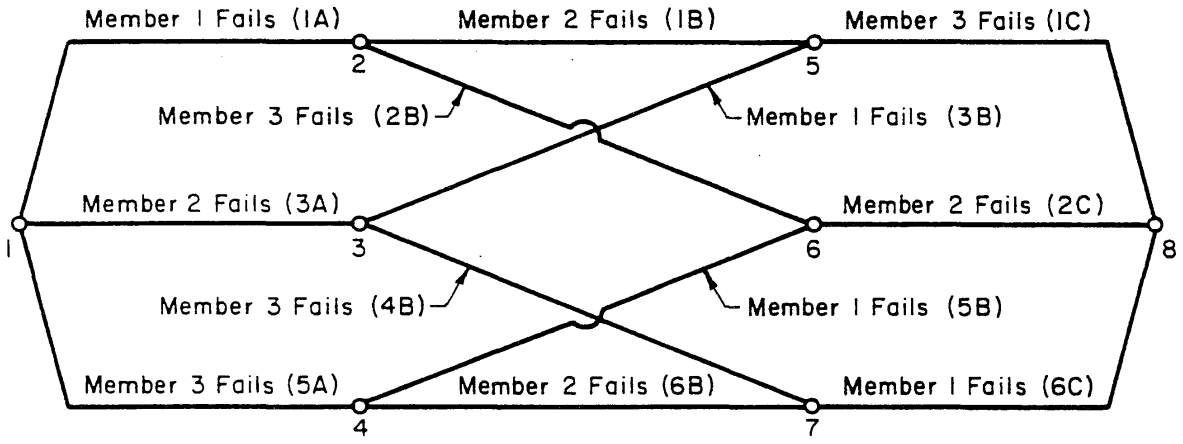


Fig. 4.3 Failure Graph for 3-Member Structure of Fig. 4.2

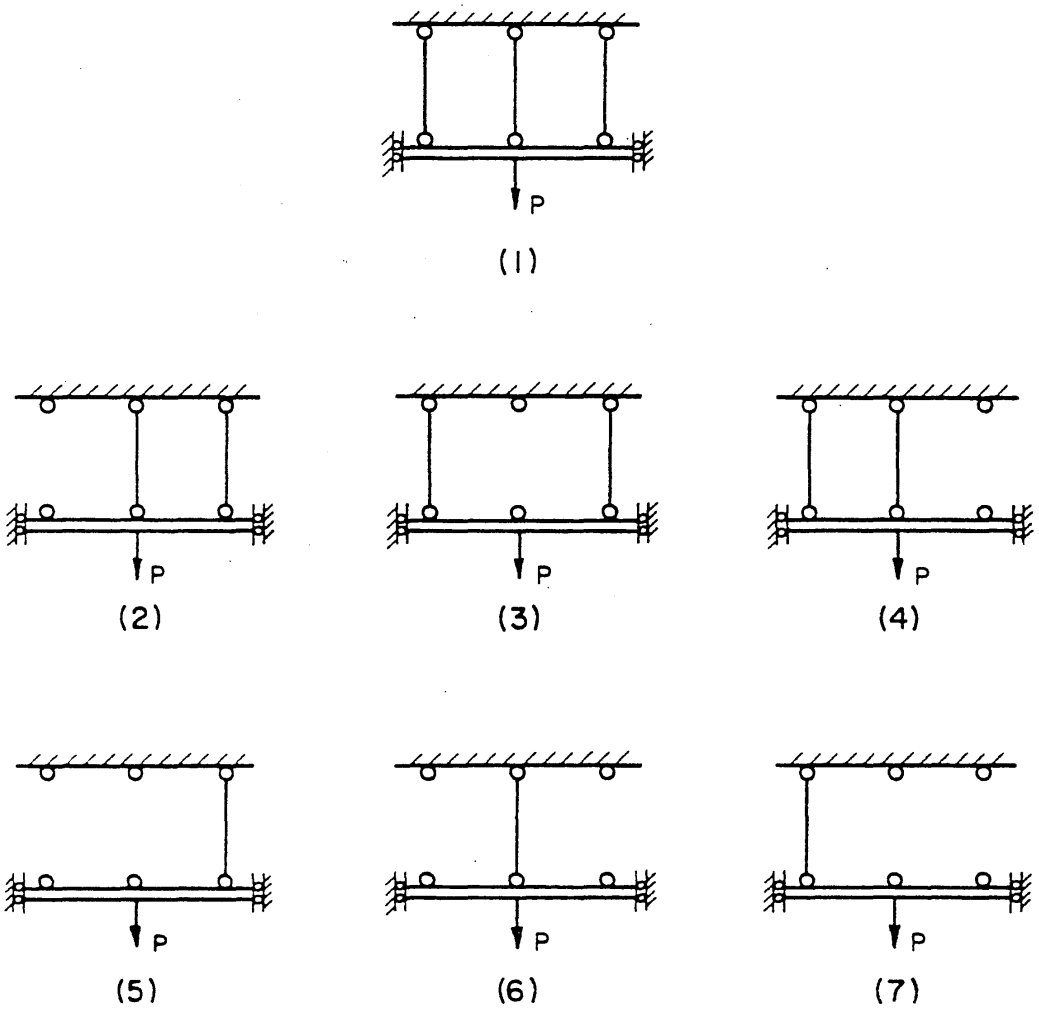


Fig. 4.4 Stable Configurations of 3-Member Structure of Fig. 4.2

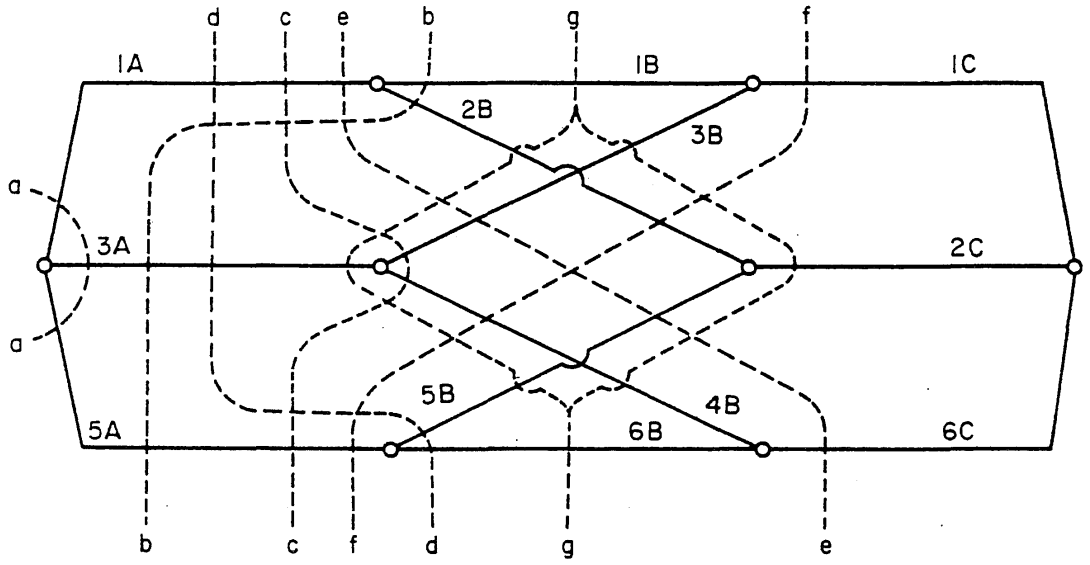


Fig. 4.5 Possible Cuts of Failure Graph of Fig. 4.3

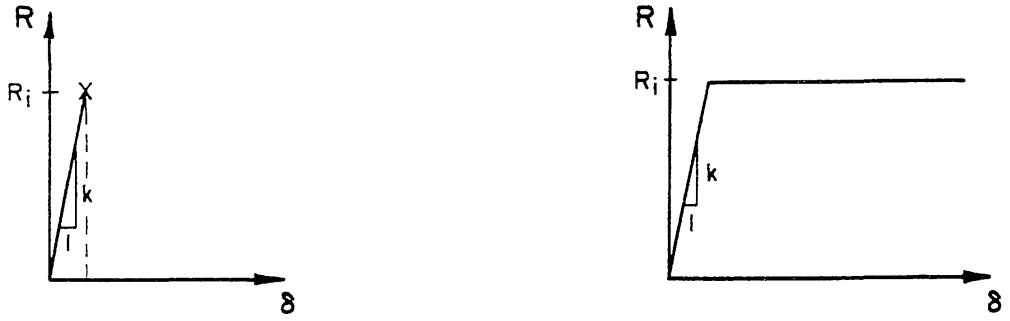


Brittle Members 1and 3

Ductile Member 2

Fig. 4.6 Load-Deformation Characteristics of Members of Structure of Fig. 4.2

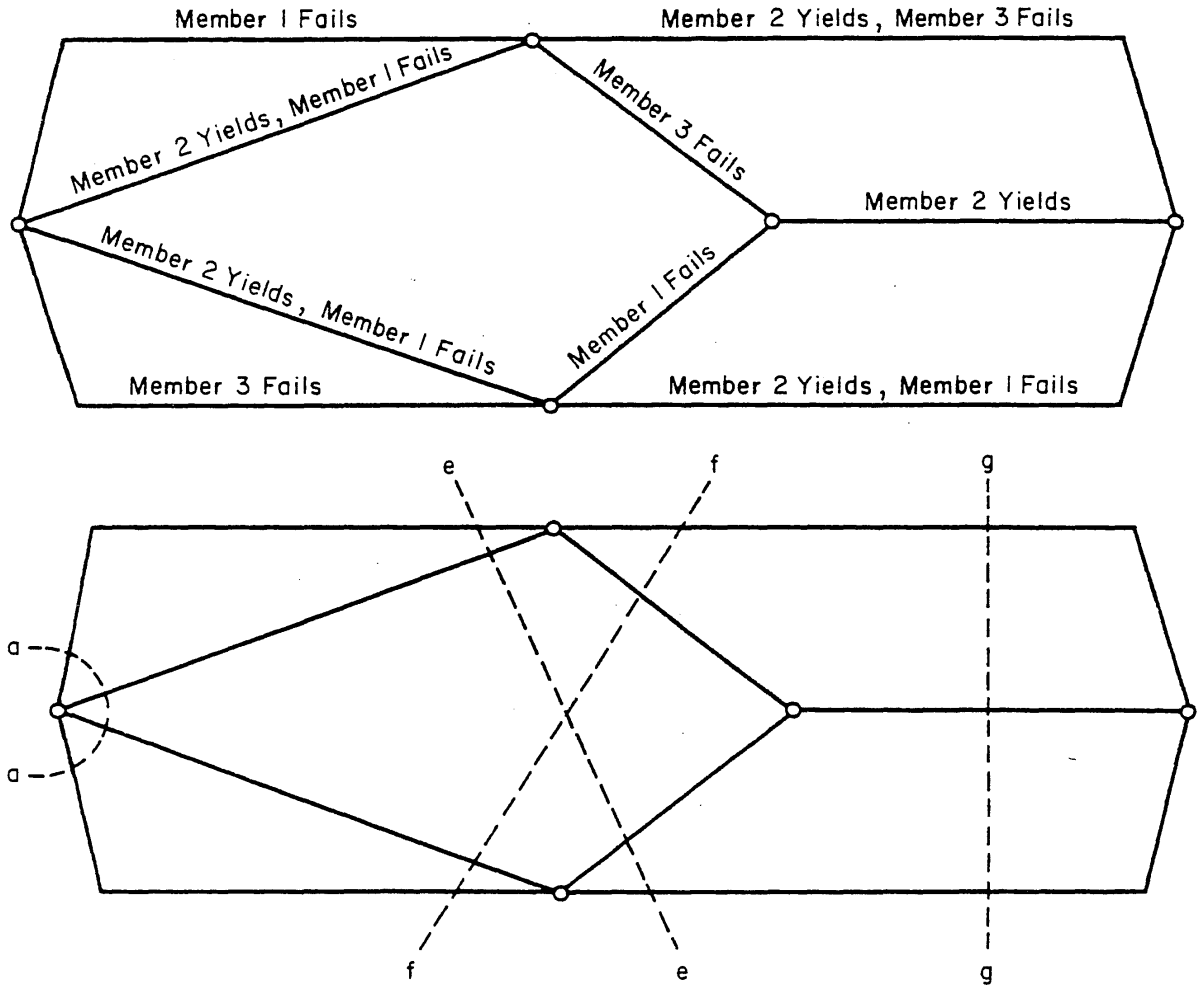


Fig. 4.7 Reduced Failure Graph and Cuts for Structure of Fig. 4.2

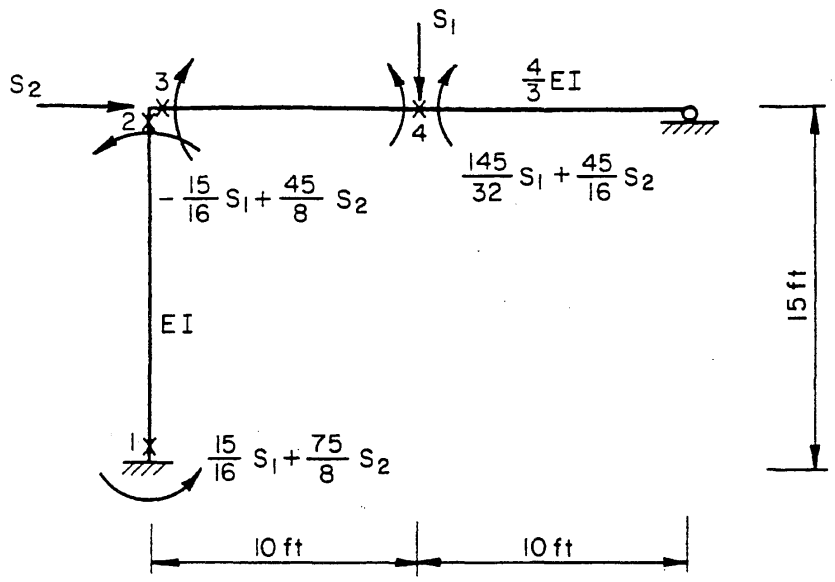


Fig. 4.8 Simple Frame Structure of Example 4.2

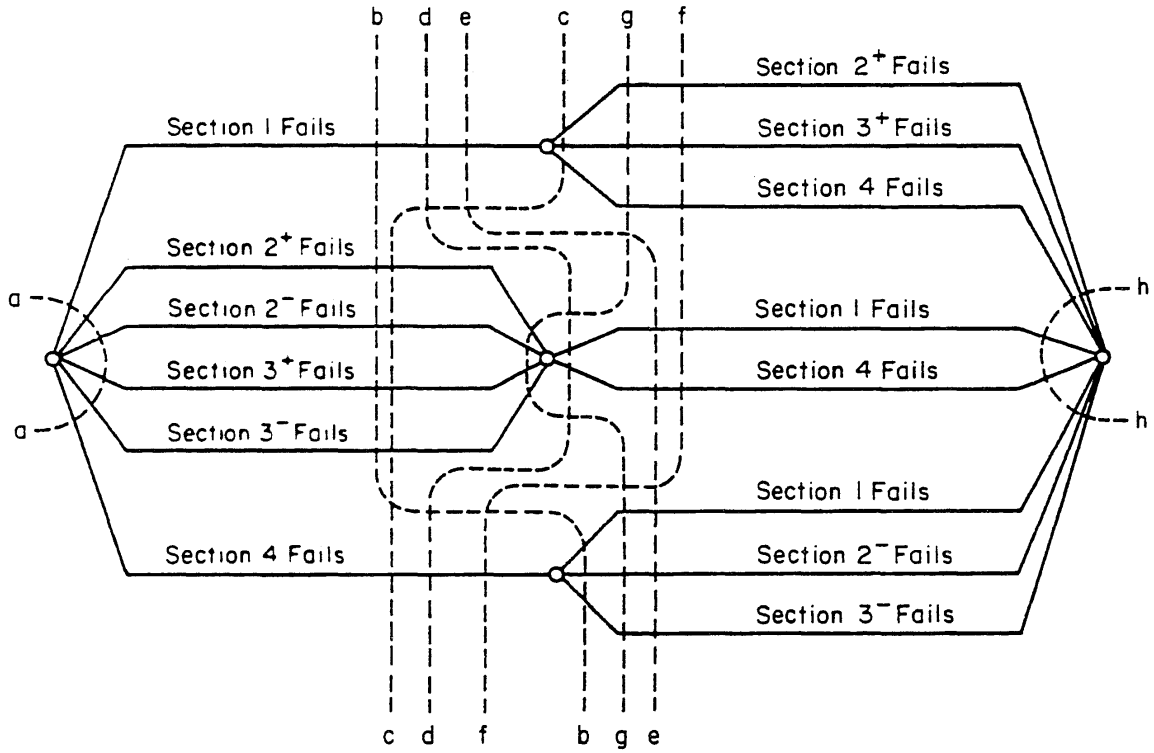


Fig. 4.9 Failure Graph for Frame of Fig. 4.8

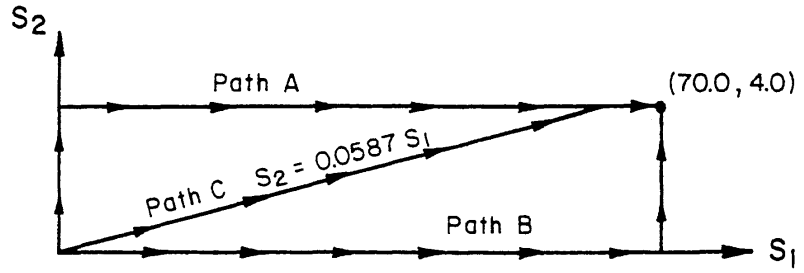


Fig. 4.10 Three Possible Loading Paths for Frame of Fig. 4.8

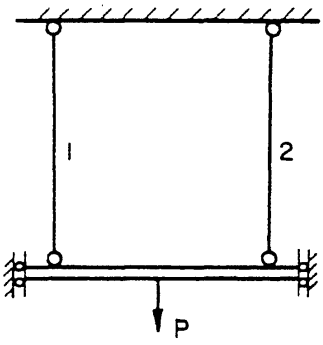


Fig. 4.11 Structure of Example 4.3

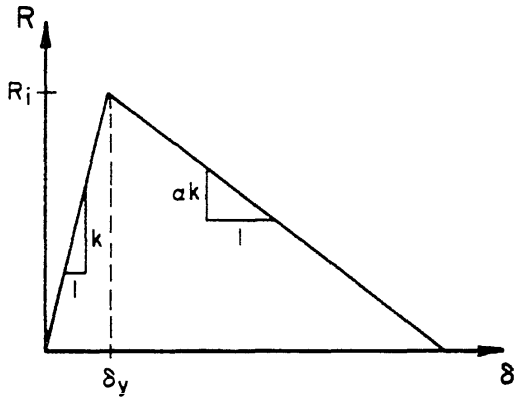


Fig. 4.12 Load-Deformation Characteristics of Members of Structure of Fig. 4.11

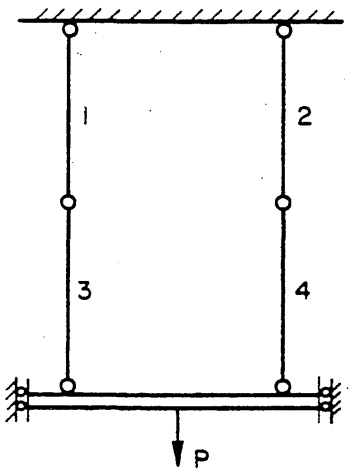


Fig. 4.13 Non-Monotonically Loaded Structure of Example 4.4

# CHAPTER 5

# COMPUTATIONAL METHODS

## 5.1 Introductory Comments

The concepts and techniques developed in the previous chapters are now combined to develop practical computational methods. The computational methods developed apply primarily to monotonically loaded structures. It is assumed that the failure mode approach leads to the determination of the probability of a union of intersections, whereas the stable configuration approach leads to the determination of the probability of an intersection of unions of events. Procedures are available (Chu and Apostolakis, 1980; Locks, 1979) for converting any combination of unions and intersections of events into unions of intersections or intersections of unions. However, care should be exercised with non-monotonically loaded structures as the first-order methods may not be applicable for the constraints.

## 5.2 Failure Mode Approach

### 5.2.1 Systematic Determination of Significant Failure Modes

For structures of any practical complexity, there will be many failure modes. Generally, however,only a limited number of these modes will be significant, i.e., will have major contributions to the unreliability of the structure. It is difficult to determine, a priori, which of the potential failure modes will be significant. Methods have been suggested and some of these will be discussed below particularly with respect to their potential applications to general systems.

Nonlinear Programming Approach--The use of nonlinear programming techniques has been applied for finding the failure modes of ductile (elastic-perfectly plastic) frames and trusses (Ma and Ang, 1981). Two different formulations of the optimization problem were suggested: one based on a general formulation of the failure modes and the other based on the linear combination of independent elementary mechanisms. The first formulation leads to a constrained optimization problem, where the constraints are defined by positive external virtual work and continuity of the structure. The second formulation leads to an unconstrained optimization problem. Even though the methods may miss some of the significant modes, they are fairly reliable in identifying most of the significant modes.

The extension of the method to non-ductile systems appears to be difficult, since there is no general approach to formulate the failure modes. However, the method as developed may prove useful for other types of problems.

The Branch and Bound Method--The most significant, i.e., the weakest mode may be found by the branch and bound optimization technique (Lawler and Wood, 1966). The method intelligently searches the failure graph to find the most significant failure mode. First, all the branches emanating from the initial node are examined and the one with the highest probability of failure is chosen. The branches emanating from the node at the end of this branch are then considered. The branch that causes the path (to this point) to have the the highest probability of failure, i.e., the branch that causes the probability of the intersection of the failure regions of the initial branch and the branch under consideration to be the greatest, is chosen next. The search can be continued in either of two ways. The first, referred to as branching from the newest active bounding problem, is to continue branching along the path, i.e., examine branches emanting from the last branch chosen. Other paths are then examined to see if it is possible for them to have a higher probability of failure. The other, referred to as branching from the lowest bound, is to search all paths and branch from the one with the highest probability of failure. Both methods eventually lead

to finding the most significant path or failure mode.

In structural reliability problems all significant failure modes are relevant and must be considered. For structural reliability purposes, modifacations have been suggested (Murotsu, et al., 1981a; Moses, 1982; Grimmelt, et al., 1983) to the general branch and bound algorithm for finding more than one significant mode.

Murotsu, et al., (1981a) suggested that the branching from the newest active bounding problem method be used to find a significant path and thus a lower bound to the system probability of failure. Other paths are then examined and are considered significant if the probability of failure of the mode is within some prescribed order of magnitude of the greatest probability of failure of any of the significant modes obtained thus far. In other words, a prescribed order of magnitude of the first-order lower bound of the system probability of failure is used as a criterion for determining if a mode is significant. Generally, an accurate estimate can be obtained by considering only those modes with a probability of failure greater than 10% of the first-order lower bound probability. Of course, better accuracy can be obtained by including more modes. Other paths for consideration can be obtained by following the method of branching from the newest active bounding problem. First, consider the paths by varying the last branch in the path. Then consider the paths by varying the last two branches in the path, and so on.

Moses (1982) suggested a similar method for obtaining the significant failure modes. The calculations are simplified by specifying all resistances equal to their respective mean values and increasing the loads to determine which members will fail.

The advantage of the branch and bound method is that the entire failure graph does not have to constructed. Instead, only the significant parts are found, thus reducing the amount of computations required.

Monte Carlo methods may also be used to find the significant failure modes. This will be discussed in Sect. 5.4.

5.2.2 Determination of the Reliability of Each Mode

The probability of each failure mode involves the determination of the probability of the intersection of the branches of the pertinent path. The failure surface representing each of the branches may be linearized using first-order techniques. It may be advantageous to linearize the failure surface at other than the failure point. Intuitively, it may be best to linearize at a point closest to the origin on the failure surface actually containing part of the failure region representing the mode. In other words, in searching for the point closest to the origin, consider only the part of the failure surface that is contained in the intersection of the individual failure regions. Unfortunately, this point may be difficult to find. This problem is discussed further in Sect. 5.2.5.

Example 5.1--Consider a failure mode composed of two branches that are defined by the following performance functions:

$$g_1 = -U_1 - \frac{U_2^2}{8} + 2$$

$$g_2 = -U_2 - \frac{U_1^2}{8} + 2$$

where $(U_1, U_2)$ are independent standard normal variates. The failure surfaces are shown in Fig. 5.1. Also shown are the linear failure surfaces obtained using first-order methods, the equivalent linear failure surface, and the linear surfaces obtained by linearizing at the point closest to the origin of the failure surface representing the failure region of the mode. The percentage errors of the various methods are tabulated in Table 5.1. It is observed that linearizing at a point on the failure surface actually containing part of the failure region representing the mode provides the best approximation.

Neglecting some branches in the determination of the probability of failure of each mode will be conservative. If some of the branches have a high probability of failure, i.e., once the structure reaches a certain configuration there is little chance of survival, it may be possible to neglect them without having any significant effect on the resulting probability of failure of the mode. Generally, the probability of failure of a branch will increase as one moves along a path in the failure graph. Thus, if a branch does not have any significant effect on the probability of a particular failure mode, the rest of the branches along the path may be neglected.

### 5.2.3 Combining of Modes

The probability of failure of a system is the probability content of the union of the failure regions of all potential failure modes. Each mode may be replaced by an approximate planar failure surface, and the origin projection distance of the plane, $\beta$, obtained as the reliability index of the mode. The direction cosines of the plane should be chosen so that the dependencies between the modes are modelled as accurately as possible. One method is to use the direction cosines of the branch in the pertinent path with the smallest failure probability. However, a better method is to view the direction cosines as sensitivity coefficients (Gollwitzer and Rackwitz, 1983); namely,

$$\alpha_i = \frac{\frac{\partial \beta}{\partial U_i}}{\left[\sum_{i=1}^{n} \left(\frac{\partial \beta}{\partial U_i}\right)^2\right]^{1/2}} \tag{5.1}$$

In general the partial derivatives would have to be evaluated numerically.

A simpler method to determine the direction cosines, and yields essentially the same accuracy as Eq. 5.1, is to use the direction

cosines of the vector from the point of the failure surface of the mode closest to the origin, i.e., the failure point of the mode. If all the failure surfaces of the branches comprising the mode are approximated by planes, the failure point can easily be found as the solution to the following constrained optimization problem:

$$\text{Mimimize} \quad U_1^2 + \ldots + U_m^2 \tag{5.2}$$

$$\text{subject to:} \quad \begin{aligned} \underline{\alpha}_1^t \underline{U} + \beta_1 &\leq 0 \\ &\vdots \\ \underline{\alpha}_m^t \underline{U} + \beta_m &\leq 0 \end{aligned}$$

An algorithm is given in Appendix A for solving this problem based on quadratic programming techniques.

To validate the methods described above, twelve different cases of a two-mode system were analyzed. The modes are listed in Table 5.2. The corresponding failure regions of the modes are shown in Fig. 5.2 along with the equivalent failure surfaces determined using the direction cosines from Eq. 5.1 and those obtained using the direction cosines of the failure point of the mode. The results of the reliability calculations and the associated errors are summarized in Table 5.3. Using the direction cosines of the failure point consistently gives the most accurate result.

One problem with using the direction cosines of the failure point is that it is possible to obtain the same direction cosines for different modes. In such cases, the two approximating hyperplanes will be perfectly correlated, whereas the modes are actually not perfectly correlated. This may lead to a slightly lower probability of failure. The error will, in general, be small and full advantage may be taken of the fact that certain planes are perfectly correlated in developing an algorithm for general systems.

Example 5.2--Consider a structure in which there are two failure modes such that the probabilities of failure of the modes are:

$$P[M_1] = P[(U_1 + 2.0 < 0)(-U_2 < 0)]$$
$$P[M_2] = P[(U_1 + 2.0 < 0)(U_2 < 0)]$$

The probability of failure of the system, i.e., the probability of the union of the two modes, is obviously

$$P[U_1 + 2.0 < 0] = 0.0228$$

The approximate plane for each mode obtained using the direction cosines of the failure point will be identical (see Fig. 5.3). The probability of failure of the system will be in error by -50% and the error in the reliability index will be 14%. This is obviously an extreme case and the error, in general, will be much less.

Neglecting failure modes will be unconservative. Often, an accurate estimate of the system probability of failure can be obtained by including only the significant modes. If it is not certain that all the significant modes have been found, the PNET method will be a good method to use to obtain the system probability of failure since significant modes that are not found will often be highly correlated with other significant modes (Ma and Ang, 1981) and, therefore, would not affect the resulting probability.

### 5.2.4 Algorithm for Analysis of General Structural Systems

The concepts and methods for failure mode analysis discussed and illustrated so far may be used to develop an algorithm for the failure mode analysis of general structural systems. It will involve searching for the significant modes while simultaneously obtaining the reliability of the respective modes. The algorithm is designed for analyzing structures that contain both brittle and ductile components.

The steps of the algorithm can be most easily described with reference to the failure graph shown in Fig. 5.4. For the purpose of description, assume that paths a through b are ductile failure modes, e.g., collapse through a plastic mechanism, whereas branches c, d, and e represent brittle failures. Similarly, branches f through g and k through ℓ represent ductile failures while the rest of the branches represent brittle failures.

Step A--Find the significant ductile modes, paths a through b, using available methods, e.g., Ma and Ang (1981). On the basis of these significant modes, calculate the best lower bound to the system probability of failure.

Step B--Compare the probability of failure of branches c, d, and e to the lower bound of the system probability of failure obtained in Step A to see if any are significant. The criterion for whether a branch or path is significant will be discussed later. Neglect any that are not significant, i.e., no longer consider them in the subsequent analysis. Find the branch with the greatest probability of failure from the significant branches; say this is branch c. Note that if there are no ductile failure modes, this step would consist only of finding the branch with the maximum probability of failure. If none of the branches are significant, then the search is completed; go to Step F.

Step C--Examine the branches that emanate from the node at the end of branch c to determine the effect that they have on the approximating plane for the mode. The significant branches of those representing ductile failures, branches f through g, can be obtained as in step A. Approximating planes are developed using the direction cosines of the failure point. If any of the branches do not have any effect on the direction cosines of the mode, i.e., the direction cosines for the approximating planes are the same as the direction cosines for branch c, follow the procedure outlined in Step E. To check whether a branch will have any effect on the direction cosines, examine to see if the failure point of the intersection of the branches in the path leading to the branch under consideration is in the failure region of the branch being considered. If it is, the branch will have no effect on the direction

cosines. For two branches, say branches c and f, if $\beta_f \leq \rho_{cf} \beta_c$ there will be no effect on the direction cosines.

Step D--Obtain the reliability for each of the paths, i.e., paths cf through cj. Check for significance. If there are any significant paths, i.e., the limit state has been reached in some mode, update the lower bound of the system failure probability. Neglect any modes that are not significant. For significant incomplete paths, determine the path with the greatest probability of failure. Return to Step C, i.e., examine the branches that emanate from the last node. For example, if path ch is significant and has the greatest probability of failure, examine branches p, q, and r. This process is continued until all paths of the failure graph are terminated either due to the limit state being reached or the path is no longer significant. Referring to Fig. 5.4, after all paths containing branch c have been terminated, branches d and e are then examined to see if they are significant. If they are, then the paths containing those branches are examined. Once all the paths have been terminated, proceed to Step F.

Step E--Assume that one of the branches emanating from branch d, say branch m, does not affect the direction cosines of the approximating plane. It is assumed that all further branches will not have any noticeable effect on the mode reliability and can be neglected. This will generally be true, but it is possible that some further branches, say branch s, may have a significant effect. Neglecting further branches will, of course, be conservative.

It may be too conservative to neglect branches k through o. In such cases, the following computational scheme is suggested. Calculate the probability of the union of all the branches (k through o) proceeding from the last node and obtain the reliability index. Use this reliability index and the direction cosines from some branch to obtain the probability of failure of the path. In other words, the probability of failure of the path is obtained as:

$$P[\{g_d < 0\}\{(g_k < 0) \cup \ldots \cup (g_o < 0)\}] \tag{5.3}$$

The branch selected for which the direction cosines are used should be a branch that does not affect the direction cosines of the path and yields the greatest probability of failure for the path, i.e., find the maximum of:

$$\{P[(g_d < 0)(g_m < 0)],\ldots,P[(g_d < 0)(g_o < 0)]\} \tag{5.4}$$

where branches m through n do not affect the direction cosines of the approximating plane. Finding this maximum could be quite laborious, especially as one proceeds further along the failure graph. As an approximation, use the branch with the maximum $[(p_F)_x][\pi_y \rho_{xy}]$, where

$(p_F)_x$ = probability of failure of branch x;
$\rho_{xy}$ = correlation coefficient between events represented by branch x and branch y;
y = varies over all branches in the path up to branch x.

If any correlation coefficient is less than 0.2, replace it by 0.2 when taking the above product. The analysis is continued for the other branches as discussed in Step D.

Step F--The significant failure modes have been found. The probability of failure of the system, or corresponding close bounds, can be evaluated.

Special Remarks--In exercising the algorithm, specific criteria are necessary for determining if a path is significant. Obviously, the less stringent the criterion, the more failure modes will be included and hence the more accurate will be the result. It is recommended that more stringent criteria be used, i.e., more paths be neglected, near the initial phase of the failure graph since the subsequent branches will reduce the failure probability of the mode. As a general guideline, it is suggested that initial branches with a failure probability of less than 10% of the lower bound system failure probability be neglected. Subsequent branches that have a probability of failure lower than 5% of the lower bound can also be neglected as being insignificant.

Step D of the algorithm can be modified to account for the fact that it is often better to linearize the failure surfaces at other than the failure point of the event when taking the intersection of events (see Example 5.1). The failure point of the mode is found by first linearizing each of the branches at their individual failure points and then using quadratic programming. A search can be made in the direction of the obtained failure point of the mode to find a point on the failure surfaces of each of the branches. The branches are linearized at these points and a new failure point of the mode is found. The process is repeated until the failure point of the mode converges to the point of linearization of each of the branches. Essentially this is the Griffith-Stewart algorithm (Griffith and Stewart, 1961) for nonlinear programming. Unless the failure surfaces are highly nonlinear and the failure point of the mode is not near the failure point of each of the branches, sufficient accuracy should be obtained with linearizing each of the branches at their respective failure points. Even in the worst cases, one cycle of Griffith-Stewart algorithm should be sufficient.

## 5.3 Stable Configuration Approach

The probability of failure of a cut is determined as the probability of the union of the branches in the cut. To avoid compounding errors arising from the first-order linearization of the branches, it is best to use equivalent linear failure surfaces for each of the branches, i.e., the first-order plane is shifted so the failure probability evaluated on the basis of the planar failure surface is the same as the best estimate of the probability content of the true failure region.

To obtain the probability of failure of the system, it is necessary to obtain the probability of the intersection of the failure regions of all the cuts. However, current computational techniques for obtaining the probability of an intersection of events with nonlinear failure surfaces are limited.

Second or higher order bounds for the intersection of events can be used to obtain the system failure probability. The bounds are based on the union of events. Since the cuts are themselves composed of the union of events and the associative property holds for unions, the probability of failure of the union of some cuts will be the probability of failure of the union of all branches in the cuts.

Often the union of three or more cuts will be equivalent to the union of just two cuts. For example, the union of $C_{a-a}$, $C_{b-b}$, and $C_{c-c}$ in Fig. 4.4 is equivalent to the union of $C_{b-b}$ and $C_{c-c}$. If all combinations of the union of three or more cuts are equivalent to the union of just two cuts, the probability of the intersection can be expanded in an analogue to Boole's formula, as follows:

$$P[\bigcap_{j=1}^{k} E_j] = \sum_{j=1}^{k} P[E_j] - \sum\sum P[E_{j_1} \cup E_{j_2}] + \sum\sum\sum P[E_{j_1} \cup E_{j_2} \cup E_{j_3}] - \ldots + (-1)^{k+1} P[\bigcup_{j=1}^{k} E_j] \tag{5.5}$$

where the repeated summation signs $\sum\sum\cdots\sum$ mean the summation over all integers $j_1, j_2, \ldots, j_m$ subject to $1 \leq j_i \leq k$, $j_1 < j_2 < \ldots < j_m$. Substitution would then yield an expression for the probability of failure in terms of just the unions of two cuts.

A reasonable estimate of the probability of failure can usually be obtained by considering only a few cuts. Generally, the significant cuts, i.e., those with small probabilities of failure, can be found by inspection. Often, only a few cuts besides the cut representing initial system damage need to be included, especially if the components fail in a brittle manner. The reliability analysis itself can also guide in the selection of cuts--if a component has a high probability of failure compared with other components in the cut, it is wise to select a cut containing the configuration with that component failed.

## 5.4 Monte Carlo Methods

Another method to estimate the reliability of structural systems is through Monte Carlo simulations. This involves generating a large number of sample structures and examining the behavior of each sample structure under a sample loading. An estimate of the probability of failure is the number of sample structures that failed divided by the total number of sample structures. It should be noted that the Monte Carlo method is only a computational technique and the formulation of the probability of failure has to be obtained before the method can be applied.

The Monte Carlo method may be time consuming and costly because of the large number of trials required. However, the number of trials needed is only a function of the probability of failure and not the dimension or complexity of the problem. The Monte Carlo method provides a useful tool for verifying other simpler computational methods.

To describe the Monte Carlo method, consider a performance function $g(X_1,\ldots,X_n)$. For a structural system this may be a very complicated function. Define an indicator function as follows:

$$I[g(X_1,\ldots,X_m)] = \begin{cases} 1 & \text{if } g(\underline{X}) > 0 \\ 0 & \text{if } g(\underline{X}) < 0 \end{cases} \tag{5.6}$$

It is well known that the probability of survival is the expected value of Eq. 5.6. The mean probability of failure is therefore,

$$P_F = E[1 - I[g(X_1,\ldots,X_m)]] \tag{5.7}$$

where E[.] is the expected value. An unbiased estimate of Eq. 5.7 is:

$$\overline{P_F} = 1 - \overline{I} = \frac{1}{n} \sum_{j=1}^{n} \{1 - I[g(x_{1j},\ldots,x_{mj})]\} \tag{5.8}$$

where $(X_{ij},\ldots,X_{mj})$ is a random observation from the joint density function of the random variables. Obtaining random observations may be somewhat difficult, especially for dependent variables. It is recommended that random observations of independent normal variables be generated and then transformed to the basic variables. If the second-moment method is used, the normal distribution can be used for purposes of generating the random observations.

It is desirable to know the closeness of the estimated probability of failure (Eq. 5.8) to the actual probability of failure, or more importantly, how many trials are required to obtain a certain accuracy. Shooman (1968), by approximating the binomial distribution with the normal distribution, developed an expression for the percent error if the maximum error is assumed to be two standard deviations of the random variable I. In other words, there is a 95% chance that the percent error will less than that given by Shooman's formula, namely,

$$\% \text{ error} = 200\sqrt{\frac{1 - p_F^*}{np_F^*}} \tag{5.9}$$

where $p_F^*$ is the estimated probability of failure and n is the number of trials. Based on this formula, the graphs in Figs. 5.5 and 5.6 were constructed to show the anticipated percent error in the probability of failure and in the reliability index, respectively. If an estimate of the probability of failure or the reliability index is available, Figs. 5.5 and 5.6 can be used to determine the number of trials that should be used to obtain a desired accuracy.

The major problem with the Monte Carlo method is the large number of trials required. To overcome this problem, several variance reduction methods, i.e., methods by which an equally accurate estimate of the probability of failure can be obtained with much fewer trials, have been suggested (Hammersley and Handscomb, 1964; Buslenko, et al., 1966; Warner and Kabaila, 1968; Ang and Tang, 1983). Two methods will be discussed here: the importance sampling technique and the extraction

of the regular part.

The use of importance sampling has been suggested by Mazumdar, et al.(1978). In this method, an arbitrary probability density function is chosen and Eq. 5.7 is rewritten as:

$$P_F = E\left[1 - I[g(X_1^*,\ldots,X_m^*)]\frac{f(x_1^*,\ldots,x_m^*)}{f^*(x_1^*,\ldots,x_m^*)}\right] \tag{5.10}$$

where:

$f(\underline{x}^*)$= = probability density function of the random variables;

$f^*(\underline{x}^*)$ = chosen probability density function.

The probability of failure is obtained as:

$$\overline{P_F} = \frac{1}{n}\sum_{j=1}^{n}\{1 - I[g(x_{1j}^*,\ldots,x_{mj}^*)]\frac{f(x_{1j}^*,\ldots,x_{mj}^*)}{f^*(x_{1j}^*,\ldots,x_{mj}^*)}\} \tag{5.11}$$

The random observations are drawn from the new density function $f^*(\underline{x}^*)$.

Obviously, the new density, $f^*(\underline{x}^*)$, should be chosen so that failure occurs more often, i.e., $g(\underline{X}^*)<0$ occurs with a greater frequency. It is difficult to say what the optimum density function is. For structural systems, great care must be taken in choosing the density. Bad choices may result in erroneous results. Unfortunately, no general guidelines seem to exist except that the chosen density function should not differ greatly from the actual density function. For components, Shinozuka (1983) has suggested that $f^*(\underline{x}^*)$ be chosen as a uniform distribution over a multidimensional rectangle. The domain of the rectangle should include the region of high likelihood around the failure point. The probability of failure is then obtained as:

$$\bar{P}_F = \frac{A}{n} \sum_{j=1}^{n} \{1 - I[g(x^*_{1j},\ldots,x^*_{mj})]f(x^*_{1j},\ldots,x^*_{mj})\} \tag{5.12}$$

where A is the area of the rectangle. Accurate results can be obtained using as few as 1000 trials for failure probabilities as small as $10^{-11}$.

Another method for reducing the variance is the extraction of the regular part, also called the method of control variates. In this method, some other function, $\ell(X_1,\ldots,X_m)$ is found such that $g(\underline{X})\simeq\ell(\underline{X})$ and the probability of the failure region, $\ell(\underline{X})<0$ can be found exactly. Monte Carlo methods are then used to obtain the difference between the actual probability of failure and the estimated probability of failure using $\ell(\underline{X})$. The probability of failure is obtained as:

$$\bar{P}_F = P[\ell(\underline{X}) < 0] + \frac{1}{n} \sum_{j=1}^{n} \{(1 - I[g(\underline{X})\ell(\underline{X})])\text{sign}[\ell(\underline{X})]\} \tag{5.13}$$

where:

$$\text{sign}[X] = \begin{cases} -1 & \text{if } X \leq 0 \\ 1 & \text{if } X > 0 \end{cases}$$

For components, $\ell(\underline{X})$ may be taken as the first-order linearization at the failure point. For structural systems, a good choice of $\ell(\underline{X})$ becomes less obvious.

An alternative method to obtain an estimate of the system probability of failure is to use Monte Carlo sampling to obtain a limited number of values of the performance function and then obtain an estimate of the probability of failure based on these values. Usually the first four moments of $g(\underline{X})$ are obtained and then a distribution is fitted to these values (Moses and Kinser, 1967; Parkinson, 1980). The Edgeworth (Murotsu, et al., 1979) or the Gram-Charlier series expansions may also be used. Care must be exercised when applying this method for

structural systems as $g(\underline{X})$ may not be unimodal.

Monte Carlo simulations may also be used to find the significant failure modes (Esteva, 1981; Gorman and Moses, 1979). A few simulations of the structural behavior are made to determine how the structure would fail. This may involve making assumptions as to how the loads should be increased so that failure would occur. A number of failure modes of the structure are thus obtained and it is assumed that these are the significant failure modes. The probability of failure is obtained using analytical methods but only considering the failure modes identified. It is difficult to predetermine the necessary number of simulations to identify the significant modes. For a structure with more than a few significant failure modes, a fairly large number of simulations will have to be made which will tend to make the method costly and may be impractical.

Table 5.1 Accuracy of Different Linearizations of the Failure Surface

| Method | Line Type* | $P_F$ | $\beta$ | % Error $P_F$ | % Error $\beta$ |
|---|---|---|---|---|---|
| Exact | Solid | 0.005351 | 2.55 | - | - |
| First Order | Long Dash | 0.000518 | 3.28 | -90.3 | 28.6 |
| Equivalent Linear Surface | Dash Dot | 0.001078 | 3.06 | -79.9 | 20.2 |
| Linearize at (1.657,1.657) | Short Dash | 0.004573 | 2.61 | -14.5 | 2.2 |

*See Fig. 5.1

Table 5.2 Failure Regions of Modes Shown in Fig. 5.2

| Case | Failure Regions | |
|---|---|---|
| | Mode 1 | Mode 2 |
| 1 | $(U_1 \leq -2.0)(U_2 \leq 1.0)$ | $(U_2 \leq -2.0)(U_1 \leq 1.0)$ |
| 2 | $(U_1 \leq -2.0)(U_2 \leq 0.0)$ | $(U_2 \leq -2.0)(U_1 \leq 0.0)$ |
| 3 | $(U_1 \leq -2.0)(U_2 \leq -0.5)$ | $(U_2 \leq -2.0)(U_1 \leq -0.5)$ |
| 4 | $(U_1 \leq -2.0)(U_2 \leq -1.0)$ | $(U_2 \leq -2.0)(U_1 \leq -1.0)$ |
| 5 | $(U_1 \leq -2.0)(U_2 \leq -1.5)$ | $(U_2 \leq -2.0)(U_1 \leq -1.5)$ |
| 6 | $(U_1 \leq -2.0)(U_2 \leq -1.8)$ | $(U_2 \leq -2.0)(U_1 \leq -1.8)$ |
| 7 | $(U_1 \leq -2.0)$ | $(U_2 \leq -1.0)(U_1 \leq -0.5)$ |
| 8 | $(U_1 \leq -2.0)$ | $(U_2 \leq -1.0)(U_1 \leq -1.0)$ |
| 9 | $(U_1 \leq -2.0)$ | $(U_2 \leq -1.0)(U_1 \leq -2.0)$ |
| 10 | $(U_1 \leq -2.0)(U_2 \leq 0.0)$ | $(U_2 \leq -1.0)(U_1 \leq -0.5)$ |
| 11 | $(U_1 \leq -2.0)(U_2 \leq 0.0)$ | $(U_2 \leq -1.0)(U_1 \leq -1.0)$ |
| 12 | $(U_1 \leq -2.0)(U_2 \leq 0.0)$ | $(U_2 \leq -1.0)(U_1 \leq -1.5)$ |

Table 5.3 Comparison of Results Using Approximate Planes with Direction Cosines as Sensitivity Coefficients and of the Failure Point of the Mode

| Case | Exact | | Sensitivity Coefficients | | | | Failure Point of Mode | | | |
|---|---|---|---|---|---|---|---|---|---|---|
| | | | | | % Error | | | | % Error | |
| | $p_F$ | $\beta$ | $p_F$ | $\beta$ | $p_F$ | $\beta$ | $p_F$ | $\beta$ | $p_F$ | $\beta$ |
| 1 | 0.037764 | 1.777 | 0.037058 | 1.786 | -1.9 | 0.5 | 0.037916 | 1.775 | 0.4 | -0.1 |
| 2 | 0.022232 | 2.010 | 0.020477 | 2.044 | -7.9 | 1.7 | 0.022621 | 2.002 | 1.7 | -0.4 |
| 3 | 0.013520 | 2.211 | 0.011718 | 2.266 | -13.3 | 2.5 | 0.013348 | 2.216 | -1.3 | 0.2 |
| 4 | 0.006700 | 2.473 | 0.005351 | 2.552 | -20.1 | 3.2 | 0.006054 | 2.509 | -9.6 | 1.5 |
| 5 | 0.002522 | 2.804 | 0.001908 | 2.893 | -24.3 | 3.2 | 0.002061 | 2.869 | -18.3 | 2.3 |
| 6 | 0.001116 | 3.057 | 0.000901 | 3.121 | -19.3 | 2.1 | 0.000933 | 3.111 | -16.4 | 1.8 |
| 7 | 0.068092 | 1.490 | 0.062899 | 1.531 | -7.6 | 2.8 | 0.065885 | 1.507 | -3.2 | 1.1 |
| 8 | 0.044312 | 1.703 | 0.039931 | 1.751 | -9.9 | 2.8 | 0.039931 | 1.751 | -9.9 | 2.8 |
| 9 | 0.022750 | 2.000 | 0.023401 | 1.988 | 2.9 | -0.6 | 0.023050 | 1.994 | 1.3 | -0.3 |
| 10 | 0.056717 | 1.583 | 0.051353 | 1.632 | -9.5 | 3.1 | 0.056954 | 1.581 | 0.4 | -0.1 |
| 11 | 0.032937 | 1.839 | 0.027787 | 1.914 | -15.6 | 4.1 | 0.031516 | 1.859 | -4.3 | 1.1 |
| 12 | 0.019365 | 2.089 | 0.014845 | 2.174 | -19.2 | 4.1 | 0.017283 | 2.113 | -5.9 | 1.2 |

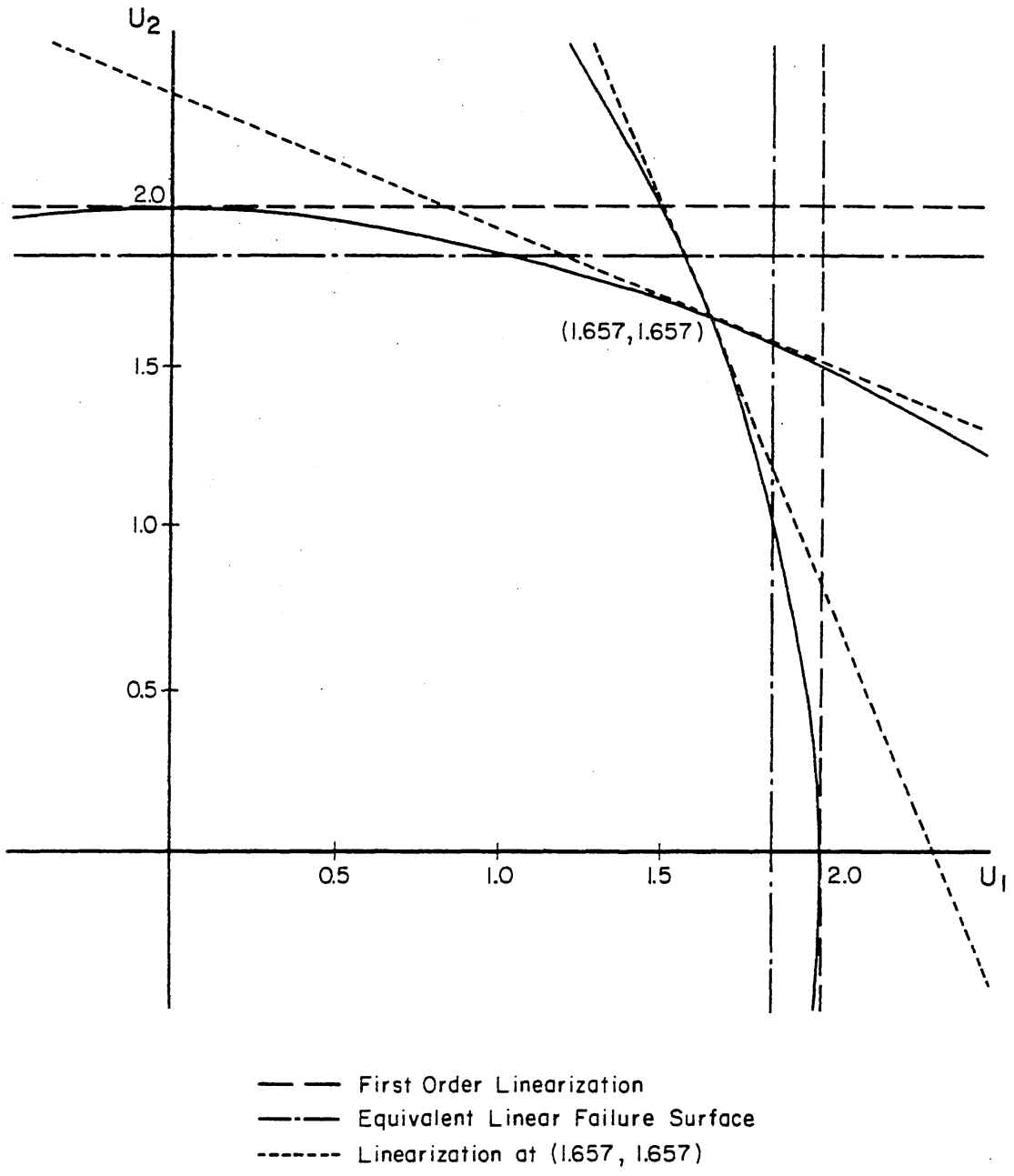


Fig. 5.1 Linearization of Failure Surfaces

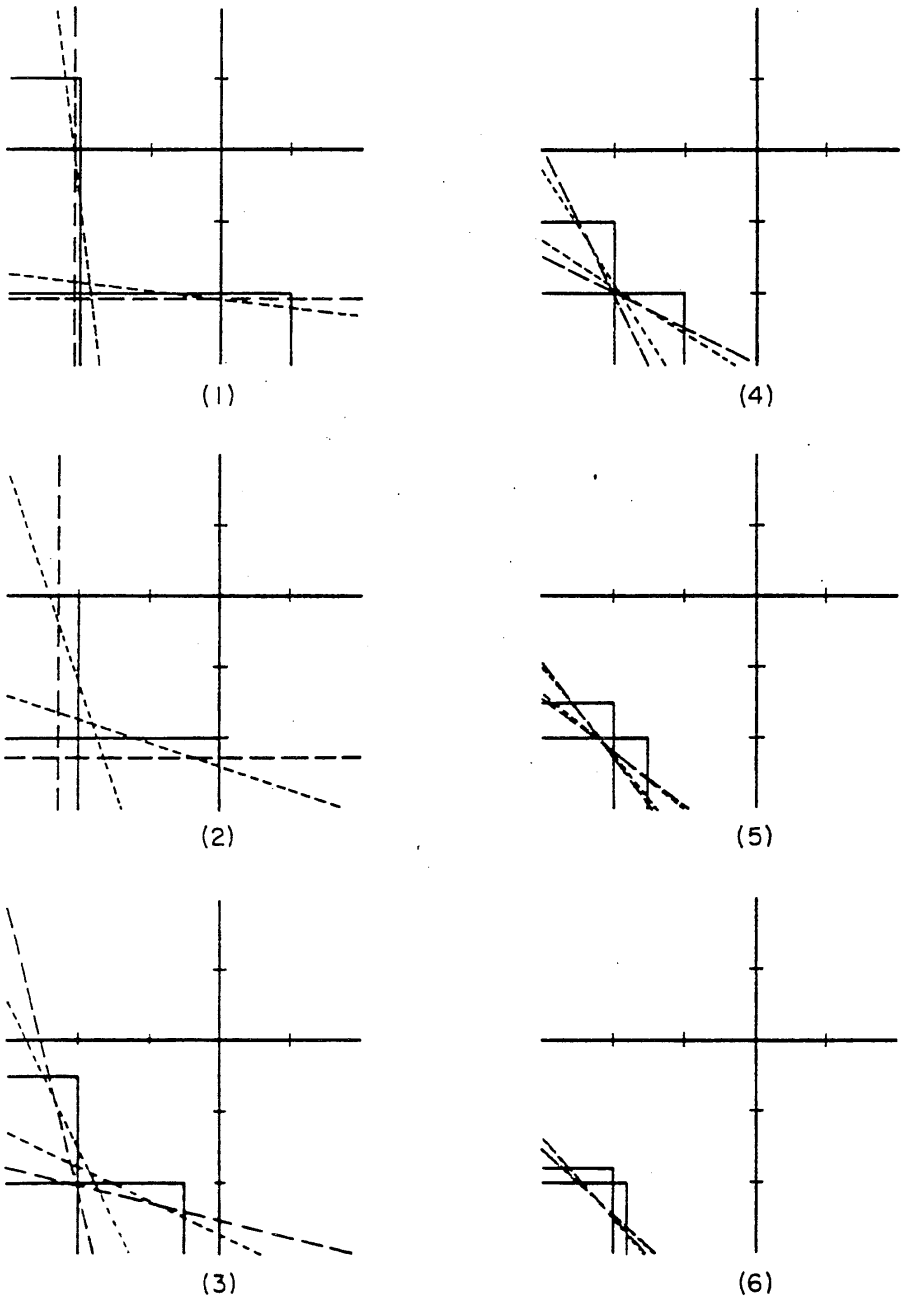


Approximate Linear Failure Surfaces

------- Direction Cosines as Sensitivity Coefficients

— — — Direction Cosines of Failure Point of Mode

Fig. 5.2 Linearization of Failure Modes

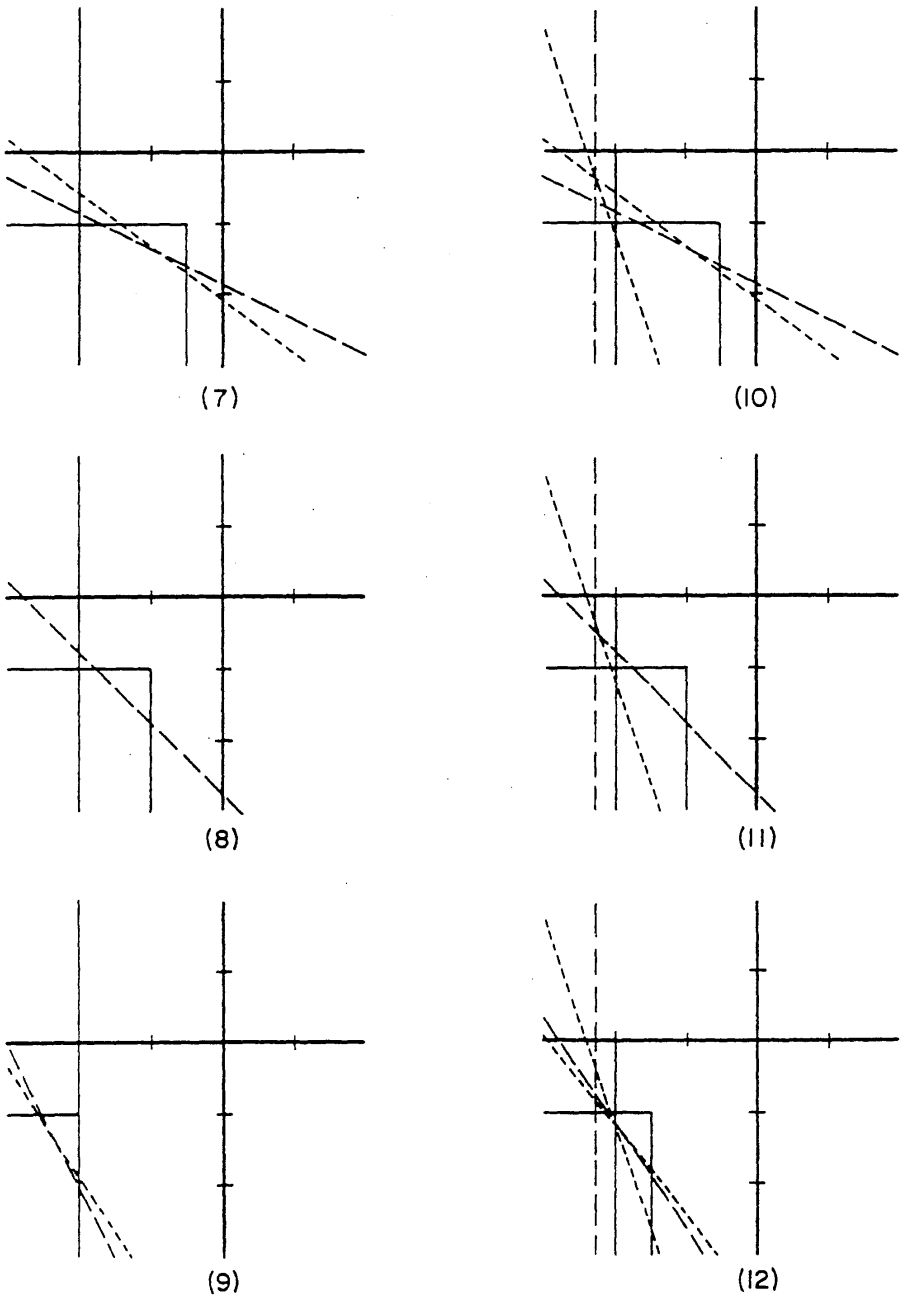


Approximate Linear Failure Surfaces

------- Direction Cosines as Sensitivity Coefficients

— — — Direction Cosines of Failure Point of Mode

Fig. 5.2 (continued)

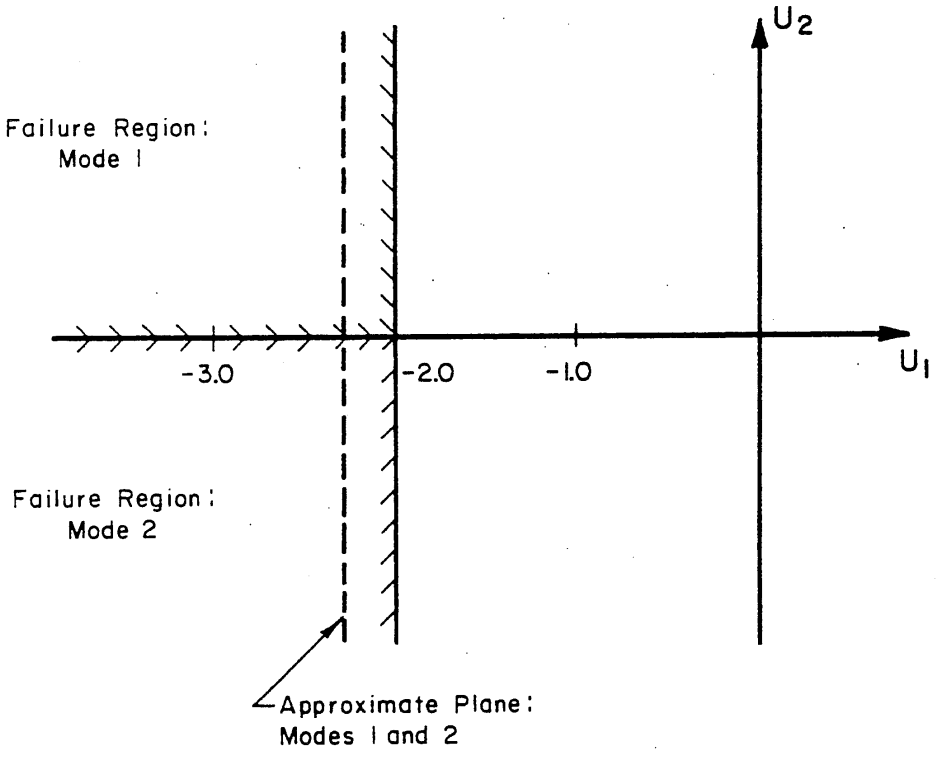


Fig. 5.3 Identical Approximate Planes

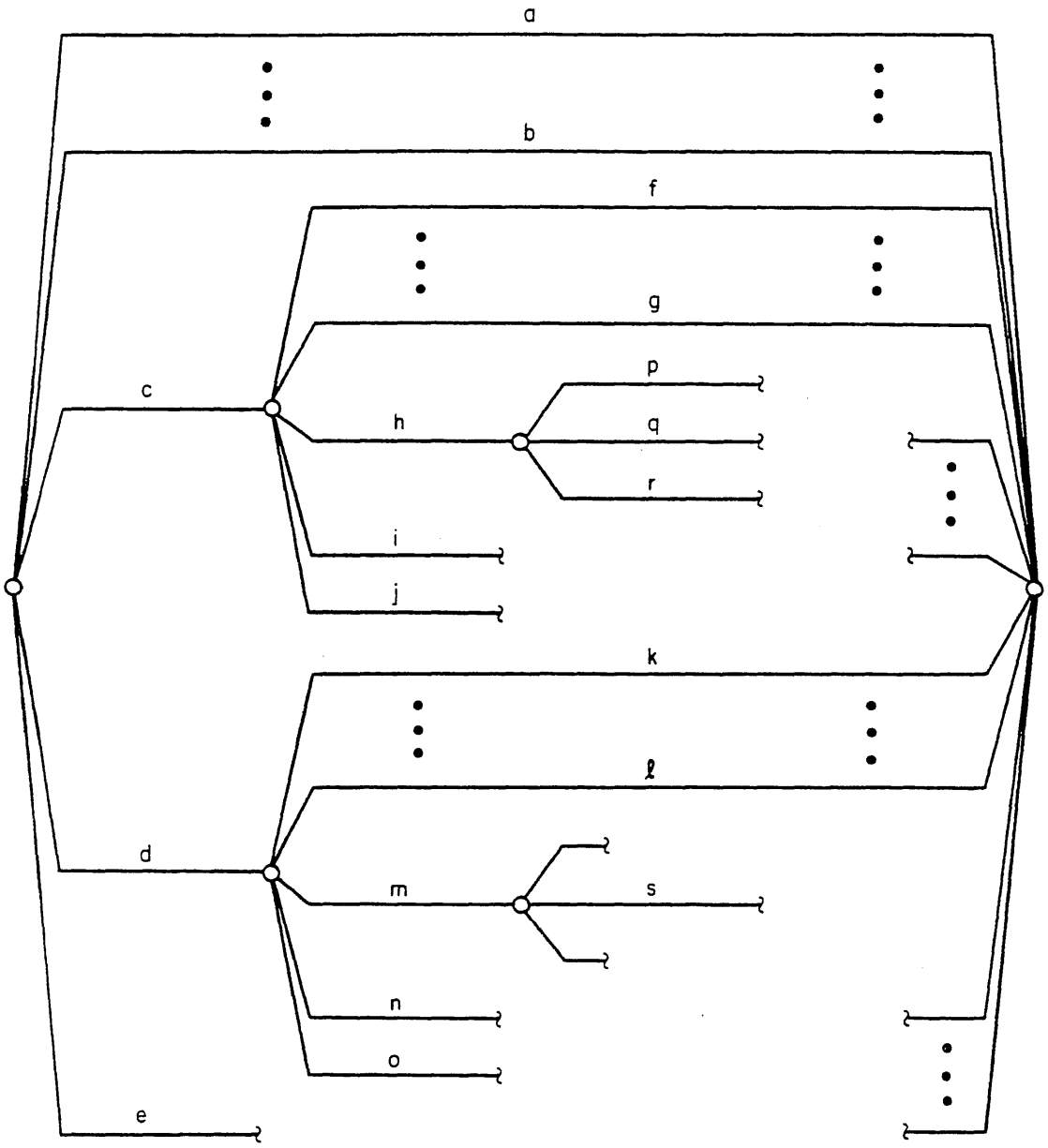


Fig. 5.4 Failure Graph for Illustrating Algorithm

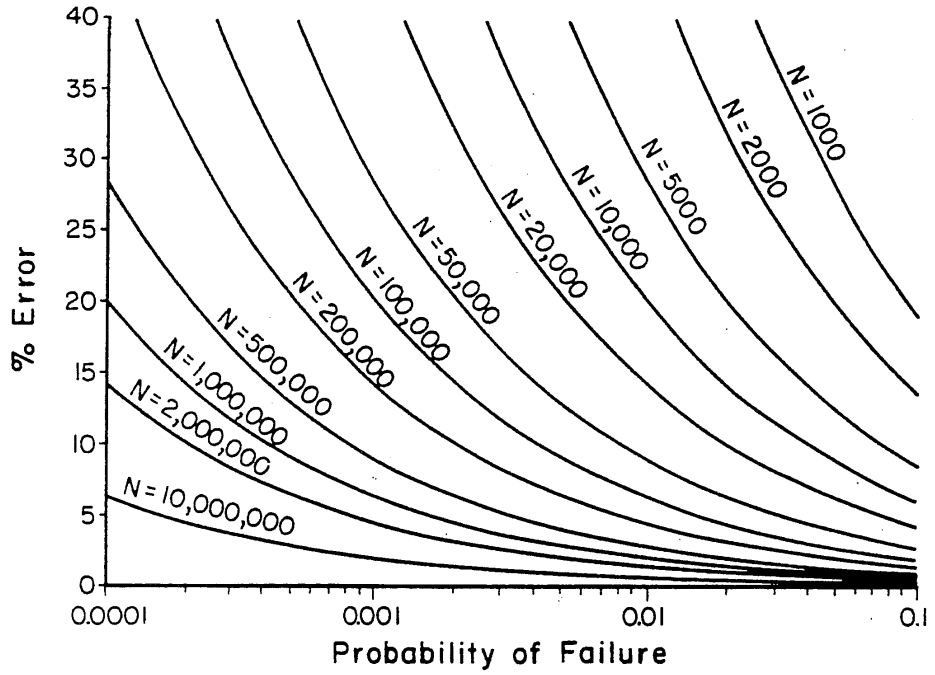


Fig. 5.5 Error in Probability of Failure from Monte Carlo Calculations

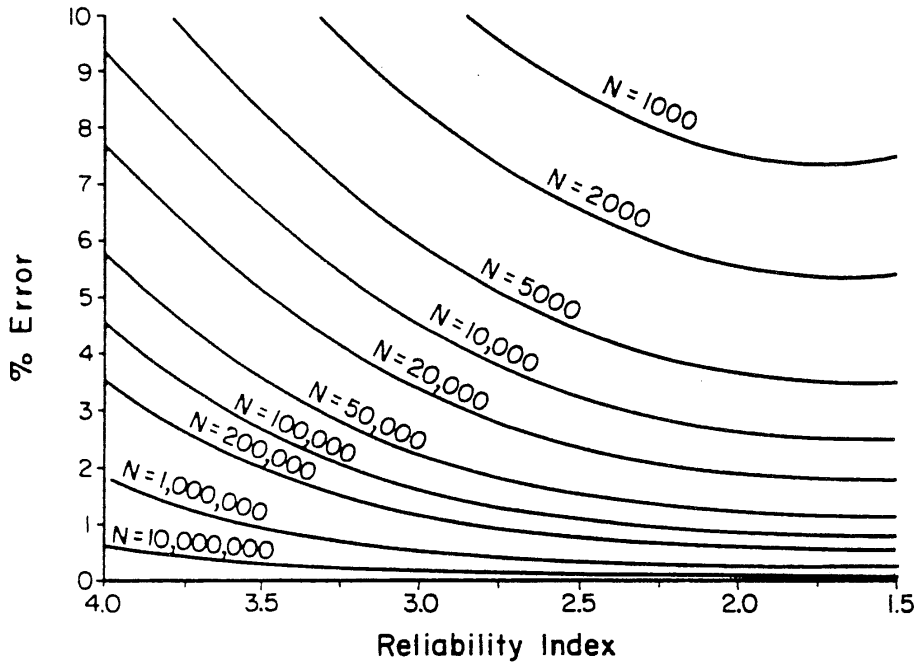


Fig. 5.6 Error in Reliability Index from Monte Carlo Calculations

# CHAPTER 6

# ILLUSTRATIVE APPLICATIONS

## 6.1 Introductory Comments

A number of different types of structures, including frames and trusses, are presented and analyzed using the methods developed in Chapter 5. The structures contain components that exhibit both ductile and brittle behavior and are selected to show how the reliability analysis techniques developed in this study can be applied to practical problems. In particular, the use of the stable configuration approach is shown to be an effective tool for estimating the probability of failure of structural systems. Where feasible, the results are verified with Monte Carlo simulations.

The applications also serve to illustrate some of the weaknesses of the present computational methods, particularly with regard to the stable configuration approach. Although the stable configuration approach is theoretically conservative, the numerical results do not necessarilly bear this out. This is due to the many approximations involved in the computations, e.g., using first-order methods to linearize each branch and using the geometric average of the bounds as a point estimate.

## 6.2 A Four-Member Parallel Structure

Consider the simple system shown in Fig. 6.1. This problem is included in the work of Daniels (1945). The fracture strengths of the members are assumed to be statistically independent random variables with identical lognormal distributions with $\mu$=5.0 kips, $\delta$=0.20 ($\lambda$=1.59,

$\zeta \approx \delta = 0.20$). The load is statistically independent of the member strengths and normally distributed with $\mu = 12.0$ kips, $\sigma = 0.30$.

The members are assumed to fail in a brittle manner; i.e., by brittle fracture, such that upon failing the capacity of the member instantaneously drops to zero. The exact cumulative distribution function of the system is, following Daniels (1945):

$$F_R(r) = 24F(r)F(\tfrac{r}{2})F(\tfrac{r}{3})F(\tfrac{r}{4}) - 12[F(r)F(\tfrac{r}{2})F^2(\tfrac{r}{4}) + F(r)F^2(\tfrac{r}{3})F(\tfrac{r}{4}) + F^2(\tfrac{r}{2})F(\tfrac{r}{3})F(\tfrac{r}{4})] + 4[F(r)F^3(\tfrac{r}{4}) + F^3(\tfrac{r}{3})F(\tfrac{r}{4})] + 6F^2(\tfrac{r}{2})F^2(\tfrac{r}{4}) - F^4(\tfrac{r}{4}) \quad (6.1)$$

where $F(.)$ is the cumulative distribution function of a member strength. The probability of failure of the system may be obtained by numerically integrating the equation,

$$P_f = \int_{-\infty}^{\infty} F_R(s) f_S(s) ds \quad (6.2)$$

where $f_S(s)$ is the probability density function of the load S. For the statistics given above, the probability of failure is determined to be $P_F = 0.1490$ and the reliability index ($\beta = -\Phi^{-1}(p_F)$) is $\beta = 1.041$.

### 6.2.1 Failure Mode Analysis

The reliability of this structure will now be obtained using the failure mode and stable configuration approaches, and also through Monte Carlo simulations. Observe that the structure is monotonically loaded and thus no constraints are needed in the formulation.

There are 24 different failure modes corresponding to the 24 different sequences in which the members could fail. The branches of the first failure mode (namely, members failing in the sequence $1 \to 2 \to 3 \to 4$) are linearized using first order methods as shown below:

| Event | $\beta$ | Direction Cosines $\alpha_{R_1}$ | $\alpha_{R_2}$ | $\alpha_{R_3}$ | $\alpha_{R_4}$ | $\alpha_S$ |
|---|---|---|---|---|---|---|
| $R_1 - S/4 < 0$ | 1.531 | 0.6630 | 0.0 | 0.0 | 0.0 | -0.7486 |
| $R_2 - S/3 < 0$ | 0.593 | 0.0 | 0.6020 | 0.0 | 0.0 | -0.7985 |
| $R_3 - S/2 < 0$ | -0.533 | 0.0 | 0.0 | 0.4941 | 0.0 | -0.8694 |
| $R_4 - S < 0$ | -1.896 | 0.0 | 0.0 | 0.0 | 0.2851 | -0.9585 |

Bounds on the reliability index of this mode are:

Second-Order Bounds: $1.675 \geq \beta \geq 1.668$

MVNI* Bounds: $1.670 \geq \beta \geq 1.635$

The failure surface of the mode is approximated by a planar surface with a distance to the origin equal to the reliability index of the mode, taken in this case as the arithmetic average of the closest bounds obtained above. The failure point of the mode (in independent standard normal space), obtained through the quadratic programming algorithm of Appendix A, is

$$u^*_{R_1} = -1.107 \; ; \quad u^*_{R_2} = 0.0 \; ; \quad u^*_{R_3} = 0.0 \; ; \quad u^*_{R_4} = 0.0 \; ; \quad u^*_S = 1.249$$

Therefore, the failure surface of this mode would be approximated by a plane with the equation:

$$0.6630U_{R_1} - 0.7486U_S + 1.669 = 0.0 \qquad (6.3)$$

It may be emphasized that six failure modes, all those for which

---

*Multivariate normal integral bounds. See Sect. 3.3.4.

member 1 fails first, will have the failure surface of Eq. 6.3, i.e., none of the branches in the mode beyond the first branch affect the direction cosines of the approximating plane. This result may also be obtained by noting that the correlation coefficient between the first and second branches is $\rho=0.5978$ and $0.593 \leq (0.5978)(1.531)$. Thus, only four failure surfaces need to be considered for determining the system reliability. The probability of failure of the system is determined to be $p_F=0.1316$ and the reliability index $\beta=1.119$. The reliability index is overestimated by 7.5%. This error is primarily due to many of the approximating planes being perfectly correlated and thus some of the modes are essentially neglected.

The estimation of the probability of failure can be improved with the algorithm outlined in Sect. 5.2.4. No branch past the first branch affects the direction cosines of any mode. Therefore, using Eq. 5.3, i.e., including the union of all branches emanating from the node at the end of the first branch, the reliability index for the failure surface representing all modes for which member 1 fails first is determined as:

$$\beta = -\Phi^{-1}(P[\{R_1 \leq \frac{S}{4}\}\{(R_2 \leq \frac{S}{3}) \cup (R_3 \leq \frac{S}{3}) \cup (R_4 \leq \frac{S}{3})\}]) \tag{6.4}$$

The reliability index for the union of the three events in Eq. 6.4 is $\beta=0.095$, and using the direction cosines of any of the individual events in the union (it makes no difference which event is used) the reliability index, Eq. 6.4, is obtained as $\beta=1.582$. Combining the four modes, the system failure probability is $p_F=0.1535$ and the reliability index $\beta=1.021$. This is 1.9% below the correct answer. This error arises from two sources: first, some of the branches in the failure graph were neglected and second, an error is associated with the linearization of the failure surfaces of the individual branches. The reliability index of the first branch is 1.2% less than the correct value (obtained through numerical integration) of $\beta=1.549$. Using this correct reliability index for the first branch results in a reliability index for the system of $\beta=1.040$, which is only 0.1% in error.

The approximate methods for calculating the system reliability are thus shown to be very accurate. The importance of accurately obtaining the component reliabilities is also emphasized.

6.2.2 Stable Configuration Analysis

For this structure there are fifteen cuts that need to be included in the stable configuration approach. Only five, however, will be considered, corresponding to the configurations shown in Fig. 6.2. The probabilities of failure of each of the five cuts and the union of any pair of cuts (off diagonal terms) are tabulated below in the form of a matrix:

| | $C_{a-a}$ | $C_{b-b}$ | $C_{c-c}$ | $C_{d-d}$ | $C_{e-e}$ |
|---|---|---|---|---|---|
| $C_{a-a}$ | 0.1675 | 0.4661 | 0.4661 | 0.4661 | 0.4661 |
| $C_{b-b}$ | | 0.4620 | 0.5100 | 0.5100 | 0.5100 |
| $C_{c-c}$ | | | 0.4620 | 0.5100 | 0.5100 |
| $C_{d-d}$ | symmetric | | | 0.4620 | 0.5100 |
| $C_{e-e}$ | | | | | 0.4620 |

The first, second, and upper third-order bounds are as follows:

| | |
|---|---|
| First-Order Bounds: | $0.0076 \leq p_F \leq 0.1675$ |
| Second-Order Bounds: | $0.1511 \leq p_F \leq 0.1634$ |
| Third-Order Upper Bound: | $p_F \leq 0.1593$ |

By observing that the union of cut a-a and any other two or more cuts is equal to the union of the other cuts and using Eq. 5.5, it is determined that the lower second-order bound gives the correct answer. The difference between the exact probability of failure is due to the linearization of the branches and not including some cuts.

For this particular structure, the redundancy is not very effective as the probability of system failure, $p_F$=0.1511, is not much smaller than the probability of initial damage, $p_D$=0.1675.

6.2.3 Monte Carlo Simulations

The problem was solved also using various Monte Carlo techniques. These solutions serve to demonstrate the usefulness and weaknesses of the Monte Carlo method.

Sample structures and corresponding sample loads were constructed using a random number generator. Since the structure is monotonically loaded, each of the failure modes are examined, irrespective of in which mode the structure will actually fail; failure occurs when the limit state of any mode is exceeded. For example, consider mode 1. If $R_1-S/4<0$, $R_2-S/3<0$, $R_3-S/2<0$, and $R_4-S<0$, then the structure fails. For 1000 and 5000 trials, Monte Carlo estimates of the expected probability of system failure yield $\bar{p}_F=0.1560$ and 0.1434 respectively. The respective errors of the these two estimates are 4.7% and -3.8%, both of which are well within the percentage error expected in light of Fig. 5.5.

Various distributions were used in conjunction with the importance sampling technique of Eq. 5.11. Most distributions, including a uniform distribution (Eq. 5.12), gave poor estimates of the system probability of failure. Almost all estimates were too low or unconservative. Using a normal distribution for the load with $\mu=16.0$ kips, $\sigma=3.6$ kips and the original distributions of the resistances in importance sampling, gave reasonable results. For 100 trials, the estimated mean probability of failure is $\bar{p}_F=0.1445$ (-3.0% error) and for 200 trials, $\bar{p}_F=0.1477$ (-0.9% error). These results seem to indicate that the use of importance sampling for Monte Carlo analysis of structural systems requires great care, particularly with regard to the selection of an appropriate alternate density function for the random variables.

The performance function of the system is

$$g(\underline{X}) = \min\{\max[(R_1-\frac{S}{4}),(R_2-\frac{S}{3}),(R_3-\frac{S}{2}),(R_4-S)], \max[(R_1-\frac{S}{4}),(R_2-\frac{S}{3}),(R_4-\frac{S}{2}),(R_3-S)], \ldots\} \quad (6.5)$$

The first four moments of $g(\underline{X})$ were obtained from 50 simulations. Based on these sample moments, the probability of failure is estimated using both the Gram-Charlier and Edgeworth expansions. In standard form, $g'=(g-\mu_g)/\sigma_g$, the probability $P(g<0)$ or $P(g'<-\mu_g/\sigma_g)$, can be obtained approximately as (Johnson and Kotz, 1970):

With Gram-Charlier Expansion

$$P(g' < x) \simeq \Phi(x) - \frac{1}{6}\sqrt{\beta_1}(x^2 - 1)\phi(x) - \frac{1}{24}(\beta_2 - 3)(x^3 - 3x)\phi(x) \quad (6.6)$$

With Edgeworth Expansion

$$P(g' < x) \simeq \Phi(x) - \frac{1}{6}\sqrt{\beta_1}(x^2 - 1)\phi(x) - \frac{1}{24}(\beta_2 - 3)(x^3 - 3x)\phi(x) - \frac{1}{72}\beta_1(x^5 - 10x^3 + 15x)\phi(x) \quad (6.7)$$

where:

$$\beta_1 = \frac{(\mu_3)_g}{(\mu_2)_g^{3/2}} \quad ; \quad \beta_2 = \frac{(\mu_4)_g}{(\mu_2)_g^2}$$

$\mu_r$ = sample $r^{th}$ moment about the mean.

Based on the moments obtained from the 50 samples, the probability of failure was obtained as follows: $p_F=0.1407$ based on the Gram-Charlier expansion (-5.5% error), and $p_F=0.1410$ based on the Edgeworth expansion (-5.4% error).

## 6.3 A Fixed-Fixed Beam

The reliability of the fixed-fixed beam shown in Fig. 6.3 is analyzed under five different assumptions of the material behavior. The uniformly applied load on the structure is normally distributed with

$\mu$=2.0 kips/ft, $\delta$=0.25, and in all cases is statistically independent of the material properties. The structure is monotonically loaded and thus can be analyzed without consideraton of any constraints.

### 6.3.1 Case I--Ductile Sections

Assume the moment-curvature relation to be elastic-perfectly plastic. The beam would collapse when a mechanism of three hinges is formed. Only one failure mode, composed of a single branch, therefore, needs to be considered. The problem reduces to finding the reliability of a component.

The plastic moments at all the sections are assumed to be lognormally distributed with $\mu_M$=20.0 kip-ft, $\delta_M$=0.10. The following correlation coefficients between the moment capacities at sections A, B, and C are assumed.

$$\rho_{M_A M_B} = 0.40 \quad ; \quad \rho_{M_A M_C} = 0.70 \quad ; \quad \rho_{M_B M_C} = 0.70$$

The performance function is

$$g = M_A + kM_B + (1 + k)M_C - \frac{wL^2}{2}\frac{k}{1+k} \tag{6.8}$$

where:

$$k = \sqrt{\frac{M_A + M_C}{M_B + M_C}}$$

Using first-order methods, the probability of failure is estimated to be $p_F$=1.281x10$^{-6}$ and $\beta$=4.703.

### 6.3.2 Case II--Brittle Sections

Assume that the random variables have the same distributions as in Case I but the material behaves in a brittle manner, i.e., once the ultimate moment at a section is reached, the capacity drops immediately

to zero. In this case, there will be six failure modes, corresponding to the six possible sequences of failure of the critical sections A, B, and C. Two of these, corresponding to section C failing first, would not be significant ($p_F < 10^{-12}$).

Consider the mode for which section A fails first, followed by section B, and finally section C. The direction cosines of the branch corresponding to the failure of section A are not affected by either of the other two branches (failures of sections B and C). In fact, the reliability index of this mode ($\beta$=2.852) is the same (to four significant figures) as the reliability index of the first branch, i.e., section A fails. Thus, the probability of failure of the system is essentially the probability that either section A or section B fails, which is $p_F$=0.003620 and $\beta$=2.686. Analyzing the structure using the stable configuration approach yields the same result. For all practical purposes, therefore, the probability of failure of the system is the same as its initial damage probability.

Twenty five thousand Monte Carlo simulations were performed. From these the probability of failure was calculated to be $\bar{p}_F$=0.00312 and $\beta$=2.74. The error in this reliability index should be less than 4% (see Fig. 5.6).

### 6.3.3 Case III--Combined Ductile and Brittle Sections

In this case, the moment-curvature diagram of the beam sections is as shown in Fig. 6.4, i.e., the material behaves in a ductile manner until some ultimate curvature is reached, and then brittle failure occurs. Five failure modes may be considered as follows:

| Mode | Definition of Failure |
|---|---|
| 1. | Collapse through plastic mechanism (3 hinges--at A, B, C) prior to reaching $\phi_u$ anywhere on the beam. |
| 2. | Curvature at section A > $\phi_u$; collapse through plastic mechanism (2 hinges--at B, C). |

3. Curvature at section B > $\phi_u$; collapse through plastic mechanism (2 hinges--at A, B).
4. Curvature at section A > $\phi_u$; followed by curvature at section B > $\phi_u$; plastic yielding at section C.
5. Curvature at section A > $\phi_u$; followed by curvature at section B > $\phi_u$; plastic yielding at section C.

There are other possible failure modes, such as the limiting curvature being reached at one section before yielding occurs at that section, but these will not be significant, and may be neglected. The failure graph is shown in Fig. 6.5.

For a concrete beam, the rotation capcity will be approximately

$$\theta = \frac{d}{2}(\phi_u - \phi_y) = \frac{d}{2}(\phi_u - \frac{M_u}{k}) \tag{6.9}$$

where d is the depth to the reinforcement and the other parameters are defined in Fig. 6.4. The performance function for the first event of the second mode is formulated as the amount of load that can be carried until the limiting curvature is reached minus the applied load, i.e.,

$$g = \frac{12\ \bar{M}_u}{L^2}(1 - \frac{d}{L}) + \frac{12kd\ \phi_u}{L^3} - w \tag{6.10}$$

All random variables are normally distributed with the following statistics:

| Variable | Mean | C.O.V. |
|---|---|---|
| $M_u^+$ | 12.0 ft-k | 0.10 |
| $M_u^-$ | 14.0 ft-k | 0.10 |
| $\phi_u^A$ | 0.10 $ft^{-1}$ | 0.25 |
| $\phi_u^B$ | 0.10 $ft^{-1}$ | 0.25 |

All random variables are assumed to be statistically independent except that:

$$\rho_{M_u^- M_u^+} = 0.30 \quad ; \quad \rho_{\phi_u^A \phi_u^B} = 0.50$$

and the negative moment capacities at the two ends of the beam (sections A and B) are perfectly correlated. The value of d is assumed to be deterministic and equal to 8 inches.

With the failure mode approach, the probability of failure is determined to be $p_F$=0.01451 and $\beta$=2.183. Using the stable configuration approach, four cuts of the failure graph need to be considered as shown in Fig. 6.5. It is found that only $C_{a-a}$ contributes significantly to the system reliability. The calculated probability of failure is the same as that obtained through the failure mode approach.

Based on 10,000 Monte Carlo trials, the mean probability of failure was determined to be $p_F$=0.0134 and $\beta$=2.21; according to Fig. 5.6, the error in the estimated reliability index should be less than 4%.

### 6.3.4 Case IV--Semi-Ductile Sections

The moment capcity of the connections at the ends of the beam may decrease abruptly to a fraction of its ultimate capacity upon failure, i.e., the moment capcity does not drop to zero. Assume that the ultimate moment capcity, $M_1$, at both ends is lognormally distributed

with $\mu_{M_1}$ =20.0 ft-kip, $\delta_{M_1}$ =0.10, and $\rho_{M_1 M_1}$ =0.80. The residual moment, $M_2$, is assumed to follow a truncated normal distribution (see Johnson and Kotz (1970) for details):

$$F_{M_2}(m_2) = \frac{\Phi(\frac{m_2 - \xi}{\alpha}) - \Phi(\frac{a - \xi}{\alpha})}{\Phi(\frac{b - \xi}{\alpha}) - \Phi(\frac{a - \xi}{\alpha})} \tag{6.11}$$

where:

$a,b$ = lower and upper truncation values, respectively;

$\xi,\alpha$ = constant parameters assumed to be 15.0 and 1.5, respectively.

Assume the lower truncation point is zero and the upper truncation point is $m_1$, i.e., $a=0$, $b=m_1$.

The moment-curvature relation for the beam is elastic-perfectly plastic; its yield moment is lognormally distributed with $\mu$=16.0 ft-k and $\delta$=0.08. The correlation coefficient between the center yield moment and $M_1$ at either end is assumed to be $\rho$=0.5. Transformation of the random variables to independent standard normal variates can be accomplished through the Rosenblatt transformation (Rosenblatt, 1952).

The failure graph for this structure would be similar to that of Fig. 4.7 with member 1 failing corresponding to $M_1$ at left being exceeded, member 2 failing corresponding to yielding at the center, and member 3 failing corresponding to $M_1$ at right being exceeded. Using the failure mode approach, bounds for the probability of system failure are as follows:

| | |
|---|---|
| Second-Order Bounds: | $0.0002073 \leq p_F \leq 0.0002133$ |
| | $3.531 \geq \beta \geq 3.523$ |
| MVNI Bounds: | $0.0002106 \leq p_F \leq 0.0002238$ |
| | $3.526 \geq \beta \geq 3.510$ |

It is interesting to examine the first mode--$M_1$ at left is exceeded,

$M_1$ at right is exceeded, and the center yields. The second event does not affect the direction cosines of the approximating plane. Thus one may conclude that it is not necessary to examine the third event. However, the third event, namely, the center yielding after $M_1$ has been exceeded at both ends, is the strongest (has the lowest probability of failure). A significant error would have been incurred if the third event was not included.

Based on the stable configuration approach, the probability of failure, using the second-order bounds for the intersection of events, is bounded as follows:

$$0.0002323 \leq p_F \leq 0.0002327$$
$$3.500 \geq \beta \geq 3.500$$

The most significant cut, i.e., the one with the lowest probability of failure, is $C_{d-d,}$ which has a probability of failure of 0.0002691 and $\beta$=3.461.

Based on 300,000 Monte Carlo trials, the mean probability of failure was estimated to be $\bar{p}_F$=0.0002433 and $\beta$=3.488. According to Fig. 5.6, the error in the reliability index should be less than 1%.

### 6.3.5 Case V--General Nonlinear Behavior

In the final case, the beam is assumed to be composed of two rigid links, as shown in Fig. 6.6, connected by nonlinear rotational springs with the following moment-curvature relations:

$$\text{Sections A and B:} \quad M = K \frac{\sigma_o}{\varepsilon_o} \alpha^2 \exp\left(\frac{-\alpha}{\varepsilon_o}\right)$$
$$\text{Section C:} \quad M = K \frac{\sigma_o}{\varepsilon_o} \left(\frac{\alpha}{3}\right)^2 \exp\left(\frac{-\alpha}{3\varepsilon_o}\right) \tag{6.12}$$

where:

$\alpha$ = angle of rotation;

$\sigma_o$ = lognormally distributed random stress with $\mu$=36 ksi, $\delta$=0.1;

$\varepsilon_o$ = lognormally distributed random strain with $\mu$=0.00124, $\delta$=0.1

K = deterministic parameter related to the beam cross section; assumed to be 12.0 $in^3$.

Assume $\rho_{\sigma_o \varepsilon_o}$=0.80. Asuume also that the rotational springs at the end will fail in a brittle manner. The maximum permissable rotation, $\theta_{max}$ is normally distributed with $\mu$=0.004 rad, $\delta$=0.125 and is independent of $\sigma_o$ and $\varepsilon_o$.

In this case, the reliability is evaluated by examining the structure at discrete values of $\theta$, say $\theta_1,\ldots,\theta_k$. A portion of the failure graph along with some of the necessary cuts is shown in Fig. 6.7. The performance function, $g(\theta_i)$, is obtained through virtual work as:

$$g(\theta_i) = \int_0^{\theta_i} M_A d\theta + \int_0^{\theta_i} M_B d\theta + \int_0^{\theta_i} M_C d\theta - \frac{wL^2}{4}\theta_i \qquad (6.13)$$

The value of $\theta$ was discretized between 0.002 and 0.005 at intervals of 0.0005. Using the failure mode approach, bounds to the probability of failure and reliability index were obtained as follows:

| | |
|---|---|
| Second-order Bounds: | $0.01186 \leq p_F \leq 0.01940$ |
| | $2.262 \geq \beta \geq 2.066$ |
| MVNI Bounds: | $0.01610 \leq p_F \leq 0.05012$ |
| | $2.142 \geq \beta \geq 1.644$ |

The geometric average of the two closest bounds may be used as the point estimate of the probability of failure, thus obtaining $p_F$=0.01768 and $\beta$=2.104.

Based on the discretized values of $\theta$ used above, there are seven cuts of the failure graph; the first three are indicated in Fig. 6.7. Using second-order bounds for the intersection of events, bounds for the probability of failure and corresponding reliability index were obtained with the stable configuration approach as follows:

$$0.02516 \leq p_F \leq 0.03124$$
$$1.958 \geq \beta \geq 1.863$$

To verify the results, 8000 Monte Carlo trials were performed. The angle of rotation, $\theta$, was not discretized; instead, the value that maximizes the resistance was determined. On this basis, the mean probability of failure was obtained as $\bar{p}_F$=0.01725 and the reliability index $\beta$=2.115. There should be less than a 4% error in the reliability index in accordance with Fig. 5.6.

Observe in this case that the stable configuration approach overestimates the probability of failure. This would be expected since not all the cuts were included because of the discretization of $\theta$. By considering more cuts (i.e., discretizing $\theta$ at finer intervals) the estimated probability should improve.

## 6.4 A Simple Grid System

A simple two member grid system is shown in Fig. 6.8. The component failures considered are the moment capacity of member 2 being exceeded at sections C, D, or E, and the combined moment and torsional capacity at sections A or B being exceeded in member 1. All failures are assumed to be brittle in nature. The limit state at section A or B is defined by:

$$1.0 - \left(\frac{m}{M}\right)^2 - \left(\frac{t}{T}\right)^2 = 0.0 \qquad (6.14)$$

where:

m = applied moment;

t = applied torque;

M = bending moment capacity;

T = torsional capacity.

Pertinent statistics for the random variables are given in Table 6.1.

This structure is non-monotonically loaded since the failure of some sections may cause the applied load effects at other sections to decrease; for example, after section A fails the torsional load at section B will drop to zero. To examine the error associated with the assumption of monotonic loading, i.e., not including the constraints, large sample Monte Carlo simulations were performed (10,000 trials). On this basis, the same mean probability of failure, $\bar{p}_F$=0.0611, was obtained whether the constraints were included or not. Therefore, the probability of failure obtained assuming the structure is monotonically loaded should give an accurate, although conservative, estimate of the true probability of failure.

The algorithm presented in Sect. 5.2.4 is used to analyze the structure with the failure mode approach. The part of the failure graph considered is shown in Fig. 6.9. The reliability index of each of the branches is also shown in Fig. 6.9 as well as an indication of which branches are insignificant (according to the recommended criteria of Sect. 5.2.4) or do not affect the direction cosines of the mode. Bounds on the system failure probability were obtained as follows:

| | |
|---|---|
| Second-Order Bounds: | $0.04910 \leq p_F \leq 0.06642$ |
| | $1.654 \geq \beta \geq 1.503$ |
| MVNI Bounds: | $0.04721 \leq p_F \leq 0.07158$ |
| | $1.673 \geq \beta \geq 1.464$ |

Using the geometric average of the two closest bounds as a point estimate, the probability of failure is estimated to be $p_F$=0.0571 and the corresponding reliability index $\beta$=1.579, which agrees well with the

Table 6.1 Statistics of Random Variables of Grid System (Fig. 6.8)

| Variable | Distribution | Mean | C.O.V. |
|---|---|---|---|
| $T_A$ | Lognormal | 14.0 ft-k | 0.125 |
| $T_B$ | Lognormal | 14.0 ft-k | 0.125 |
| $M_A$ | Lognormal | 20.0 ft-k | 0.10 |
| $M_B$ | Lognormal | 20.0 ft-k | 0.10 |
| $M_C$ | Lognormal | 20.0 ft-k | 0.10 |
| $M_D$ | Lognormal | 45.0 ft-k | 0.10 |
| $M_E$ | Lognormal | 50.0 ft-k | 0.10 |
| P | Normal | 10.0 kip | 0.25 |

Correlation Coefficient Matrix

| | $T_A$ | $T_B$ | $M_A$ | $M_B$ | $M_C$ | $M_D$ | $M_E$ | P |
|---|---|---|---|---|---|---|---|---|
| $T_A$ | 1.0 | 0.8 | 0.5 | 0.4 | 0.0 | 0.0 | 0.0 | 0.0 |
| $T_B$ | | 1.0 | 0.4 | 0.5 | 0.0 | 0.0 | 0.0 | 0.0 |
| $M_A$ | | | 1.0 | 0.8 | 0.0 | 0.0 | 0.0 | 0.0 |
| $M_B$ | | | | 1.0 | 0.0 | 0.0 | 0.0 | 0.0 |
| $M_C$ | | | | | 1.0 | 0.5 | 0.6 | 0.0 |
| $M_D$ | | symmetric | | | | 1.0 | 0.5 | 0.0 |
| $M_E$ | | | | | | | 1.0 | 0.0 |
| P | | | | | | | | 1.0 |

result of Monte Carlo simulations.

Three cuts of the failure graph are considered with the stable configuration approach, as shown in Fig. 6.9. The bounds and point estimates of the probability of failure of each of the cuts are as follows:

| | Bounds | Point Estimate |
|---|---|---|
| $C_{a-a}$ | $0.0501 \leq p_F \leq 0.0652$ | 0.0571 |
| $C_{b-b}$ | $0.2130 \leq p_F \leq 0.2149$ | 0.2141 |
| $C_{c-c}$ | $0.1413 \leq p_F \leq 0.1511$ | 0.1461 |

The lower and upper second-order bounds for the probability of an intersection are identical and yield a probability of failure of $p_F=0.0570$. In this case, therefore, the redundancy has little positive effect, as the failure probability is $p_F=0.0570$ versus the initial damage probability, $P[C_{a-a}]$, of $p_D=0.0571$.

## 6.5 A Simple Rigid Frame

Consider the one-story one-bay frame shown in Fig. 6.10. The probability of collapse through plastic mechanisms for this same structure was analyzed by Ma and Ang (1981). It is assumed that the fully plastic moment capacities of the columns are perfectly correlated and are statistically independent of the moment capacity of the beam.

For the present example, it is further assumed that the base plates can fail in a brittle manner; the capacities of the base plates are assumed to be statistically independent of each other and of the member resistances. All random variables are assumed to be normally distributed with the following statistics.

| Variable | Mean | C.O.V. |
|---|---|---|
| $M_1$ | 360 ft-k | 0.15 |
| $M_2$ | 480 ft-k | 0.15 |
| $M_3$ | 400 ft-k | 0.20 |
| $M_4$ | 400 ft-k | 0.20 |
| $S_1$ | 100 kip | 0.10 |
| $S_2$ | 50 kip | 0.30 |

6.5.1 Failure Mode Analysis

For structural analysis purposes, the columns are specified to be W14x68 sections and the beam to be a W24x62 section. Under these conditions, there are at least 132 possible failure modes.

Assuming that the loading is monotonic, and using the algorithm outlined in Sect. 5.2.4, 34 modes were obtained. Among the 132 modes, 41 modes were eliminated as not being significant, whereas other modes were neglected because some of the branches do not have any effect on the direction cosines of the corresponding mode. Based on the 34 modes identified, bounds to the system probability of failure were obtained by failure mode analysis as follows:

| | |
|---|---|
| Second-Order Bounds: | $0.05617 \leq p_F \leq 0.1516$ |
| | $1.588 \geq \beta \geq 1.030$ |
| MVNI Bounds: | $0.06792 \leq p_F \leq 0.2220$ |
| | $1.491 \geq \beta \geq 0.766$ |

Using the geometric average of the two closest bounds, a point estimate is $p_F$=0.1015 and $\beta$=1.273. In this case, the wideness of the bounds is due to the high probability of failure.

6.5.2 Stable Configuration Analysis

The stable configuration approach can be used effectively to obtain the probability of failure of the frame structue. In this case, only two cuts are considered, the cut corresponding to the initial damage, where damage is defined as the brittle failure of a base plate, and the cut through all branches representing plastic collapse and all branches representing failures after the right base plate fails. To simplify the calculations, the events in each of the cuts corresponding to failure of a base plate after at least one plastic hinge has formed are not considered. Although this introduces unconservatism, it is counteracted by the conservative error introduced using only two cuts and the conservatism introduced in ignoring the non-monotonic loading. The unconservatism introduced is also small since the events neglected are highly correlated with the event of a base plate failing before any plastic hinge forms. Also, many of the events neglected are insignificant.

Calling the two cuts a-a and b-b respectively, the following point estimates are obtained:

$$P[C_{a-a}] = 0.1324 \; ; \quad P[C_{b-b}] = 0.3221 \; ; \quad P[C_{a-a} \cup C_{b-b}] = 0.3611$$

A point estimate of the probability of failure of the system is, therefore, $p_F=0.0934$ and $\beta=1.320$. Including other cuts in the formulation, e.g., the cut corresponding to the stable configurations associated with the left base plate failure, did not change the estimated probability of failure. The result agrees well with the result of the failure mode analysis of Sect. 6.5.1. This also serves to illustrate that a good estimate of the system probability of failure can be obtained by including only a limited number of cuts.

6.5.3 Monte Carlo Analysis

To examine the effect of non-monotonic loading, 200 Monte Carlo trials were performed. The reason for the relatively small number of Monte Carlo simulations was the complicated analysis required when taking into account the non-monotonic loading, e.g., including the constraints in the formulation. This should be sufficient to examine the effect or error of monotonic loading.

Among the 200 trials, 16 failures were observed using the monotonic loading formulation, giving a mean probability of failure of $\bar{p}_F=0.080$. Taking into account the non-monotonic loading and assuming that the structure is loaded along path B in Fig. 4.10 ($S_1$ is applied followed by $S_2$), yielded 13 failures or a mean failure probability of $\bar{p}_F=0.065$. Alternatively, assuming the structure is loaded along path A ($S_2$ is applied and then $S_1$) yielded the same 13 failures plus one additional failure for a mean failure probability of $\bar{p}_F=0.070$. The additional failed structure was not obtained under the assumption of monotonic loading. The failed structure corresponded to the right base plate failing; the two loads then provided counteracting moments at the left base. The full load $S_1$ provided enough of a counteracting moment to prevent failure. However, the vertical load that caused failure at the right base plate did not provide enough of a counteracting moment to prevent failure of the left base plate. After failure of the left base plate, the structure collapsed. The possibility of a counteracting moment not being present was not taken into account in the monotonic loading formulation and therefore this failure was overlooked.

In this example, radically different loading paths apparently had little effect on the reliability of the structure. Also, assuming monotonic loading, the probability of failure is overestimated by about 20%.

## 6.6 An Unsymmetrical Two-Story Two-Bay Frame

The unsymmetrical two-story two-bay frame, shown in Fig. 6.11, considered by Ma and Ang (1981) is modified to include the possiblity of some components failing in a brittle manner. Similar to the simple framed structure in Sect. 6.5, it is assumed that failure will occur through the formation of plastic hinge mechanisms, and the base plates may fail in a brittle manner. The statistics of the load and resistance random variables are summarized in Table 6.2. All variables are assumed to be statistically independent. Sections labeled with the same symbol in Fig. 6.11 are assumed to be perfectly correlated.

The structure is subject to some non-monotonic loading. However, the probability of failure can be estimated with the stable configuration approach assuming monotonic loading.

Three cuts of the failure graph are used with the stable configuration analysis. The first cut, a-a, corresponds to the initial configuration of the structure, i.e., cutting through all branches emanating from the initial node. From the analysis of this cut it was determined that the probability of failure of the base plates at the center and on the right ($M_7$ and $M_8$) was much higher than the failure probability of the base plate on the left ($M_6$). Therefore, two more cuts were included (cuts b-b and c-c) corresponding to the configurations with the center base plate failed and the right base plate failed, respectively.

Based on the results of Sect. 6.5 and in order to simplify the calculations, the failure of the base plate after the formation of a plastic hinge somewhere in the structure was not considered. Point estimates of the probabilities of failure for each of the cuts and the union of any two cuts are as follows:

| | $C_{a-a}$ | $C_{b-b}$ | $C_{c-c}$ |
|---|---|---|---|
| $C_{a-a}$ | 0.013337 | 0.034010 | 0.038921 |
| $C_{b-b}$ | | 0.029404 | 0.055266 |
| $C_{c-c}$ | | | 0.036917 |

Table 6.2 Statistics of Random Variables of Two-Story Two-Bay Frame (Fig. 6.11)

| Variable | Mean | C.O.V. |
|---|---|---|
| $M_1$ | 100 ft-k | 0.15 |
| $M_2$ | 190 ft-k | 0.15 |
| $M_3$ | 90 ft-k | 0.15 |
| $M_4$ | 110 ft-k | 0.15 |
| $M_5$ | 150 ft-k | 0.15 |
| $M_6$ | 140 ft-k | 0.20 |
| $M_7$ | 140 ft-k | 0.20 |
| $M_8$ | 140 ft-k | 0.20 |
| $F_1$ | 38 kip | 0.15 |
| $F_2$ | 20 kip | 0.25 |
| $F_3$ | 26 kip | 0.25 |
| P | 7 kip | 0.25 |

Note: All random variables are statistically independent.

Observe that

$$P[C_{a-a} \cup C_{b-b} \cup C_{c-c}] = P[C_{b-b} \cup C_{c-c}]$$

Therefore,

$$\begin{aligned} p_F &= P[C_{a-a}]+P[C_{b-b}]+P[C_{c-c}]-P[C_{a-a} \cup C_{b-b}]-P[C_{a-a} \cup C_{c-c}] \\ &\quad -P[C_{b-b} \cup C_{c-c}]+P[C_{a-a} \cup C_{b-b} \cup C_{c-c}] \\ &= P[C_{a-a}]+P[C_{b-b}]+P[C_{c-c}]-P[C_{a-a} \cup C_{b-b}]-P[C_{a-a} \cup C_{c-c}] \end{aligned} \quad (6.15)$$

Thus, the probability of failure is $p_F=0.006727$ and the corresponding reliability index is $\beta=2.377$.

The above estimate appears reasonable for two reasons. First, the inclusion of several other cuts did not have any noticeable effect on the previously computed bounds. Secondly, the probability of plastic collapse ignoring the possibility of base plate failures is $p_F=0.006122$, which is slightly less than the above result as expected. It is highly likely that a plastic hinge will form in a column before the corresponding base plate fractures; therefore, it is reasonable that there would only be a slight increase in the probability of failure when including the possibility of base plate failures.

## 6.7 A Two-Tier Truss

A two-tier truss similar to that analyzed by Gorman and Moses (1979) is considered. The structure is shown in Fig. 6.12 and the statistics of the random variables are given in Table 6.3. The structural members are assumed to be ductile and collapse may occur through the formation of plastic mechanisms. However, the cross bracings may also fail through brittle fracture if they are loaded in tension. All load and resistance variables are assumed to be

Table 6.3 Statistics of Random Variables of Two-Tier Truss (Fig. 6.12)

| Member | Area (Sq. in.) | Tension | | Compression | |
|---|---|---|---|---|---|
| | | Mean (kips) | C.O.V. | Mean (kips) | C.O.V. |
| 1 | 2.0 | 40.0 | 0.10 | 22.0 | 0.10 |
| 2 | 1.0 | 20.0 | 0.10 | 11.0 | 0.10 |
| 3 | 1.0 | 20.0 | 0.10 | 11.0 | 0.10 |
| 4 | 2.0 | 40.0 | 0.10 | 22.0 | 0.10 |
| 5 | 0.8 | 15.0 | 0.10 | 8.0 | 0.10 |
| 6 | 0.8 | 15.0 | 0.10 | 8.0 | 0.10 |
| 7 | 0.6 | 13.0 | 0.10 | 2.5 | 0.10 |
| 8 | 0.6 | 13.0 | 0.10 | 2.5 | 0.10 |
| 9 | 0.6 | 13.0 | 0.10 | 2.5 | 0.10 |
| 10 | 0.6 | 13.0 | 0.10 | 2.5 | 0.10 |

| | Mean | C.O.V. |
|---|---|---|
| S (Load) | 4.0 kips | 0.20 |
| Brittle Fracture | 13.0 kips | 0.15 |

Note: All random variables are statistically independent.

statistically independent normal variates.

Furthermore, there is a 0.025% chance that the compression bracings will fail in a brittle manner independently of the applied load. The cause of this failure could be due to enviromental causes, e.g., wave action or ice loading in an offshore tower, or this could be a means for taking account of construction errors. The performance function for this failure is simply,

$$g(\underline{X}) = Z \tag{6.16}$$

where Z is a normal variate with $\mu$=3.481, $\sigma$=1.00.

The probability of failure of this system is evaluated with the stable configuration approach and assuming montonic loading. Four cuts are considered, corresponding to the configurations of no damage, member 8 failed in a brittle manner, member 10 failed in a brittle manner, and both members 8 and 10 failed in a brittle manner. Point estimates of the probabilities of failure for each of the cuts and the union of any pairs of cuts are as follows:

| | $C_{a-a}$ | $C_{b-b}$ | $C_{c-c}$ | $C_{d-d}$ |
|---|---|---|---|---|
| $C_{a-a}$ | 0.001401 | 0.013127 | 0.010633 | 0.021214 |
| $C_{b-b}$ | | 0.012880 | 0.021153 | 0.020969 |
| $C_{c-c}$ | | | 0.010385 | 0.020969 |
| $C_{d-d}$ | | | | 0.020724 |

Define

$$A = C_{a-a} \quad ; \quad B = C_{b-b} \quad ; \quad C = C_{c-c} \quad ; \quad D = C_{d-d}$$

By expanding the intersection of the cuts using Eq. 5.5 and observing the following relations among the cuts,

$$P[A \cup B \cup C] = P[B \cup C] \quad ; \quad P[A \cup B \cup D] = P[A \cup D]$$
$$P[A \cup C \cup D] = P[A \cup D] \quad ; \quad P[A \cup B \cup C \cup D] = P[A \cup D]$$

the probability of failure can be obtained as:

$$P[F] = P[A] + P[B] + P[C] + P[D] - P[A \cup B] - P[A \cup C] - P[B \cup D] - P[C \cup D] + P[A \cup D] \quad (6.17)$$

The probability of failure of the system is then determined to be $P_F$=0.0009060; the corresponding reliability index is $\beta$=3.119.

Based on 100,000 Monte Carlo simulations, the mean probability of failure is $\bar{p}_F$=0.00105 and $\beta$=3.07. According to Fig. 5.6, the error in the reliability index is within 2%. Observe that the Monte Carlo solution gives a higher probability of failure than the stable configuration approach, even though the stable configuration approach is theoretically conservative. The main reason is that in the solution with the stable configuration approach, differences of probabilities that are close to each other are required. Errors in the probabilities of cuts or union of pairs of cuts could significantly affect the resulting system failure probability.

The probability of initial damage, $P[C_{a-a}]$, is about 1.5 times the probability of failure. Thus, the effectiveness of the redundancy in this example is observed.

The significance of the possibility of tensile brittle fracture may be examined by increasing the mean value of the fracture resistance of the cross bracings to 15.0 kips. The corresponding probability of failure is reduced to $p_F$=0.0003682 and $\beta$=3.376. Thus, in this example, a slight increase in the resistance to brittle fracture reduces the probability of failure by about 60%. These results may also be compared with the probability of plastic collapse (i.e., with no brittle failures) which is $p_F$=0.00024158 and $\beta$=3.490.

## 6.8 A Truss Structure

The truss structure shown in Fig. 6.13 is used to illustrate the reliability of systems with deterioration. Assume that collapse of the

structure is caused by the yielding of the members, either in tension or compression, and that the yield capacities in tension and compression of a member are equal. All random variables are assumed to be statistically independent with the statistics given in Table 6.4.

6.8.1 Failure Mode Analysis

Bounds and a point estimate (based on the geometric average of the bounds) of the probability of system failure obtained by failure mode analysis are as follows:

Second-Order Bounds: $0.01749 \leq p_F \leq 0.02085$

$2.109 \geq \beta \geq 2.037$

Point Estimate: $p_F = 0.01909$ ; $\beta = 2.073$

In this case, the second-order bounds are always closer than the corresponding MVNI bounds.

Assume that over time, the lower chord members (members 8, 9, and 10) deteriorate such that these may subsequently fail in a brittle manner; however, the ultimate strength remains the same as the original yield strength. On this basis, the probability of failure of the structure remains the same (to four significant figures).

Suppose that further deterioration takes place so that the strengths of the lower chord members are reduced to $\mu$=17.5 kips, $\sigma$=2.0 kips and that failure will be brittle. The corresponding bounds and point estimate of the system failure probability become:

Second-Order Bounds: $0.04167 \leq p_F \leq 0.04948$

$1.732 \geq \beta \geq 1.650$

Point Estimate: $p_F = 0.04541$ ; $\beta = 1.691$

The structure may remain in service even though the probability of failure has more than doubled. An alternative may be to reduce the allowable load. For instance, from Fig. 6.14, it is seen that if the

Table 6.4 Statistics of Random Variables of Truss Structure (Fig. 6.13)

Resistances*

| Member | Area (sq. in.) | Mean (kips) | C.O.V. |
|---|---|---|---|
| 1 | 9.0 | 28.0 | 0.10 |
| 2 | 3.0 | 11.0 | 0.10 |
| 3 | 3.0 | 11.0 | 0.10 |
| 4 | 3.0 | 11.0 | 0.10 |
| 5 | 3.0 | 11.0 | 0.10 |
| 6 | 9.0 | 28.0 | 0.10 |
| 7 | 9.0 | 25.0 | 0.10 |
| 8 | 6.0 | 20.0 | 0.10 |
| 9 | 6.0 | 20.0 | 0.10 |
| 10 | 6.0 | 20.0 | 0.10 |

*All are lognormally distributed.

Loads**

| Load | Mean (kips) | C.O.V. |
|---|---|---|
| $P_1$ | 12.0 | 0.20 |
| $P_2$ | 12.0 | 0.20 |

**Both are normally distributed.

Note: All random variables are statistically independent.

mean value of the two applied loads is 11.4 kips (C.O.V.=0.20), the probability of failure would be approximately the same as that of the original structure.

With time, further deterioration may take place; suppose that the strengths of the lower chords are reduced to $\mu$=15.0 kips, $\sigma$=2.0 kips. Bounds and point estimate of the probability of failure are now:

Second-Order Bounds: $0.22652 \leq p_F \leq 0.23295$

$0.750 \geq \beta \geq 0.729$

Point Estimate: $p_F = 0.22971$ ; $\beta = 0.740$

At this stage, the structure may require retrofitting; e.g., by adding cables between the lower joints (see Fig. 6.15). The cables are assumed to fail in a ductile manner. The strengths between the cables are assumed to be statistically independent and also independent of the truss members. Suppose the cable strengths follow a lognormal distribution with $\mu$=10.0 kips, $\sigma$=1.0 kips. Assuming that the cables and the original lower chords share the load equally, bounds and point estimate of the probability of failure would be:

Second-Order Bounds: $0.01749 \leq p_F \leq 0.01959$

$2.109 \geq \beta \geq 2.062$

Point Estimate: $p_F = 0.01851$ ; $\beta = 2.085$

The structure is, therefore, slightly safer than it was originally.

The original lower chord members continue to deteriorate so that members 8 and 10 have a strength $\mu$=12.0 kips, $\sigma$=2.0 kips, and member 9 has a strength $\mu$=5.0 kips, $\sigma$=1.5 kips. In this case, the bounds and point estimate of the failure probability become:

Second-Order Bounds: $0.01718 \leq p_F \leq 0.02322$

$2.116 \geq \beta \geq 1.991$

Point Estimate: $p_F = 0.01997$ ; $\beta = 2.054$

The probability of failure is approximately the same as that of the original structure.

The failure mode approach is well suited for this example problem since the failure modes that did not contain failures of the bottom chord members did not change and thus had to be analyzed only once.

### 6.8.2 Stable Configuration Analysis

The reliability of the truss structure can also be obtained with the stable configuration approach. For the original structure, where all members are ductile, the stable configuration formulation will be the same as the failure mode formulation, i.e., each path of the failure graph contains only one branch and thus only one cut is needed.

Up until the time of retrofitting, the stable configuration analysis will yield the same result as the failure mode analysis. Only one cut, the cut representing the initial damage, contributes significantly to the result. Even after retrofitting when the strengths of the lower chords are $\mu$=15.0 kips, $\sigma$=2.0 kips, only the cut representing the initial damage contributes significantly to the result. When further deterioration has taken place such that members 8 and 10 have strengths of $\mu$=12.0 kips, $\sigma$=2.0 kips, and member 9 has a strength of $\mu$=5.0 kips, $\sigma$=1.5 kips, the probability of initial damage is $p_D$=0.18147. Member 9 has a relatively high probability of failure compared with the other members so the cut corresponding to member 9 failed is analyzed to obtain $p_F$=0.02261. The probability of the union of the two cuts is $p_F$=0.18371 yielding a system failure probability of $p_F$=0.02037 and a corresponding reliability index of $\beta$=2.046. Including other cuts did not significantly change the failure probability. This result agress well with that obtained earlier with the failure mode approach.

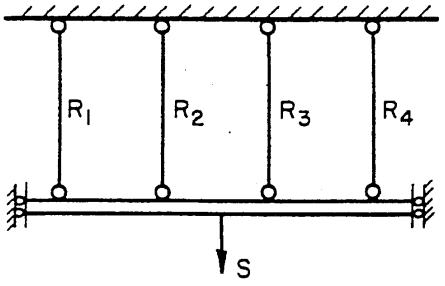


Fig. 6.1 Four-Member Parallel Structure

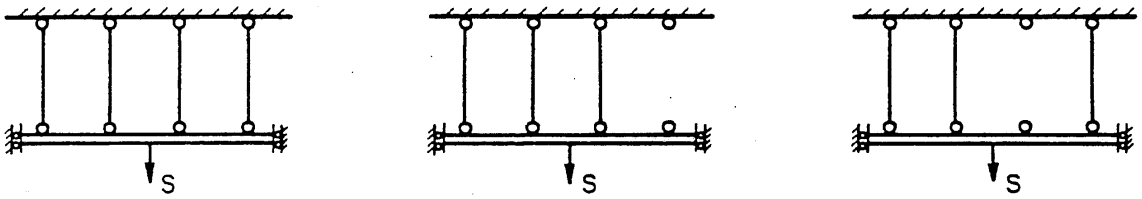


Configuration A Configuration B Configuration C

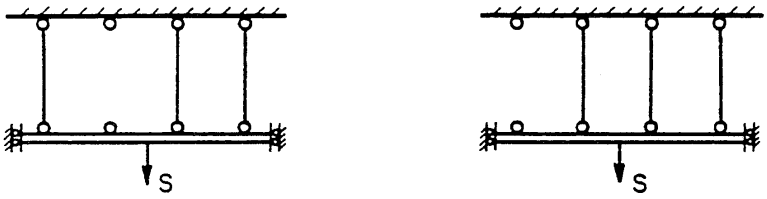


Configuration D Configuration E

Fig. 6.2 Stable Configurations Considered

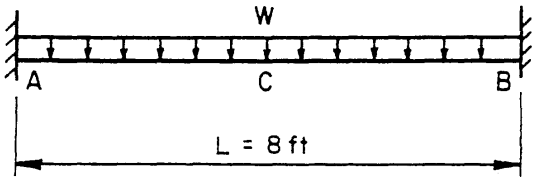


Fig. 6.3 A Fixed-Fixed Beam

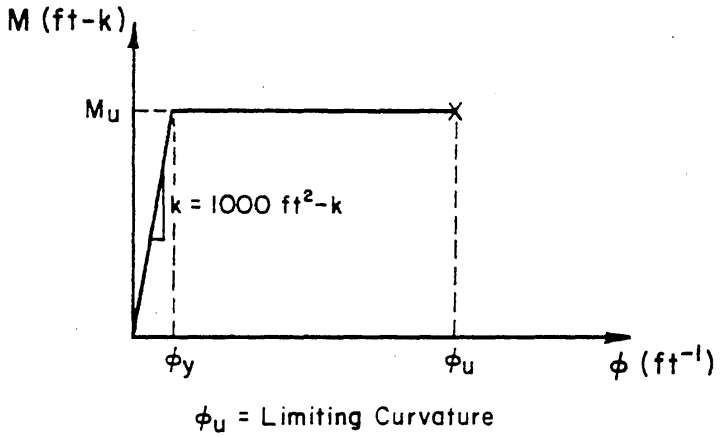


Fig. 6.4 Moment-Curvature Diagram for Beam, Case III

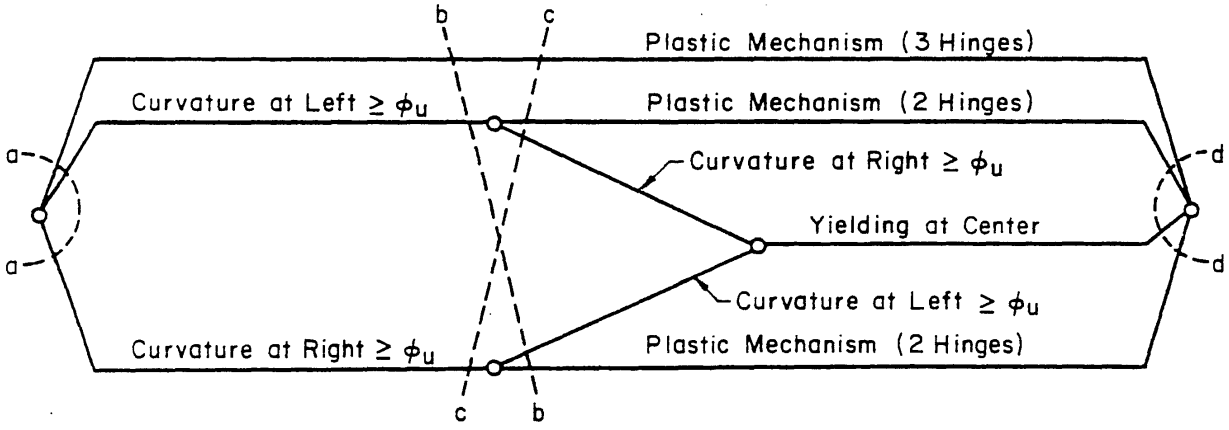


Fig. 6.5 Failure Graph for Beam, Case III

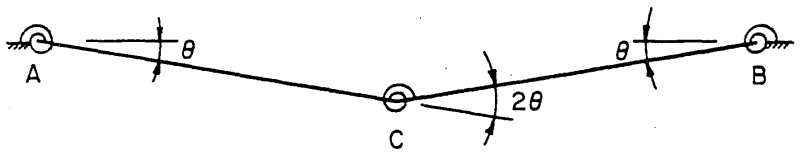


Fig. 6.6 Modelling of Beam, Case V

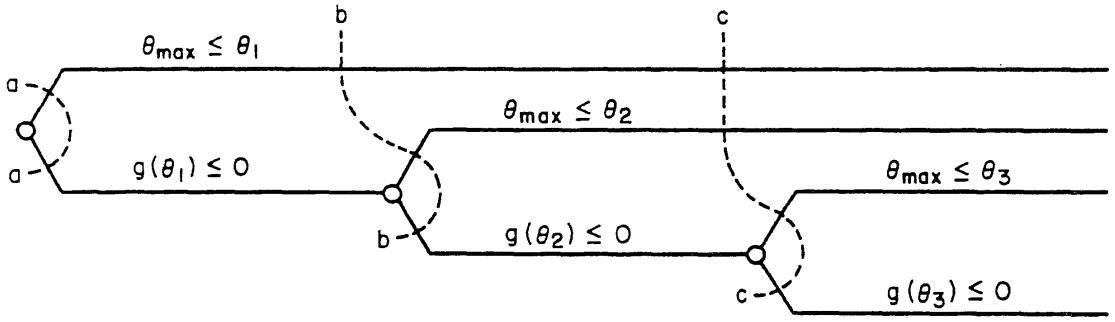


Fig. 6.7 Portion of Failure Graph for Beam, Case V

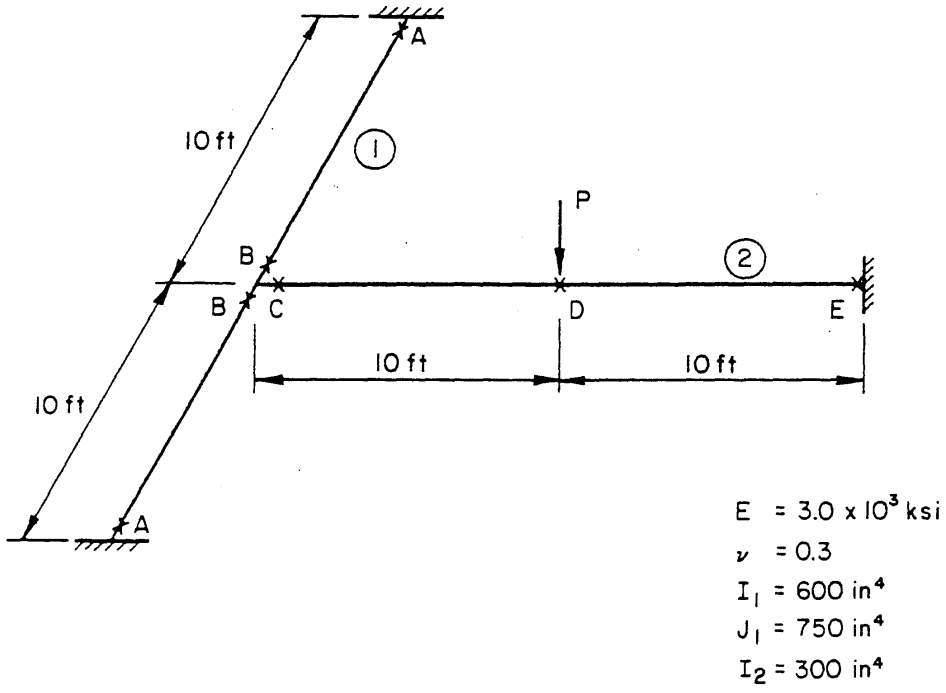


Fig. 6.8 A Simple Grid System

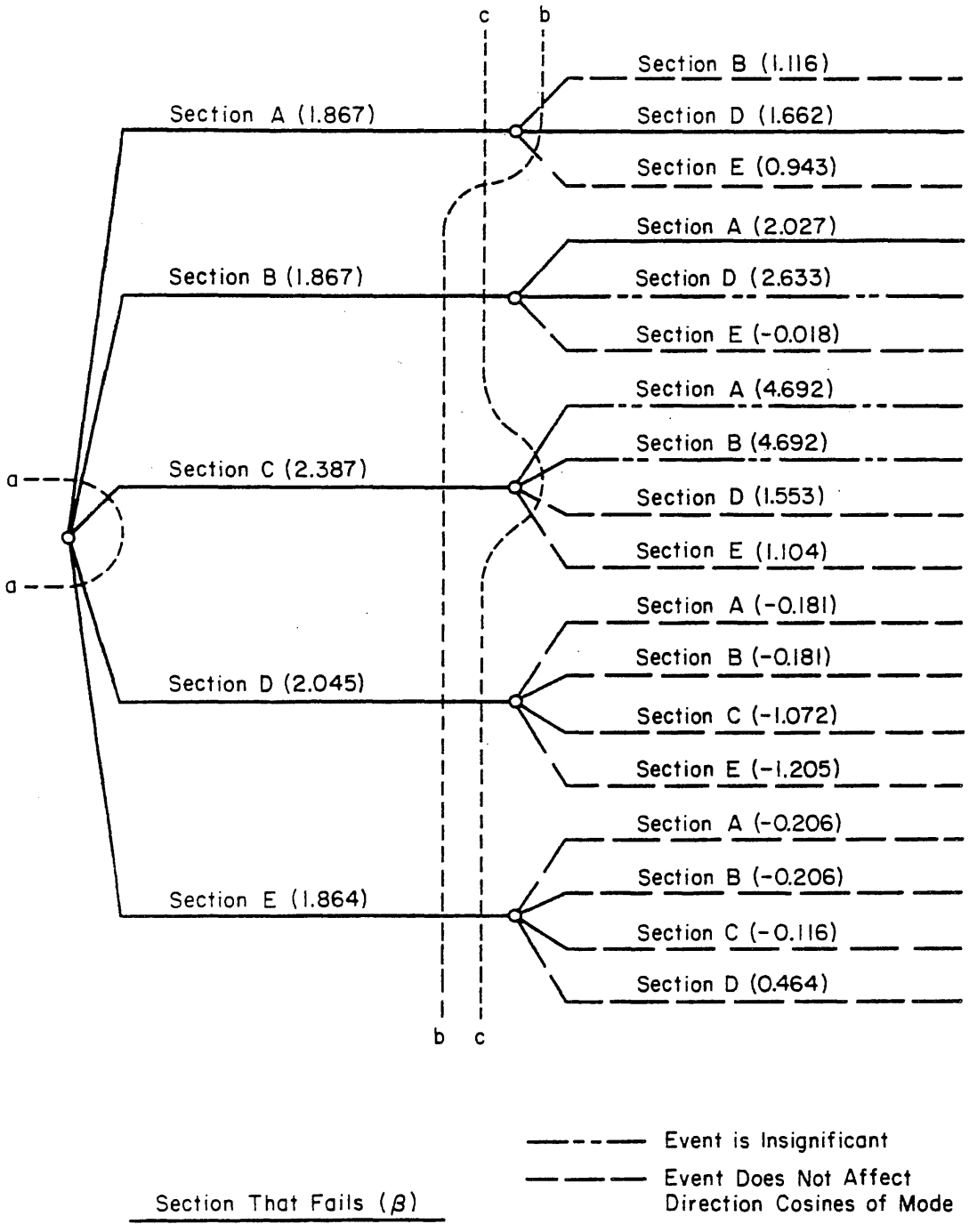


Fig. 6.9 Failure Graph for Grid System

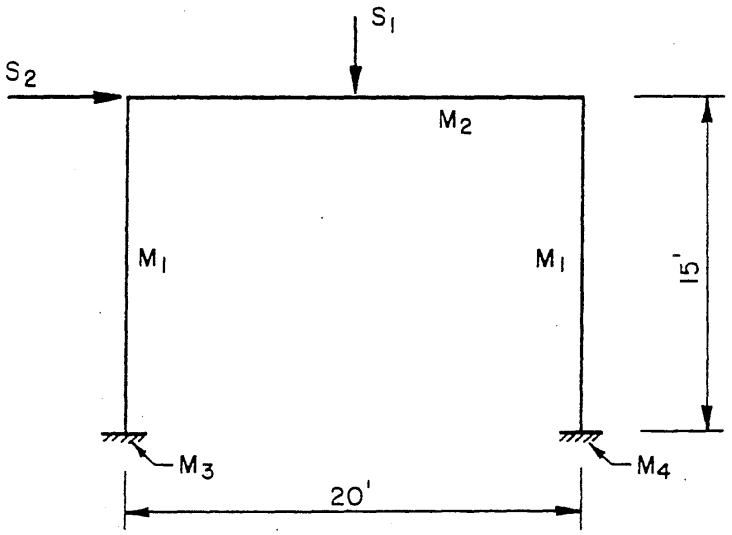


Fig. 6.10 One-Story One-Bay Frame

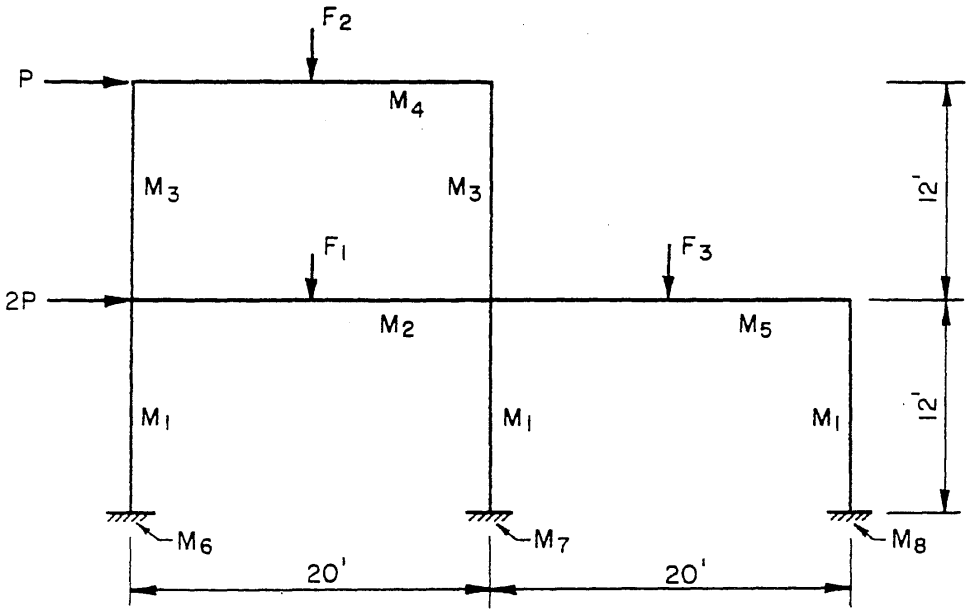


$I_1 = 204$ in.$^4$ $I_4 = 204$ in.$^4$

$I_2 = 448$ in.$^4$ $I_5 = 375$ in.$^4$

$I_3 = 156$ in.$^4$

Fig. 6.11 Two-Story Two-Bay Frame

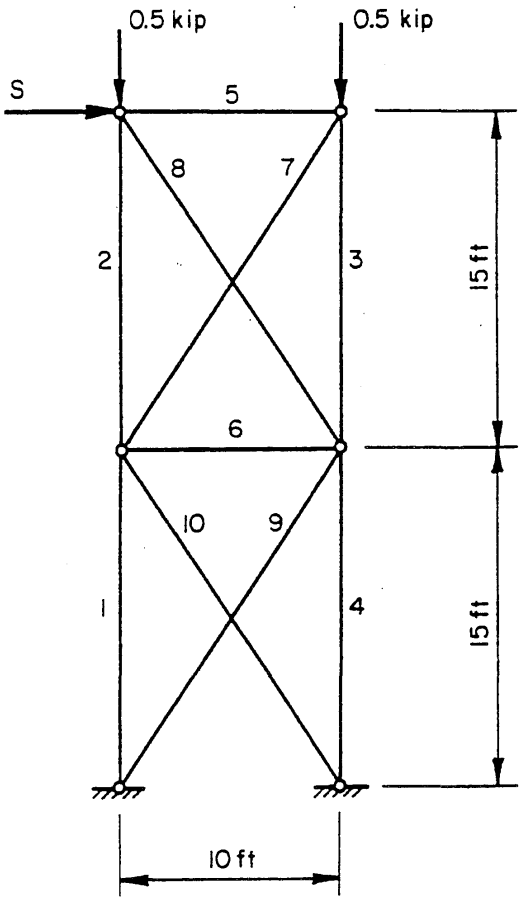


Fig. 6.12 Two-Tier Truss System

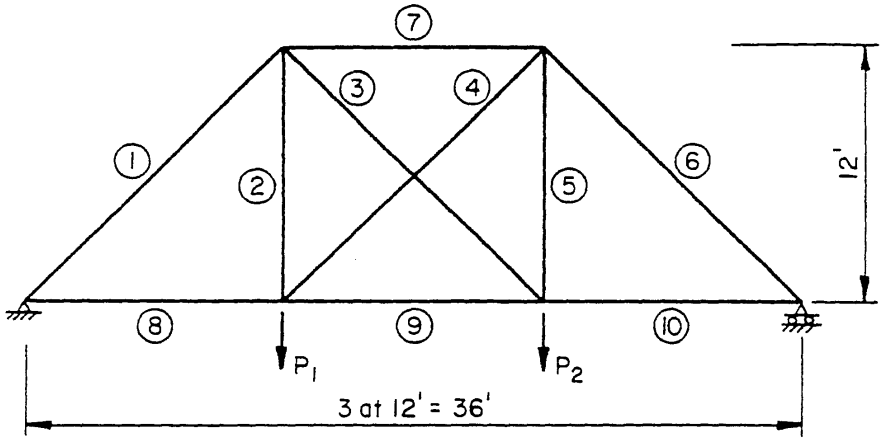


Fig. 6.13 A Truss Structure

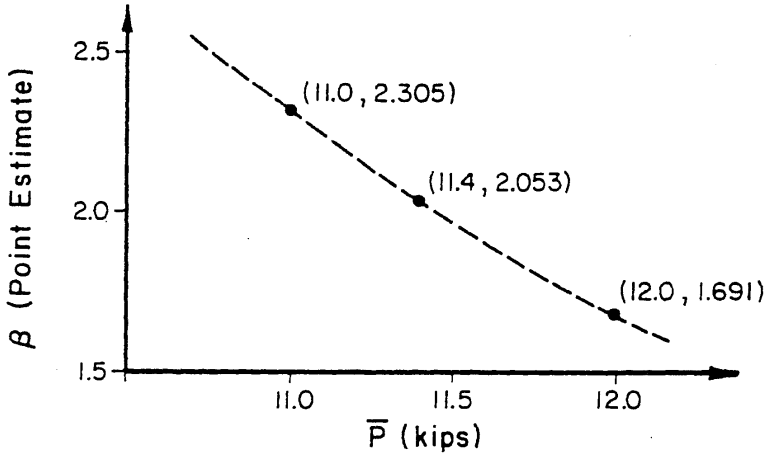


Fig. 6.14 $\beta$ vs. $\bar{P}$

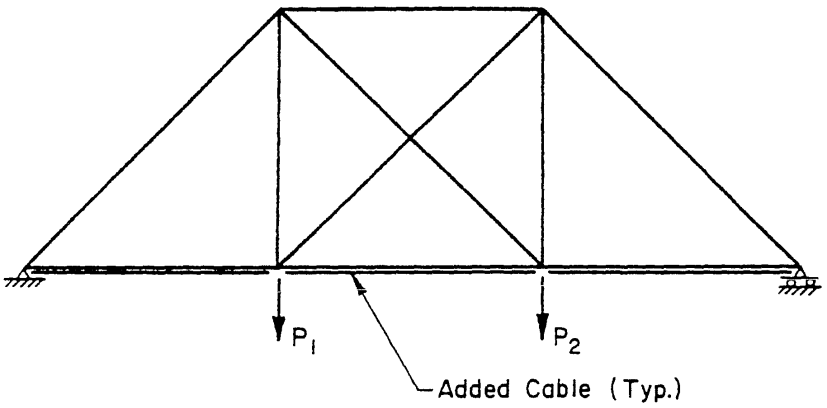


Fig. 6.15 Retrofitted Truss Structure

# CHAPTER 7

# SUMMARY AND CONCLUSIONS

## 7.1 Summary

Two formulations have been developed for the determination of the reliability of general structural systems, including systems with brittle components. One is the failure mode approach, which is based on ways in which a structure can fail. The other is the stable configuration approach, which is based on ways in which a structure can carry an applied load. For a class of structures, in which the load effects on the surviving elements never decrease with the failures of other elements, simplified formulations are introduced. Such simplifications for this type of structure result from the fact that the constraints may be neglected, i.e., the sequence in which the elements may fail is irrelevant. Results of the simplified formulaton are on the conservative side.

To aid in the development of the formulations, the failure graph concept is introduced, a failure graph being a directed graph of all possible sequences of component failures that lead to the prescribed limit state. Each path from the initial node to the terminal node of the graph represents a failure mode. A branch represents a component failure and each node of the graph (except the terminal node) represents a stable configuration of a structure. A cut is defined as a set of branches containing one branch from every path.

The failure mode approach results in the probability of failure being determined as the probability of the union of the individual failure modes (paths). Each failure mode is composed of the intersection of events; the load-carrying capacity of each of the stable configurations that can be formed from the structure, as components

fail, will have to be exceeded for the mode to fail, i.e., all the branches in the path must fail.

A practical computational algorithm is developed for the failure mode approach. Generally, less error is incurred in the system calculations than is introduced through the linearization of the individual events. The method also allows the combination of failure modes and thus reduces the number of modes that need to be considered.

The stable configuration approach leads to the probability of the intersection of the failures of the cuts; if any cut survives there is no possible path from the initial node to the terminal node of the failure graph. The failure of a cut is the union of the failure events of each of the components represented by the branches comprising the cut.

A bounding method is suggested for the computations involved with the stable configuration approach.

## 7.2 Conclusions

Based on the results of the present study, the following conclusions may be derived:

1. The reliability of structural systems can often be obtained by assuming monotonic loading, i.e., ignoring the constraints. For non-monotonically loaded structures, the monotonic loading assumption will lead to conservative results. The degree of conservatism will generally be tolerable.

2. Conceptually, the stable configuration approach has advantages over the failure mode approach; in particular, the effect of the redundancy of a system is easily discernable and the correct probability of failure is approached from above, i.e., neglecting cuts or possible stable configurations will lead to conservative results, whereas neglecting potential failure modes will yield

unconservative results. Practically, a few cuts may be sufficient to obtain an estimate of the system failure probability. Most importantly, the significant cuts are easily found, either through intuition or from the analysis of other cuts.

## 7.3 Critical Overview and Recommendations for Further Study

Since structural reliability, and particularly structural system reliability, is a relatively new field of research, many unanswered questions remain. This study has served to clarify some concepts and extended the available computational techniques.

Continued study and research are obviously necessary in several directions. In particular, the stable configuration approach merits further examination and developments. The formulation aspects, especially for non-monotonically loaded systems, need to be examined further. Continued developments and extensions of the computational techniques available for the stable configuration approach are needed as at present this is the primary weakness of the method.

This study has only considered systems reliability problems involving single load applications. In reality, a structure will experience different load applications or different combinations of loadings.

The development of methodologies is emphasized in the present study; the application to actual structural systems was limited to relatively simple systems. Further studies should also include the application of the methods and algorithms developed herein to structural systems of practical complexity and dimension.

# APPENDIX A

## QUADRATIC PROGRAMMING ALGORITHM FOR FINDING THE FAILURE POINT OF FAILURE MODES

A quadratic programming algorithm is presented for obtaining the solution to the following minimization problem.

$$\text{Minimize} \quad U_1^2 + U_2^2 + \ldots + U_n^2 \tag{A.1}$$

$$\text{subject to} \quad \underline{\alpha}_1^t \underline{U} + \beta_1 \leq 0$$

$$\vdots$$

$$\underline{\alpha}_m^t \underline{U} + \beta_m \leq 0$$

where n is the number of variables and m the number of constraints. The algorithm consists of two parts. The first part finds a feasible starting point based on the work of Rosen (1960). The second part finds the failure point given a feasible starting point based on the algorithms of Fletcher (1971) and Avriel (1976).

Part A: To Find a Feasible Starting Point

A1. Find the constraint with the largest $\beta$. Assume this is constraint 1. Set q=1, $\underline{u}_o = -\beta_1 \underline{\alpha}_1$, $\underline{\underline{H}} = \underline{\underline{I}} - \underline{\alpha}_1 \underline{\alpha}_1^t$, and $\underline{\underline{A}} = \underline{\alpha}_1$. $\underline{\underline{H}}$ is an nxn matrix, $\underline{\underline{I}}$ is the identity matrix, and $\underline{\underline{A}}$ is an nxq matrix.

A2. Find $\gamma = \max_j \{\underline{\alpha}_j^t \underline{u}_o + \beta_j\}$, j=q+1,...,m. If $\gamma<0$ then a feasible point has been found; proceed to Part B. Otherwise, assume that $\gamma$ occurs at j=q+1.

A3. If $|\underline{\underline{H}}_q \underline{\alpha}_{q+1}| = 0$, go to Step A4. Otherwise add constraint q+1 to the active constraints, those constraints for which the inequality is an equality. Update $\underline{\underline{H}}$ and $\underline{\underline{A}}$ using the rules given below (after Part B). Set $\underline{u}_o = \underline{u}_o - \gamma \underline{a}_{q+1}$, where $\underline{a}_{q+1}$ is the q+1 column of the matrix $\underline{\underline{A}}$. Set q=q+1 and return to Step A2.

A4. Calculate $\underline{r} = \underline{\underline{A}}^t \underline{\alpha}_{q+1}$. If $r_i \leq 0$, i=1,...,q, then no feasible solution exists. If $r_i > 0$ for at least one constraint, say i=t, delete constraint t from the active constraints and add constraint q+1. Update $\underline{\underline{H}}$ and $\underline{\underline{A}}$ according to rules given below (after Part B). Set $\underline{u}_o = \underline{u}_o - \gamma \underline{a}_{q+1}$ and return to Step A2.

Part B: To Find the Failure Point

B1. Compute $\underline{z} = \underline{\underline{H}} \underline{u}_o$. If $z_i = 0$, i=1,...,n, go to Step B3.

B2. Obtain $\kappa^* = \min\{1, \kappa\}$ where

$$\kappa = \min_j \left\{ \frac{-\underline{\alpha}_j^t \underline{u}_o + \beta_j}{\underline{\alpha}_j^t \underline{z}} : \underline{\alpha}_j^t \underline{z} \geq 0 \right\} \qquad j=q+1,\ldots,m \qquad \text{(A.2)}$$

Assume that $\kappa$ occurs at j=q+1. Set $\underline{u}_o = \underline{u}_o - \kappa^* \underline{z}$. If $\kappa^* < 1$, add constraint q+1 to the active constraints, update $\underline{\underline{H}}$ and $\underline{\underline{A}}$ (see below), set q=q+1, and return to Step B1.

B3. Compute $\underline{\lambda} = \underline{\underline{A}}^t \underline{u}_o$. Find $\lambda^* = \max\{\lambda_i\}$, i=1,...,q. Say this occurs at i=r. If $\lambda^* \leq 0$, then stop, the failure point has been obtained. If $\lambda^* > 0$, drop constraint r from the active constraints, update $\underline{\underline{H}}$ and $\underline{\underline{A}}$, set q=q-1, and return to Step B1.

Rules for Updating $\underline{\underline{H}}$ and $\underline{\underline{A}}$

I. Add constraint q+1.

$$\underline{\underline{H}} = \underline{\underline{H}} - \frac{\underline{\underline{H}}(\underline{\alpha}_{q+1})(\underline{\alpha}_{q+1})^t \underline{\underline{H}}}{(\underline{\alpha}_{q+1})^t \underline{\underline{H}}(\underline{\alpha}_{q+1})} \tag{A.3}$$

$$\underline{\underline{A}} = \begin{bmatrix} & & 0 \\ & \underline{\underline{A}} & \cdot \\ & & \cdot \\ & & 0 \end{bmatrix} + \frac{\underline{\underline{H}}\,\underline{\alpha}_{q+1}}{(\underline{\alpha}_{q+1})^t \underline{\underline{H}}(\underline{\alpha}_{q+1})} (-\underline{\alpha}_{q+1}^t \underline{\underline{A}}, 1) \tag{A.4}$$

II. Delete constraint q.

$$\underline{\underline{H}} = \underline{\underline{H}} + \frac{\underline{a}_q \underline{a}_q^t}{\underline{a}_q^t \underline{a}_q} \tag{A.5}$$

$$\begin{bmatrix} & & 0 \\ & \underline{\underline{A}} & \cdot \\ & & \cdot \\ & & 0 \end{bmatrix} = \underline{\underline{A}} - \frac{\underline{a}_q \underline{a}_q^t \underline{\underline{A}}}{\underline{a}_q^t \underline{a}_q} \tag{A.6}$$

where $\underline{a}_q$ is the $q^{th}$ column of $\underline{\underline{A}}$ before updating.

REFERENCES


1. Ang, A. H-S., "Structural Risk Analysis and Reliability-Based Design," Journal of the Structural Division, ASCE, Vol. 99, No. ST9, September, 1973, pp. 1891-1910.

2. Ang, A. H-S. and Amin, M., Studies of Probabilistic Safety Analysis of Structures and Structural Systems, Structural Research Series No. 320, University of Illinois, Urbana, 1967.

3. Ang, A. H-S. and Cornell, C. A., "Probability Basis of Structural Safety and Design," Journal of the Structural Division, ASCE, Vol. 100, No. ST9, September, 1974, pp. 1755-1769.

4. Ang, A. H-S. and Ma, H-F., "On the Reliability Analysis of Framed Structures," Probabilistic Mechanics and Structural Reliability, ASCE, 1979, pp. 106-111.

5. Ang, A. H-S. and Ma, H-F., "On the Reliability of Structural Systems," Structural Safety and Reliability, ICOSSAR '81, Elsevier Scientific Publishing Co., Amsterdam, Netherlands, 1981, pp. 295-314.

6. Ang, A. H-S. and Tang, W. H., Probability Concepts in Engineering Planning and Design, Volume II, John Wiley & Sons, New York, NY, 1983.

7. Augusti, G. and Baratta, A., "Limit Analysis of Structures with Stochastic Strength Variations," Journal of Structural Mechanics, Vol. 1 No. 1, 1972, pp. 43-62.

8. Avriel, M., Nonlinear Programming: Analysis and Methods, Prentice-Hall, Inc., Englewood Cliffs, New Jersey, 1976.

9. Barlow, R. E. and Proschan, F., Statistical Theory of Reliability and Life Testing, Holt, Rinehart, and Winston, Inc., New York, NY, 1975.

10. Bennett, R. M. and Ang, A. H-S., Discussion of "System Reliability Bounding by Conditioning," accepted by Journal of Engineering Mechanics, ASCE, 1983.

11. Buslenko, N. P., Golenko, D. I., Shreider, Yu. A., Sobol, I. M., and Sragovich, V. G., The Monte Carlo Method, translated by G. J. Tee, Pergamon Press, Oxford, England, 1966.

12. Chen, X. and Lind, N. C., "A New Method of Fast Probability Integration," University of Waterloo, Paper No. 171, June, 1982.

13. Chu, T. L. and Apostolakis, G., "Methods for Probabilistic Analysis of Noncoherent Fault Trees," IEEE Transactions on Reliability, Vol. R-29, No. 5, December, 1980, pp. 354-360.

14. Cornell, C. A., "Bounds on the Reliability of Structural Systems," Journal of the Structural Division, ASCE, Vol. 93, No. ST1, February, 1967, pp. 171-200.

15. Curnow, R. N. and Dunnett, C. W., "The Numerical Evaluation of Certain Multivariate Normal Integrals," Annals of Mathematical Statistics, Vol. 33, No. 2, June, 1962, pp. 571-579.

16. Daniels, H. E., "The Statistical Theory of the Strength of Bundles of Threads, I," Proceedings of the Royal Society, London, Series A, Vol. 183, No. 995, June, 1945, pp. 405-435.

17. DerKiureghian, A. and Moghtaderi-Zadeh, M., "An Integrated Approach to the Reliability of Engineering Systems," Nuclear Engineering and Design, Vol. 71, No. 3, August, 1982, pp. 349-354.

18. Ditlevsen, O., "Generalized Second Moment Reliability Index," Journal of Structural Mechanics, Vol. 7, No. 4, 1979, pp. 435-451.

19. Ditlevsen, O., "Narrow Reliability Bounds for Structural Systems," Journal of Structural Mechanics, Vol. 7, No. 4, 1979, pp. 453-472.

20. Ditlevsen, O. and Madsen, H. O., Discussion of "Optimal Reliability Analysis by Fast Convolution," Journal of the Engineering Mechanics Division, ASCE, Vol. 106, No. EM3, June, 1980, pp. 579-583.

21. Dumonteil, P., Discussion of "Optimal Reliability Analysis by Fast Convolution," Journal of the Engineering Mechanics Division, ASCE, Vol. 106, No. EM2, April, 1980, p. 420.

22. Dunnett, C. W. and Sobel, M., "Approximations to the Probability Integral and Certain Percentage Points of a Multivariate Analogue of Student's t-Distribution," Biometrika, Vol. 42, June, 1955, pp. 258-260.

23. Esary, J. D., Proschan, F., and Walkup, D. W., "Association of Random Variables, with Applications," Annals of Mathematical Statistics, Vol. 38, No. 5, October, 1967, pp. 1466-1474.

24. Esteva, L., "Uncertainty, Reliability, and Decisions in Structural Engineering," Structural Safety and Reliability, ICOSSAR '81, Elsevier Scientific Publishing Co., Amsterdam, Netherlands, 1981, pp. 559-577.

25. Fiessler, B., Neumann, H-J., and Rackwitz, R., "Quadratic Limit States in Stuctural Reliability," Journal of the Engineering Mechanics Division, ASCE, Vol. 105, No. EM4, August, 1979, pp. 661-676.

26. Fletcher, R., "A General Quadratic Programming Algorithm," Journal of the Institute of Mathematics and its Applications, Vol. 7, No. 1, February, 1971, pp. 76-91.

27. Frankland, F. H., Discussion of "The Safety of Structures," Transactions, ASCE, Vol. 112, 1947, pp. 160-162.

28. Freudenthal, A. M., "The Safety of Structures," Transactions, ASCE, Vol. 112, 1947, pp. 125-180.

29. Garson, R. C., "Failure Mode Correlation in Weakest-Link Systems," Journal of the Structural Division, ASCE, Vol. 106, No. ST8, August, 1980, pp. 1797-1810.

30. Gollwitzer, S. and Rackwitz, R., "Equivalent Components in First-Order System Reliability," Reliability Engineering, Vol. 5, No. 2, 1983, pp. 99-115.

31. Gorman, M. R. and Moses, F., "Reliability of Structural Systems," Report No. 79-2, Case Western Reserve University, 1979.

32. Griffith, R. E. and Stewart, R. A., "A Nonlinear Programming Technique for the Optimization of Continuous Processing Systems," Management Science, Vol. 7, No. 4, July, 1961, pp. 379-392.

33. Grigoriu, M., "Methods for Approximate Reliability Analysis," Structural Safety, Vol. 1, No. 2, December, 1982, pp. 155-165.

34. Grigoriu, M. and Lind, N. C., "Optimal Estimation of Convolution Integrals," Journal of the Engineering Mechanics Division, ASCE, Vol. 106, No. EM6, December, 1980, pp. 1349-1364.

35. Grimmelt, M. J. and Schueller, G. I., "Benchmark Study on Methods to Determine Collapse Probabilities of Redundant Structures," Structural Safety, Vol. 1, No. 2, December, 1982, pp. 93-106.

36. Grimmelt, M. J., Schueller, G. I., and Murotsu, Y., "On the Evaluation of Collapse Probabilities," Recent Advances in Engineering Mechanics and Their Impact on Civil Engineering Practice, ASCE, 1983, pp. 859-862.

37. Hammersley, J. M. and Handscomb, D. C., Monte Carlo Methods, Methuen & Co., London, England, 1964.

38. Henley, E. J. and Williams, R. A., Graph Theory in Modern Engineering, Vol. 98, Mathematics in Science and Engineering Series, Academic Press, New York, NY, 1973.

39. Hohenbichler, M., "Approximate Evaluation of the Multinormal Distribution Function," Studies on the Reliability of Redundant Structural Systems, Technical University of Munich, No. 58, 1981, pp. 55-66.

40. Hohenbichler, M. and Rackwitz, R., "Non-Normal Dependent Vectors in Structural Safety," Journal of the Engineering Mechanics Division, ASCE, Vol. 107, No. EM6, December, 1981, ppp. 1227-1238.

41. Hohenbichler, M. and Rackwitz, R., "Reliability of Parallel Systems Under Imposed Uniform Strain," Journal of Engineering Mechanics, ASCE, Vol. 109, No. 3, June, 1983, pp. 896-907.

42. Hohenbichler, M. and Rackwitz, R., "First-Order Concepts in System Reliability," Structural Safety, Vol. 1, No. 3, April, 1983, pp. 177-188.

43. Hunter, D., "An Upper Bound for the Probability of a Union," Journal of Applied Probability, Vol. 13, No. 3, September, 1976, pp. 597-603.

44. Ishizawa, J., "On the Reliability of Indeterminate Structural Systems," Ph.D. thesis, University of Illinois, Urbana, 1968.

45. Johnson, N. L., "Systems of Frequency Curves Generated by Methods of Translation," Biometrika, Vol. 36, 1949, pp. 149-176.

46. Johnson, N. L. and Kotz, S., Distributions in Statistics: Discrete Distributions, John Wiley & Sons, New York, NY, 1969.

47. Johnson, N. L. and Kotz, S., Distributions in Statistics: Continuous Univariate Distributions - 1, John Wiley & Sons, New York, NY, 1970.

48. Johnson, N. L. and Kotz, S., Distributions in Statistics: Continuous Multivariate Distributions, John Wiley & Sons, New York, NY, 1972.

49. Jorgenson, J. L. and Goldberg, J. E., "Probability of Plastic Collapse Failure," Journal of the Structural Division, ASCE, Vol. 95, No. ST8, August, 1969, pp. 1743-1761.

50. Klingmuller, O., "Redundancy of Structures and Probability of Failure," Structural Safety and Reliability, ICOSSAR '81, Elsevier Scientific Publishing Co., Amsterdam, Netherlands, 1981, pp. 331-340.

51. Kounias, E. G., "Bounds for the Probability of a Union, with Applications," Annals of Mathematical Statistics, Vol. 39, No. 6, December, 1968, pp. 2154-2158.

52. Lawler, E. L. and Wood, D. E., "Branch-and-Bound Methods: A Survey," Operations Research, Vol. 14, No. 4, July-August, 1966, pp. 699-719.

53. Locks, M.O., "System Reliability Analysis: A Tutorial," Microelectronics and Reliability, Vol. 18, No. 4, 1978, pp. 335-345.

54. Locks, M. O., "Inverting and Minimizing Boolean Functions, Minimal Paths and Minimal Cuts: Noncoherent System Analysis," IEEE Transactions on Reliability, Vol. R-28, No. 5, December, 1979, pp. 373-375.

55. Ma, H-F. and Ang, A. H-S., Reliability Analysis of Redundant Ductile Structural Systems, Structural Research Series No. 494, University of Illinois, Urbana, 1981.

56. Mazumdar, M., Marshall, J. A., and Chay, S. C., "Propagation of Uncertainties in Problems of Structural Reliability," Nuclear Engineering and Design, Vol. 50, No. 2, October II, 1978, pp. 163-167.

57. Moses, F., "System Reliability Developments in Structural Engineering," Structural Safety, Vol. 1, No. 1, September, 1982, pp. 3-13.

58. Moses, F. and Kinser, D. E., "Analysis of Structural Reliability," Journal of the Structural Division, ASCE, Vol. 93, No. ST5, October, 1967, pp. 147-164.

59. Murotsu, Y., Nakayasu, H., Mori, K., and Kase, S., "New Method of Relating Safety Factor to Failure Probability in Structural Design," Advances in Reliability and Stress Analysis, ASME, 1979, pp. 23-35.

60. Murotsu, Y., Okada, M., Yonezawa, M. and Taguchi, K., "Reliability Assessment of Redundant Structure," Structural Safety and Reliability, ICOSSAR '81, Elsevier Scientific Publishing Co., Amsterdam, Netherlands, 1981, pp. 315-329.

61. Murotsu, Y., Okada, M., Yonezawa, M., Grimmelt, M. and Taguchi, K., "Automatic Generation of Stochastically Dominant Modes of Structural Failure in Frame Structure," Bulletin of University of Osaka Prefecture, Series A, Vol. 30, No. 2, 1981.

62. Owen, D. B., "Tables for Computing Bivariate Normal Probabilities," Annals of Mathematical Statistics, Vol. 27, No. 4, 1956, pp. 1075-1090.

63. Parkinson, D. B., "Four-Moment Reliability Analysis for Static and Time-Dependent Problems," Reliability Engineering, Vol. 1, No. 1, September, 1980, pp. 29-42.

64. Pinjarkar, S.G., "Fault Tree Analysis to Anticipate Potential Structural Failure," Probabilistic Mechanics and Structural Reliability, ASCE, 1979, pp. 372-376.

65. Phoenix, S. L., "The Random Strength of Series-Parallel Structures with Load Sharing Among Members," Probabilistic Mechanics and Structural Reliability, ASCE, 1979, pp. 91-95.

66. Rackwitz, R. and Feissler, B., "Structural Reliability Under Combined Random Load Sequences," Computers and Structures, Vol. 9, No. 5, November, 1978, ppp. 489-494.

67. Rackwitz, R. and Peintinger, B., "General Structural System Reliability," Structural Analysis, Bulletin d'Information No. 154, Comite Euro-International du Beton, April, 1982, pp. 127-191.

68. Rosen, J. B., "The Gradient Projection Method for Nonlinear Programming, Part I, Linear Constraints," Journal of the Society for Industrial and Applied Mathematics, Vol. 8, No. 1, March, 1960, pp. 181-217.

69. Rosenblatt, M. "Remarks on a Multivariate Transformation," Annals of Mathematical Statistics, Vol. 23, No. 3, September, 1952, pp. 470-472.

70. Shinozuka, M., "Basic Analysis of Structural Safety," Journal of Structural Engineering, ASCE, Vol. 109, No. 3, March, 1983, pp. 721-740.

71. Shinozuka, M. and Itagaki, H., "On the Reliability of Redundant Structures," Annals of Reliability and Maintainability, Vol. 5, 1966, pp. 605-610.

72. Shinozuka, M., Yao, J. T-P., and Nishimura, A., "A Note on the Reliability of Redundant Structures," Proceedings, Sixth International Symposium on Space Technology and Science, Tokyo, 1965, pp. 431-438.

73. Shooman, M. L., Probabilistic Reliability: An Engineering Approach, McGraw-Hill, New York, NY, 1968.

74. Slepian, D., "The One-Sided Barrier Problem for Gaussian Noise," Bell System Technical Journal, Vol. 41, No. 2, March, 1962, pp. 463-501.

75. Stevenson, J. and Moses, F., "Reliability Analysis of Frame Structures," Journal of the Structural Division, ASCE, Vol. 96, No. ST11, November, 1970, pp. 2409-2427.

76. Vanmarcke, E. H., "Matrix Formulation of Reliability Analysis and Reliability-Based Design," Computers and Structures, Vol. 3, No. 4, July, 1973, pp. 757-770.

77. Warner, R. F. and Kabaila, A. P., "Monte Carlo Study of Structural Safety," Journal of the Structural Division, ASCE, Vol. 94, No. ST12, December, 1968, pp. 2847-2859.

78. Yao, J. T-P. and Yeh, H. Y., "Safety Analysis of Statically Indeterminate Trusses," Annals of Reliability and Maintainability, Vol. 6, 1967, pp. 54-62.

79. Yao, J. T-P. and Yeh, H. Y., "Formulation of Structural Reliability," Journal of the Structural Division, ASCE, Vol. 95, No. ST12, December, 1969, pp. 2611-2619.